UNIVERSIDAD AUTÓNOMA DE NUEVO LEÓN

FACULTAD DE CIENCIAS DE LA TIERRA

EVALUACIÓN DEL PELIGRO SÍSMICO EN EL ESTADO DE TABASCO Y CASOS DE ESTUDIO EN ZONAS URBANAS

POR

CARMEN MARICELA GÓMEZ ARREDONDO

COMO REQUISITO PARCIAL PARA OBTENER EL GRADO DE
DOCTOR EN CIENCIAS CON ORIENTACIÓN EN GEOCIENCIAS

ENERO, 2025

UANL®
UNIVERSIDAD AUTÓNOMA DE NUEVO LEÓN

FCT®
FACULTAD DE CIENCIAS DE LA TIERRA

EVALUACIÓN DEL PELIGRO SÍSMICO EN EL ESTADO DE TABASCO Y CASOS DE ESTUDIO EN ZONAS URBANAS

APROBACIÓN DE LA TESIS

DR. JUAN CARLOS MONTALVO ARRIETA
DIRECTOR DE TESIS

DR. MIGUEL ÁNGEL SANTOYO GARCÍA GALIANO
CO-DIRECTOR

DR. FRANÇOISE COURBOULEX
MIEMBRO DE LA COMISIÓN DE LA TESIS

DR. ARTURO IGLESIAS MENDOZA
MIEMBRO DE LA COMISIÓN DE LA TESIS

DR. UWE JENCHEN
MIEMBRO DE LA COMISIÓN DE LA TESIS

DR. FERNANDO VELASCO TAPIA
SUBDIRECTOR DE POSGRADO

EVALUACIÓN DEL PELIGRO SÍSMICO EN EL ESTADO DE TABASCO Y CASOS DE ESTUDIO EN ZONAS URBANAS

ESTE TRABAJO FUE REALIZADO EN EL **DEPARTAMENTO DE GEOFÍSICA**, EN LA **FACULTAD DE CIENCIAS DE LA TIERRA** DE LA **UNIVERSIDAD AUTÓNOMA DE NUEVO LEÓN**, BAJO LA DIRECCIÓN DEL DR. JUAN CARLOS MONTALVO ARRIETA Y LA CO-DIRECCIÓN DEL DR. MIGUEL ÁNGEL SANTOYO GARCÍA GALIANO.

DR. JUAN CARLOS MONTALVO ARRIETA
DIRECTOR DE TESIS

Acknowledgments

Al **Dr. Juan Carlos Montalvo Arrieta**, porque aparte de su guía y enseñanza, sus consejos serán un gran apoyo en mi camino profesional. Quien por su amor a la sismología me ha guiado con paciencia y sabiduría ¡Gracias por ser una fuerte y humilde inspiración!

A la Dra. **Françoise** Courboulex: Merci beaucoup pour votre soutien et votre confiance dans cette chemin de la sismologie. Merci d'avoir accepté de faire partie de ce rêve!

al Dr. **Miguel** Ángel Santoyo: Muchas gracias por su disposición y consejos para la mejora de este trabajo. Su apoyo, confianza y enseñanzas, serán claves en mi desarrollo personal y profesional.

al Dr. **Arturo** Iglesias Mendoza:: Gracias por su apoyo, consejos, conocimiento y por acompañarme nuevamente en mi camino hacia la sismología.

al Dr. **Uwe** Jenchen: agradezco mucho sus consejos, motivación y enseñanzas para lograr un sueño profesional más. ¡Gracias por su cálida motivación!

Al Dr. **Fernando** Velasco Tapia, por sus consejos, sus regaños motivadores y mucho más; porque aparte de su apoyo en la formación de profesionistas, su sabiduría nos ha sido una gran ayuda para ser mejores personas y mejores seres humanos.

Este proyecto de investigación ha sido posible gracias a la Universidad Juárez Autónoma de Tabasco, con beneficio del programa PISA (Programa Institucional de Superación Académica), al PRODEP (Programa para el Desarrollo Profesional Docente) y al CONHACYT (Consejo Nacional de Humanidades Ciencias y Tecnologías).

Agradezco infinitamente los profesores compañeros de la **Universidad Juárez Autónoma de Tabasco**, que me apoyaron, al **Dr. Gerardo Delgadillo Piñón, al M.T. Abel Cortazar May, a la Dra. Hermicenda Pérez Vidal** y al personal académico y administrativo de la División Académica de Ciencias Básicas. ¡Gracias infinitas!

A **Daniel, Guillermo** y **Carlos Mario**, más que compañeros, amigos, agradezco por sus enseñanzas, motivación y entusiasmo hacía el crecimiento y la enseñanza.

A la **Joaquina**, **ZGLL** por ser más que mi apoyo antes, durante y después de este trabajo. Sin mi otra persona, no se como hubiera cruzado este camino.

Por último y no menos importante. **Luis** Gerardo por su apoyo y amistad sismológica desde antes que decidirme entrar a este mundo de ondas.

To:

Mamá, Papá,
Cris, Cristian,
Valente.

Consuelo Arredondo y José Gómez: *mi primer amor. Sus enseñanzas me han traído aquí.*
Cristina Gónez y Cristian Zúñiga: *Alegría y ternura inmensa de tenerlos.*
Valente: *Mi esposo, mi compañero de vida, mi amor infinito.*

Contents

Resumen

La evaluación probabilística del peligro sísmico a través de la metodología Cornell-McGuire, para periodos de retorno de 95, 238, 475 y 950 años, se llevó a cabo para el Sureste de México, con enfoque en el estado de Tabasco. La necesidad de una actualización de los mapas de peligro sísmico se justifica con el crecimiento poblacional, la importancia socioeconómica, los peligros naturales que han afectado a la entidad y a la construcción en esta zona, de la refinería más importante del país. Este trabajo se inició con la actualización de un catálogo sísmico que cubre los periodos pre-instrumental e instrumental de 1533 a 2020 con un rango de magnitudes $3.5 \leq M_w \leq 8.6$ y un total de eventos de 62,965. Un primer estudio para caracterizar la sismicidad natural e inducida para un grupo de eventos en el sur del Golfo de México fue llevado a cabo dentro del catálogo. Después se propuso un modelo de fuentes sísmicas formado por 21 zonas considerando la sismicidad, tectónica, geología e información geofísica. Entre dichas zonas se tienen las corticales, de interface, de intraplaca superficiales y de intraplaca profunda. Los parámetros M_{max}, a y b fueron calculados para cada región. Las ecuaciones de predicción del movimiento del suelo que permiten la integración de V_{S30} fueron usadas primero en roca con valores $V_{S30} \geq 800$ m/s, mientras que en los valores de $180 \geq V_{S30} \geq 300$ m/s se contemplan los efectos locales de sitio, los cuales fueron obtenidos a través de la técnica *Multichannel Analysis of Surface Waves,* en algunas zonas del estado de Tabasco. Las funciones de transferencia y los cocientes espectrales H/V fueron utilizados para la obtención de los sismogramas sintéticos para el municipio de Centro y a su vez se correlacionaron con evidencias de daños del terremoto de Chiapas de M_w8.2, demostrado que eventos regionales pueden causar severos daños estando incluso a una distancia de 350 km. Todo lo anterior muestra que el estado de Tabasco, aunque geográficamente no cuenta con registros de terremotos de grandes magnitudes, es una región vulnerable daños por eventos sísmicos y que presenta un considerable peligro sísmico.

Abstract

A probabilistic seismic hazard assessment using the methodology by Cornell-McGuire focuses on Tabasco's state has been performed for 95, 238, 475, and 950 years return period. The population growth, socioeconomic importance, natural hazards affecting Tabasco state, and the current construction of the biggest oil refinery show the necessity to update the seismic hazard maps and better understand Tabasco's seismicity. At the beginning of this research, an updated seismic catalog was prepared for a period of 1533 to 2020 covering a pre-instrumental and an instrumental period, with a magnitude range of $3.5 \leq M_w \leq 8.6$ with a total of 62,965 events. An analysis of natural and induced seismicity was carried out for a cluster of seismicity in the southern Gulf of Mexico, defining the events as natural seismicity. Next, a new model is proposed formed by 21 seismic zones for crustal, interface, shallow inslab, and deep inslab sources. M_{max}, a and b parameters were evaluated for each region. The Ground Motion Prediction Equations that allow the integration of the Vs_{30} in their equations were used considering values of $V_{S30} \geq 800$ m/s for rock and $180 \geq V_{S30} \geq 300$ m/s to contemplate local site effects, where surficial wave values were obtained through Multichannel Analysis of Surface Waves technique for some places of Tabasco's state. Transfer function and H/V spectral ratio were used to perform the synthetic seismogram for Centro Municipality and correlated with damage evidence of the M_w8.2 Chiapas earthquake, proving that regional events can cause several damages with 350 km of epicentral distance. All these data evidence that even if Tabasco's state is a geographic entity missing large magnitude events recorded, it is a vulnerable region for distant seismic events and has a considerable seismic hazard.

Hypothesis

By evaluating the seismic hazard, and its representation using maps of the variation of the ground motion parameters (peak and spectral values) for different levels of probability of exceedance, the behavior for future earthquakes in the Southeast of Mexico with implications in Tabasco is determined. This work performs the first approximation to estimate the degree of exposure of the state's urban centers to seismic events of different distances and magnitudes, as well as to contribute to the mitigation of damage and the review of construction codes.

Aims

Evaluate the seismic hazard in the Southeast of Mexico, focusing on the Tabasco state from ground motion parameters (peak values, A_{max}, $V_{max,}$ and spectral values from pseudo acceleration, pseudo velocity, and pseudo displacement) for different levels of probability of exceedance, taking into account the seismotectonic setting of the region.

Specifics

- Compilate a unique catalog of the historical and instrumental seismicity for the study area.
- Characterize damage and intensities generated by historical events.
- Evaluate the seismotectonic setting of the region.
- Generate the seismic regionalization.
- Evaluate parameters of recurrence laws.
- Select the Ground Motion Prediction Equations valid for each zone.
- Estimate the site effect of Tabasco state.

Motivation and contribution

The primary purpose of this thesis is to assess the probabilistic seismic hazard for Tabasco state, a region traditionally considered aseismic. A significant event in southern Mexico that impacted Tabasco was the M_w8.2 Chiapas earthquake, which occurred on September 8, 2017. This earthquake caused damage to several buildings (Figure 1.1) and resulted in the death of one person in the region. Following this event, some facts were highlighted, emphasizing the need for a more thorough understanding of the seismic risk in the state. Notably, it was noted that there is a lack of seismic criteria for building construction even though the event had an epicentral distance of 350 km. The following questions were asked at the beginning of the study to know the state of the knowledge of this topic in the territory:

- Can we perform a feasible seismic hazard analysis without a dense network of seismic stations?
- Can we estimate and relate the seismic site effect with the seismic hazard in Tabasco state?
- How is the behavior of the sedimentary quaternary material where Tabasco is lying?
- Which geological structures are related to earthquakes? and if there is a relationship, how this kind of seismicity has affected Tabasco?
- Is there evidence of historical seismicity that had caused damage to Tabasco's state?
- Can I compute the Uniform Hazard Spectrum for Tabasco's state?

It is essential to mention that in this work, some contributions were made to develop the seismic hazard assessment in southern Mexico, focusing on Tabasco state, as follows:

- With the development of a new seismic source model created from a new seismic catalog of southern Mexico, the recompilation of focal mechanism, a geological and tectonic bibliographic compilation, seismic information of pre-instrumental earthquakes, a more comprehensive model will be proposed encompassing southern Mexico state and focusing Tabasco state.

- The urban zones of Tabasco have been growing up on sedimentary rocks and old lagoons, which means that they are lying in unconsolidated material; adding that the entity has a complex hydraulic system, and frequent floods are a recurrent phenomenon, is relevant to evaluate the local site effect that can amplify the seismic waves generated by earthquakes with local and regional distances. The M_w8.2 earthquake had an epicentral distance of 360 km, and generated Modified Mercalli Intensities (MMI) up to VII in Villahermosa city, the most populated urban center of Tabasco; adding that some buildings were damaged during the seismic event, it can be evidence of the site effect in Tabasco.

- Seismic hazard studies for Tabasco state still need to be included; it will be the first seismic hazard study focused on the entity.

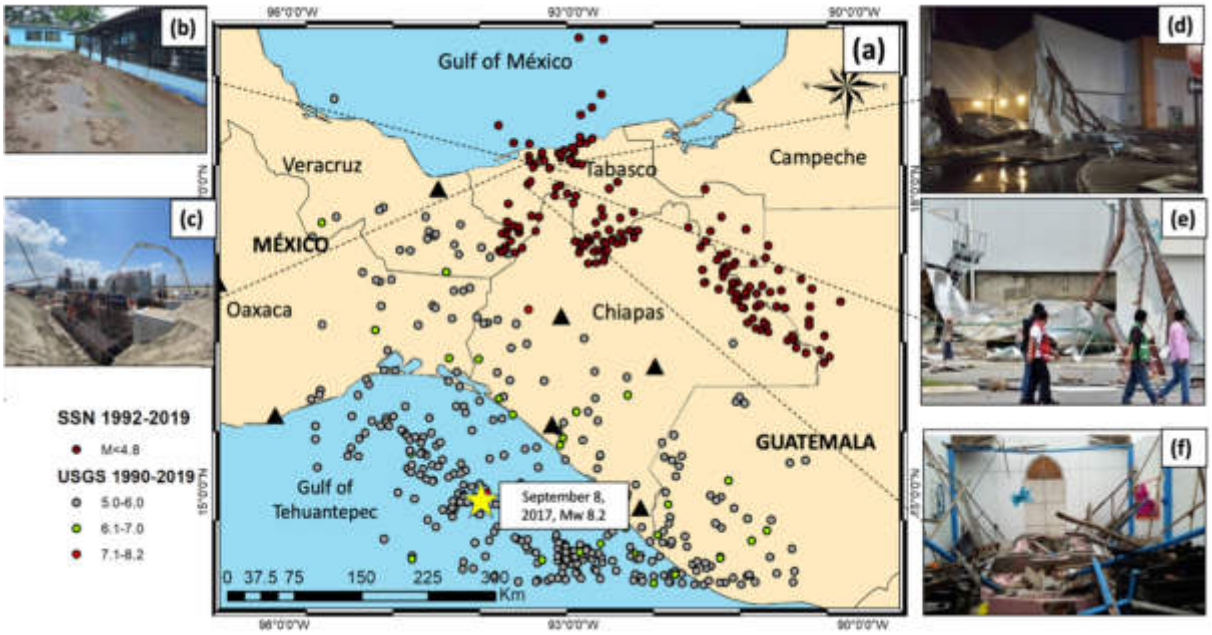

Figure 1.1. (a) Display of Southern Mexico area; dark red circles are the epicenters reported for Tabasco state by the Servicio Sismológico Nacional (SSN, Spanish acronym); gray, green, and red color circles are some epicentral locations reported by USGS. Triangles indicate the location of seismic stations belonging to the SSN. The star shows the location of the September 08, 2017, of M_w8.2; figures (b), (d), (e), and (f) exhibit damages happened during M_w8.2 earthquake; and (c) represent the construction of Paraiso, Tabasco's refinery the biggest one of Mexico.

1.1 Background

Natural hazards are natural phenomena capable of causing significant damage and loss in different regions across the world (*e.g.* Pelc and Kodeman, 2018; Ward *et al.,* 2020). Some examples of them are volcanic activity, landslides, floods, and seismic hazards. Earthquakes are one of the most catastrophic phenomena, and their consequences in Mexico have been devasting and left hundreds of affectations. An example is the April 4, 2010 earthquake, El Mayor-Cucapah with M_w7.2 that occurred in Baja California; it caused 4 deaths and injured 104 others (Trugman *et al.,* 2014); the September 9, 2017, Chiapas earthquake with M_w8.2 left 100 deaths and 900 injuries (Xiang *et al.,* 2019; Ortiz *et al.,* 2021); during September 19, 2017, Puebla-Morelos event with M_w7.1 collapsed 46 buildings which resulted in 219 deaths (Galvis *et al*., 2017). The society has witnessed major catastrophes with economic solid implications (León *et al*., 2022); for example, El Mayor-Cucapah earthquake (M_w7.2) generated damage up to 1.15 million dollars (CRED 2016), Chiapas earthquake (M_w8.2) and Puebla-Morelos (M_w7.1) caused damage by 1012.3 million dollars (Jiménez, 2018; Singh *et al*., 2018; CENAPRED, 2021).

Southeastern Mexico (SEM) lies in a tectonic active region, which is not exempt from damage by natural phenomena. Within this area is Tabasco, an entity affected by volcanic, meteorological, and seismological phenomena. On March 28, 1982, the last eruption of the Chichonal volcano in Chiapas took place and caused 2,000 deaths and the displacement of 20,000 people; the most urbanized areas of Tabasco were in dark more than one week (De la Cruz Reyna and Martín del Pozzo, 2009). In October 2007 an intense runoff hit Tabasco; about 70% of the state was flooded and 850,000 inhabitants were affected with losses of 3 billion dollars (Perevochtchikova and Lezama de la Torre, 2010). On the other hand, large-magnitude earthquakes in bordering states such as Chiapas and Oaxaca have affected Tabasco. On September 8, 2017, an intraplate earthquake with normal fault occurred in the subducted Cocos slab in the SEM. Rupture initiated at a depth of 50 km is estimated to have broken the subducted lithosphere ~35 km (Melgar *et al*., 2018). This event had an epicentral distance 360 km and caused damage to infrastructure and two deaths, in Tabasco state (Figure 1.1). Although there is no evidence of moderate and large magnitude earthquakes with epicenter on the entity, those that occurred at regional distances have presented MMI up to VII (SSN, 2023).

Significant damage from large earthquakes has been evidenced in historical and recent seismic activity in SEM.

The losses of life, infrastructure damage, and socioeconomic consequences caused by natural phenomena such as earthquakes in SEM, show the importance of updating and developing some provisions to ensure that buildings can resist the seismic forces. The seismic hazard analysis allows evaluation of the intensity of ground shaking for a specific site. There are two methodologies to perform the evaluations, Probabilistic Seismic Hazard Assessment (PSHA) and Deterministic Seismic Hazard Assessment (DSHA).

PSHA is widely considered in seismology to help determine the risk that a seismic area is exposed. It can be understood as assessing the annual frequency of exceedance of the ground motion parameters (PGA, Peak Ground Acceleration, PGV, Peak Ground Velocity, Displacement, and Spectral Ordinates). Its history starts at the beginning of the 1960s with studies of earthquakes affecting buildings and ground motion, considering their magnitude, distance, and their relationship with the frequency of occurrence of the earthquakes and the frequency of occurrence of the ground motion in a site. An important concept was that the optimal design in the constructions/buildings/structures could be achieved considering the probability of the occurrence of a seismic event or the ground motion associated and the faults resulting in engineering (McGuire, 2008).

Knowing the data mentioned above for a specific site or region, the last step is performing an earthquake engineering analysis to ensure the structures/buildings can withstand ground shaking. It depends on future earthquakes' location, size, and shaking intensity. An important work that involves the link between a seismic hazard assessment and the aspects related to the ground motion characterization in a specific site, which may be seen as the last study point on a PSHA, was developed by Cabañas *et al.,* 1999. If all information cited is considered for studying an area, it means that a complete work in seismic hazard assessment has been done.

1.1.1 Seismotectonic in Southeastern Mexico

The Middle American Trench (MAT) is one of the more complex convergent margins of the Earth. Southern Mexico is located in this tectonically active region.

Along the MAT, there is the convergence zone where the Cocos plate is subducting underneath North American and Caribbean plates, creating an interesting geological structure in Southern Mexico (Figure 1.2).

Near the Tehuantepec Isthmus is the Tehuantepec Ridge (TR) a transformant fault that originated in the East Pacific Rise; the subduction zone near the TR has different characteristics than the rest of the Middle American Trench. In the proximity of the TR, the subducted Cocos plate drastically changes the subduction angle; to the east of Tehuantepec Isthmus, the subduction geometry is about 45° in Chiapas state and Guatemala (Franco *et al.,* 2012), and to the west, the plate subducts about 25° in Oaxaca and Guerrero states (Hayes *et al.,* 2018). In the zone of TR also there is a change in the convergence rate from 6.4 cm/yr to 7.2 cm/yr (DeMets *et al.*, 1994).

In SEM also there is a transforming boundary between the Caribbean and North American plates related to the Polochic-Motagua fault system (PMFS). The PMFS is a left lateral transform boundary that extends from Hispaniola Island to the Middle American Trench; the fault system is located in its onshore part in Guatemala. It is a seismically active region (White *et al*., 2004; Andreani *et al.,* 2008a; Guzmán Speziale, 2010).

SEM is located near the triple junction of the Cocos-North American-Caribbean plates. This is a not well understanding region, and its surface expression is unclear (*e.g.* Manea *et al*., 2013). Based on seismicity or seismic reflection and well data, some authors support that the NorthAmerica-Caribbean boundary extends to the Sierra de Chiapas, in Chiapas state (*e.g.* Andreani *et al.,* 2008b; Witt *et al.,* 2012). Guzmán Speziale *et al.,*1989 and Guzmán-Speziale and Meneses-Rocha, 2000, suggest that the joining of these three plates corresponds to a wide deformation zone that extends to the center of Chiapas, where the motion extinguished in the Strike-Slip Fault Province. Guzmán-Speziale and Meneses-Rocha (2000), mention that the Reverse Fault Province is part of the North America-Caribbean plate boundary. However, triple junction geometry is ambiguous and is yet under discussion.

On the other hand, all this tectonic activity in SEM is evidenced by seismicity. The study area has witnessed large earthquakes; some examples are mentioned as follows:

- March 28, 1787, M_w8.6, interplate earthquake.
- July 22, 1816, M7.7, Guatemala earthquake, occurred in Chixoy-Polochic fault.
- January 14, 1903, M_w7.2, Chiapas earthquake, intraplate.
- September 23, 1902, M7.8, Chiapas earthquake, intraplate.
- September 17, 2017, M_w 8.2, Chiapas earthquake, intraplate.

Far away from the tectonic boundaries, seismicity has been present:

- May 30, 1743, M7.4-8.2, Chiapas shallow earthquake.
- August 26, 1964, M_w 6.4, Veracruz earthquake, crustal.

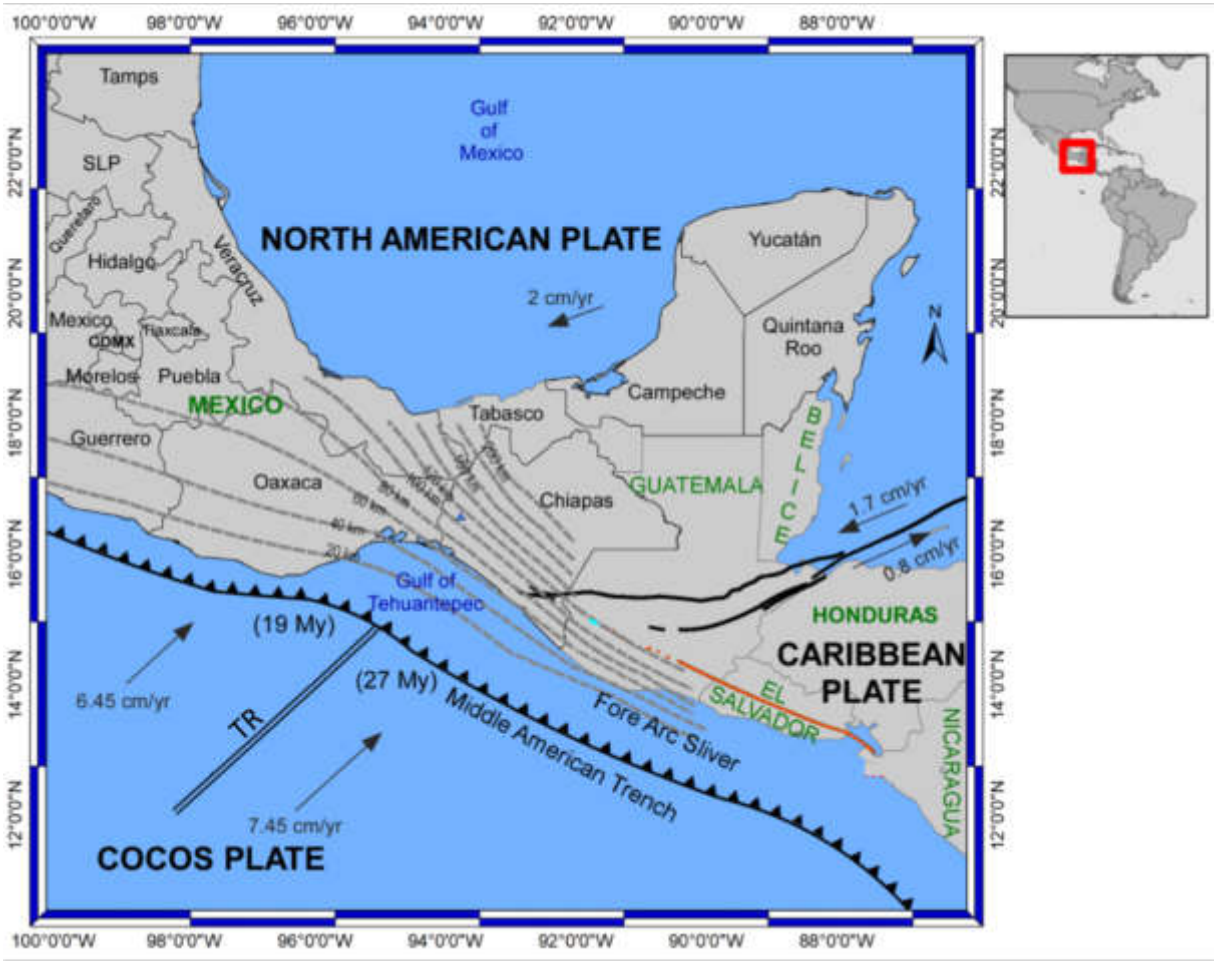

Figure 1.2. Tectonic setting in Southern Mexico. Continuous black lines represent the Polochic-Motagua tectonic boundary. Continuous line with black triangles depicts the convergent boundary between Cocos and North American plates. Gray lines show the depth of Cocos plate subducting North American plate (Hayes et al., 2018). Arrows are the velocities vector in the different plates (Authemayou et al, 2011, Calò, 2021). TR:Tehuantepec Ridge.

As shown, there is evidence of seismicity before the XX century in SEM. The April 19, 1902, occurred an earthquake with M_w7.8, in Guatemala; in September 23 of the same year, one earthquake with M_w7.4 took place with epicenter in Chiapas. Both events are classified as intraplate events within the Cocos Plate (Suárez, 2021). The earthquake of January 14, 1903, M_w7 is also considered as an intraplate event (Nishenko and Sing, 1987). Suárez (2021) argues that is an intraplate event and it may be interpreted as similar to the recent earthquake of September 8, 2017, with M_w8.2.

Conversely, the shallow seismicity in the North American and Caribbean plates is related to crustal deformation. In the PMFS, a shred of clear evidence is the February 4, 1976 earthquake *Ms*7.5 which ruptured ~230 km of the segment of Motagua fault (Plafker, 1976). Historically the earthquake of July 22, 1816, is related to the Polochic fault (White, 1985). In Chiapas state, there are Strike-slip and reverse provinces that are also seismically active. Guzmán-Speziale *et al.*, 1989, documented focal mechanisms with strike-slip solutions, which parallels strike-slip faults. Furthermore, some seismic catalogs have reported earthquakes related to some crustal faults in Chiapas state and Guatemala (*e.g.* Guzmán-Speziale 1989; Peraldo and Montero, 1999; White et al., 2004) in their seismic catalogs.

1.1.2 Seismological implications in Tabasco state

Tabasco state is lying ~300 km of distance from the convergent boundary of Cocos-North America and the transformant PMFS. Nevertheless, there is evidence of shallow and large events that have affected the region (Ambraseys and Adams, 1996; Suárez, 2021). The diversity of seismic sources gives as a result different effects in the attenuation of the seismic waves. There is evidence of historical crustal and subduction events (intraplate and interplate) that have shown damage to regional distance reaching Tabasco. As a matter of fact, an earthquake that occurred in 1652 generated great damage in Tabasco and Guatemala (García Acosta and Suárez Reynoso, 1996). Another one is the event of July 22, 1816 with *M*7.5-7.7 that took place in the Ixcan fault. initiating its rupture in the PMFS but spreading to Concordia fault, causing damage in San Cristobal de las Casas, Chiapas, and Tabasco. The September 23, 1902 *Mw*7.8 event was reported with similar damage to 1652 suggesting similar sources (White *et al*., 2004, Guzman-Speziale, 2010), demonstrating that Chiapas and Tabasco suffered the major effects even with an epicentral distance greater than 200 km (Böse 1903).

The earthquake of January 14, 1903, (M_w7.4) had epicenter in the Gulf of Tehuantepec but in some locations of Tabasco had MMI VI, which resulted in injuries in the entity (Cornú and Ponce, 1989; Suárez 2021). The earthquake of August 6, 1942, M_w7.7 also was described as felt with strong ground motion in Tabasco (Ambrasseys and Adams, 1996).

The mentioned events are some examples of earthquakes showing that large events with regional distances and coming from different settings tectonics can damage Tabasco's state.

Adding that Tabasco presents low to moderate seismicity, it becomes a challenge to figure out the effect that large and distant events may have on civil structures and small buildings, taking into account that the seismic design is not considered for the constructions and that the state is on a sedimentary basin.

1.2 History overview

The Probabilistic Seismic Hazard Assessment (PSHA) has been used worldwide to determine seismic design levels. It was with the collaboration of two researchers in the 1960s that the concept of PSHA was introduced (McGuire, 2008). The first studies covered earthquake ground motion, their dependence on magnitude and distance, and the relationship between the frequency of occurrence of earthquakes at a site. Afterward, the optimal design of buildings considering the mentioned parameters could be achieved by accounting for the probabilities of earthquake occurrence and the associated ground motions, and the resulting engineering failures. These concepts were well recognized and noticed that applying them for any site required a ground motion hazard curve (ground motion amplitude *vs* annual frequency of exceedance). It is known as a probabilistic seismic hazard.

The first information of seismic hazard for Mexico was published by Esteva, 1963, which was based on estimates of recurrence intervals of large magnitudes in seismic zones, attenuating the ground motion to estimate intensity in various zones, and equation of the ground motion return periods to the earthquake recurrence intervals. In 1970 (Esteva, 1970) published the first PGA and PGV map for Mexico for periods of 50, 100 and 500 years (Figure 1.3).

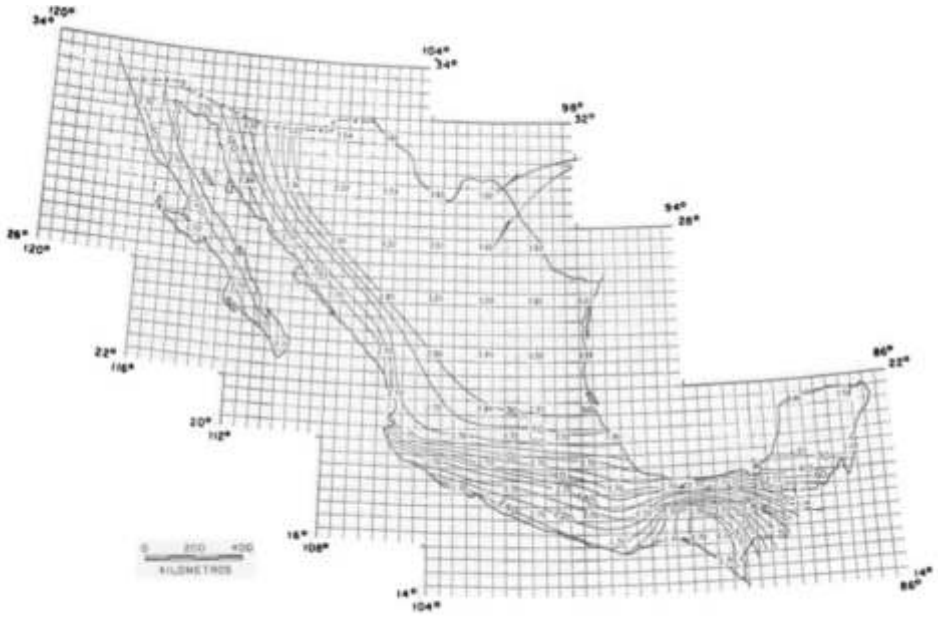

Figure 1.3 First seismic hazard map for Mexico. PGA for a return period (Tr) 500 años (Esteva, 1970).

The *Comisión Federal de Electricidad* (*CFE, Spanish acronym*) through the chapter MDOC (*Manual de Diseño de Obras Civiles, spanish acronym*) has been the base document presenting the seismic criteria design for Mexico, which means it has been the critical document to elaborate design norms and in municipals and states.

The institution shows seismic design criteria embodied in three versions: 1) 1993: This version gave recommendations to obtain seismic spectra designs based on seismic regionalization and considering many structure types. 2) 2008: The presentation was modified and conducing to continue seismic hazard with a probabilistic approach; in this version, new structural/buildings systems were added, and 3) 2015: It considers the acceleration parameter depending on a specific return period for rock sites (Figure 1.4).

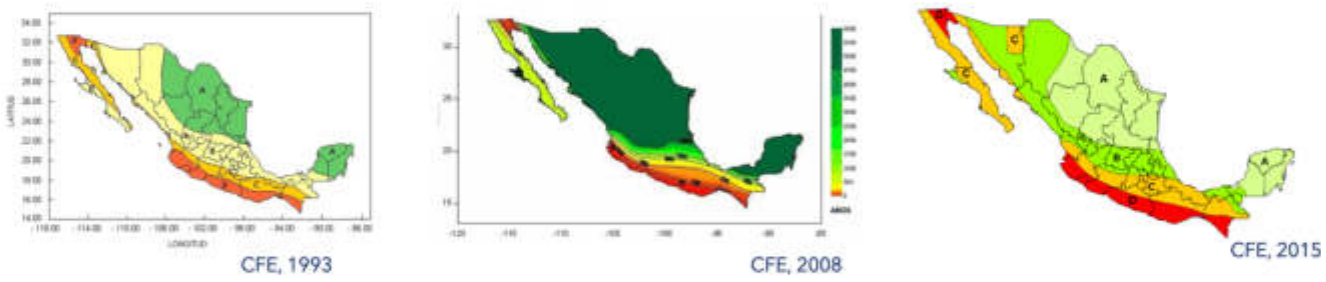

Figure 1.4. Evolution of the seismic zonation maps created by CFE (MDOC, 1993, 2008, and 2015)

A regional seismic hazard analysis aims to create maps expressing different levels of exceedance probability *vs* a ground motion intensity parameter; this kind of work is the first approximation to generating other studies induced by earthquakes as landslides and liquefaction. Determination of seismic hazards for an engineering application can be accomplished through deterministic and probabilistic perspectives. They are explained in the next section.

1.3 Methodology and methods used in previous works

Seismic hazard evaluation analyzes a ground motion parameter (PGA, PGV, and so on) expected in a specific area in a constant return period. There are two forms to evaluate the seismic hazard using a deterministic and probabilistic method. In a deterministic analysis, DSHA (Deterministic Seismic Hazard Analysis) is necessary to determine the expected maximum magnitude earthquake that may occur in the individual faults and the shortest source-to-site distance, then the worst scenario is determined. On the other hand, the PSHA estimates the probability that a particular ground-shaking intensity measure A is equal to or exceeds the ground-shaking level A_0.

The last method for seismic hazard estimations involves the effects of all the earthquakes that could affect a site or area. Thus, instead of only taking into account the maximum magnitude earthquake, all events having a magnitude within a chosen range are considered.

The probabilistic approach overcomes the deterministic one because it takes into account all magnitudes, all relevant hypocentral locations, not only the nearest one, and the uncertainties in the seismic analysis.

SEM lies in a tectonically active region. Consequently, a high level of seismicity is present; it is, therefore, better to consider all region events and integrate them over this area than choose only one representative event. For this reason, PSHA will be used to assess the seismic hazard in the region.

The methodology used in the PSHA is based on Cornell, 1968, it involves four steps (Figure 1.5)

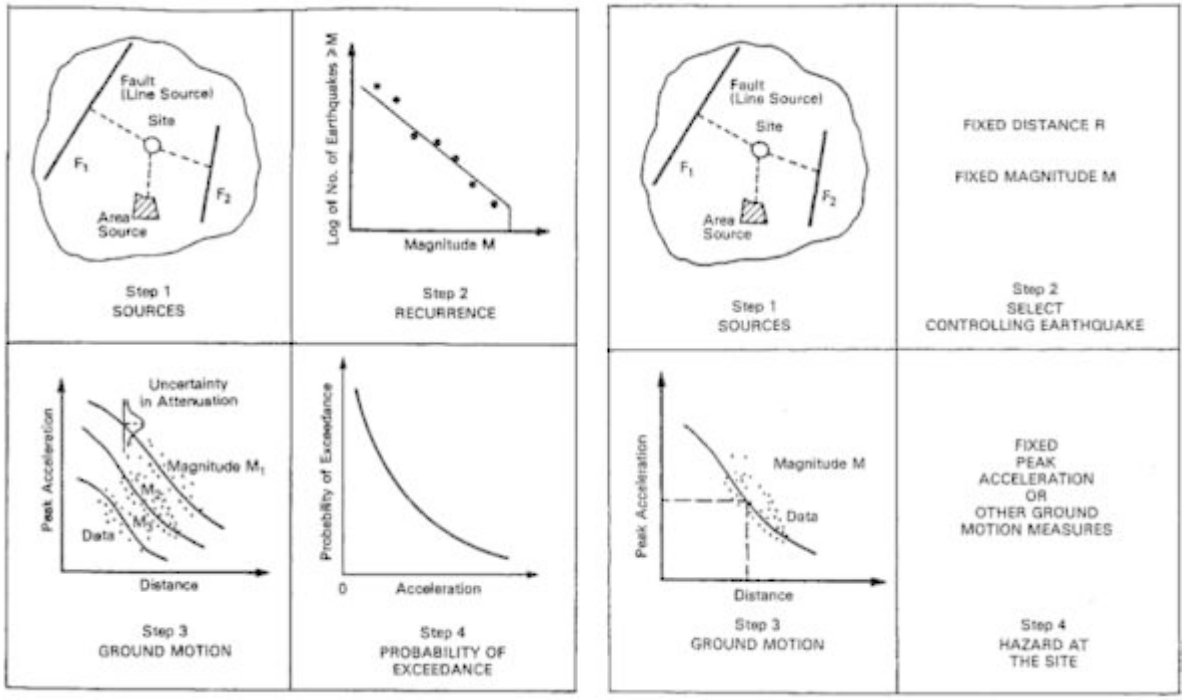

Figure 1.5. Right: Steps for assessing DSHA. Left: Basic steps for evaluating the PSHA. (Marmureanu et al., 2010)

I. The first step in a PSHA is to determine the seismic sources. This means that within the area delimited by a horizontal polygon, an assumption is made in the sense that the probability of occurrence of a given earthquake, of a given size, is constant throughout the entire source with a defined depth interval.

   The seismogenic source is defined by the seismicity, the geological features, the tectonic setting, and the geophysical information available.

Nevertheless, the deterministic method, in which the closest source-to-site distance is considered the probabilistic method, demand amalgamation of the entire source, taking into account a broad range of distances from all possible location in the source, because earthquakes are assumed may occur anywhere within the seismic source. The knowledge or judgment of the experts in the area shall help to a better estimation of the seismic source and its parameters.

II. The next step for a probabilistic evaluation is the ocurrrence relationship for each delimited source model. Each source needs a model for the rate of earthquakes exceeding a given magnitude. The classic Gutenberg-Richter relationship is shown by:

$$log_{10}N(M \geq m) = a - bm \qquad (1.1)$$

often seen as a linear trend in the frequency of earthquakes. It is representing the best fit through the data set of observations. In the equation, N is the number of earthquakes, related to the rate of events with magnitude $M \geq m$. The number of earthquakes described in log_{10} scale can be described by a-bm, where a is the intercept, it is the logarithm of the number of earthquakes of magnitude zero or greater expected to occur during the same time, b is the slope term indicating the relative frequency of large magnitude events versus small magnitude events. The G-R occurrence relationship has a negative exponential functional form, in which the occurrence rate decreases with increasing magnitude. It gives the probability that an event occurs anywhere of a certain magnitude within the bounds of the source area in a specific time period. Under this scope is important to use a complete dataset likewise inappropriate values will be found. For low seismicity regions where there is missing a dense seismic network, not all seismic events may be recorded and consequently, it is useful to choose a lower bound magnitude.

Not considering the lowest magnitudes than a minimum magnitude is allowed since small magnitudes events are tough to have a meaningless contribution to the seismic hazard. Nonetheless, the seismic parameters are estimated by these magnitudes.

A complete characterization of a potential seismic source is determining the upper boundary of the magnitude distribution, which means, better known as M_{max}.

For a deterministic approach, M_{max} is the only element to describe the seismic potential in a seismogenic source, thus, its obtention is a key element to the seismic design of civil structures. There are different denominations for the boundary mentioned, within the nuclear industry, the 'safe shutdown earthquake' is defined as the maximum earthquake potential for which certain structures, systems, and comprise important to safety, are designed to sustain and remain functional. For dam safety are 'Maximum credible earthquake' described as the largest earthquake magnitude that could occur along a recognized fault or within a particular seismotectonic province or source area under the current tectonic framework; and 'Maximum design earthquake' is the earthquake that produces the maximum level of ground motion for which a structure is to be designed or evaluated. Maximum earthquake magnitude for area sources is generally estimated from historical events, an advantage is that there are plenty of data, so this might be an appropriate estimation of the maximum magnitude.

Another point regarding in seismic hazard studies is that the acceptance of a Poisson model implies the assumption that the occurrence of earthquakes is random in time and space, and, that these are independent random events. This is valid when the catalog used contemplates all seismic sources, so if a Poissonian model is assumed is important that foreshocks and aftershocks be removed from the seismic catalog. Also is valid when the probabilities of occurrence are calculated for short time periods, typically those used for engineering works.

III. The third step in the determination of seismic hazard analysis is the estimation of the ground motion caused by an earthquake. The ground motion prediction equations (GMPE) or attenuation relationships are a basic component of a probabilistic study. If there are no relationships computed for the area under question, such relations are based on data from different regions but with a similar tectonic setting. Again, judge of the experts is needed to decide which curve is that best fit for the region of interest. The development of ground motion prediction equations is based on several statistical regression techniques available. Ground motion depends on source type, travel path, travel distance and local site conditions (*e.g.* Douglas 2003), it is defined in a standard shape as (Arroyo and Ordaz, 2010):

$$y(T) = \alpha_1(T) + \alpha_2(T)(M_w - 6) + \alpha_3(T)(M_w - 6)^2 + \alpha_4(T)\ln(R) + \alpha_5(T)R \qquad 1.2$$

Where $y(T)$ is the ground motion parameter to be estimated, α_1 to α_5, are the coefficients to be determined in the regression, M_w is the moment magnitude of the earthquakes, R is the closest distance of the rupture area. It gives as a result an attenuation curve in which the shape is dependent on the parameter before mentioned. So, a curve with respect to distance changes if some of these parameters are modified. Attenuation functions are in terms of peak ground acceleration (PGA). They are obtained from a statistical adjustment of maximum values recorded in the accelerographs, in function of magnitude and distance of different earthquakes.

From an engineering point of view, the more important components are horizontals since they are usually the most damaged.

Most of these relationships are preferably created to use moment magnitude M_0; however, others use, for example, surface waves M_S, even if there are conversions equations, which is often avoided because it increases uncertainties. GMPE's are usually made for a type of magnitude. Another parameter to take into consideration is the distance, R (Figure 1.6, Table 1)

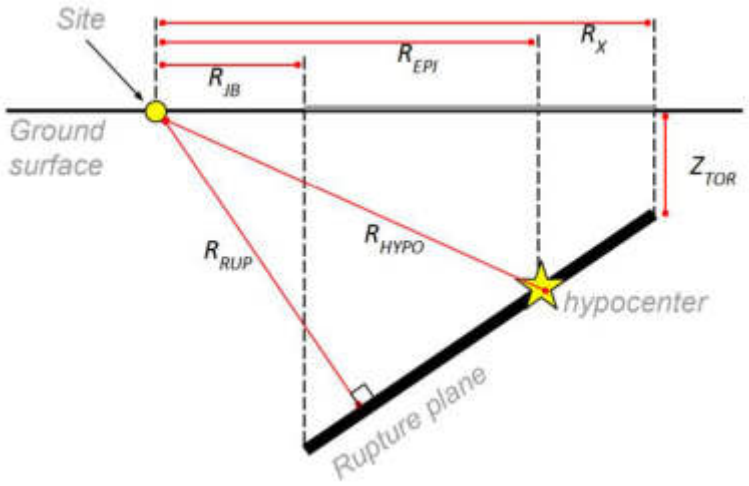

Figure 1.6. Types of distance measures used in different seismic hazard processing software. (e.g. R-Crisis, OpenQuake)

Table 1.1. Description of different distances used in seismic hazard analysis.

Distance definition	Symbol	Description
Epicentral	R_{EPI}	Distance between the epicenter and the site
Hypocentral	R_{HYPO}	Distance between the hypocenter and the site
Joyner and Boore	R_{JB}	Closest distance between the site and the surface projection of the rupture
Closest distance to the rupture	R_{RUP}	Closest distance between the site and the rupture surface
Horizontal top-edge distance	R_X	Horizontal distance between the site and the top-edge of the rupture
Horizontal off-end distance	R_{Y0}	Horizontal distance off the end of the rupture measured parallel to strike
Top of rupture depth	Z_{tor}	Depth to the top edge of the rupture

Most used distance measures are those from earthquake fault rupture or epicentral/hypocentral distance. They can be used in area sources since small earthquakes can be treated as point sources rather than fault planes, taking into account that for area sources no fault planes are defined.

An important issue to mention is for short source-to-site distances the selection of distance measure is an important parameter, while for large source-to-site distances the difference between these definitions is small. As an outcome, the selection of attenuation relationships might be consistent with the distance type chosen.

Aside from the mentioned parameters as magnitude and distance, the local site conditions can influence the ground motion. Different material types, amplify in different ways which have a greater effect near the receiver. Sites with low surface wave velocities and low density will experience higher amplitudes values in comparison to those with ones with the highest values. Site classes are often classified as hard rock, rock, very dense soil, stiff soil, soft soil, and soil needed from specific evaluation. Some of the GMPE involve the effects of the underlying material. Since changes in material properties cause reflection in the seismic waves, an outcoming is a change in the wave amplitude. Therefore, is important to make a distinction in the site class lying in the region of interest.

IV. The last step is to compute all the effects of all events, of all different sizes, which occurred anywhere in different sources, and probabilities of occurrence are united to estimate the seismic hazard given by:

$$E(z) = \sum_{i=1}^{N} \alpha_i \int_{m_0}^{m_u} \int_{r=0}^{r=\infty} f_i(m) g_i(r)\, P(Z > z|m,r) dr dm \qquad (1.3)$$

where E(z) is the expected number of exceedances of ground motion level z during a specific time period. Due to the summation over *i*, all sources are considered. α_i is the mean rate of occurrence of earthquakes of the considered magnitudes in the *i*-th source, $f_i(m)g_i(r)$ are the probability density distributions of magnitude, and distance between the various locations within source *i* and the site for which the hazard is being estimated. $P(Z > z|m,r)$ is the probability that an earthquake of magnitude *m* and distance *r* will exceed ground motion level *z*, which is determined from the GMPE. As a matter of fact, the integration is with respect to distance and magnitude to involve all locations in the source *i* and all earthquakes of magnitudes within the considered range.

1.4 Comparison between published seismic zones

In global framework studies by Ordaz *et al*., 2014, conducted a PSHA dividing into a set of seismogenic areas and assigning a predominant tectonic environment to obtain spectral acceleration with 5% damping. Recently, Silva *et al.,* 2020, conceived a seismic risk model, developing seismic hazard models and showing probability exceedance curves for specific return periods, among others, using a compilation of various countries. Nevertheless, they mention the importance of creating national or regional studies with more detailed and reliable information.

Mexico lies in a seismic active region where subduction zones, spreading centers, and strike-slip faults are present. Nowadays, different seismic source models have been developed around the country that may be used for assessing the seismic hazard (*e.g.* Zúñiga *et al*., 2017, Rodríguez Lomelí and García-Mayordomo, 2019, Sawires *et al*, 2021). In Central America which is one of the most active zones in the world some seismological zonation have been proposed (*e.g.* Benito *et al*., 2012, Alvarado *et al.,* 2017). All of them are based on their seismic catalog taken from a local and regional seismic database or other studies.

SEM region concentrates an important level of seismicity; this region has hosted large historical and recent earthquakes (*e.g.,* Peraldo and Montero, 1999; White *et al.,* 2004; Suárez, 2021). This is why evaluating seismic hazards becomes a challenge.

At the beginning of seismic zonation for seismic hazard assessment in SEM, data go back to the work of Zúñiga *et al*. (2017) with a first-order seismic regionalization for the whole country and defining *a* and *b*-values of Gutenberg-Richter relationship for the 18 regions proposed. Rodriguez-Lomelí and García-Mayordomo (2019) generated a new definition for a new seismic zonation model focusing on the Chiapas state. They proposed 17 seismic zones and obtained PSHA for 500, 1000, and 2500 return periods to 600, 700, and 950 cm/s^2 PGA values. Alamilla *et al*. (2021) generated a seismic zonation using an incomplete catalog for the Gulf of Mexico, providing that it must not be treated as a single zone but rather as a different approach. Recently, Sawires *et al.* (2021) prepared a seismic source model defined by 37 area sources from a detailed review of the main tectonic features and the seismicity of the subduction zone.

For Central America Benito *et al.* (2012), proposed regional seismic zonation encompassing the easternmost of Mexico. They developed a PSHA for 500, 1000, and 1500 years return periods. Alvarado *et al.* (2017), propose a model with 41 zones defined as active crustal, 10 zones for interface subduction, and 7 zones for inslab subduction covering the Central American area (Figure 1.7). One of the most recent works is from Garcia-Peláez *et al*. (2023) where the authors show a seismic source characterization discretized in 40 source zones. However, those studies are not focused on the effects of sedimentary basins as where Tabasco state is located, they point out the PSHA for regions tectonically active.

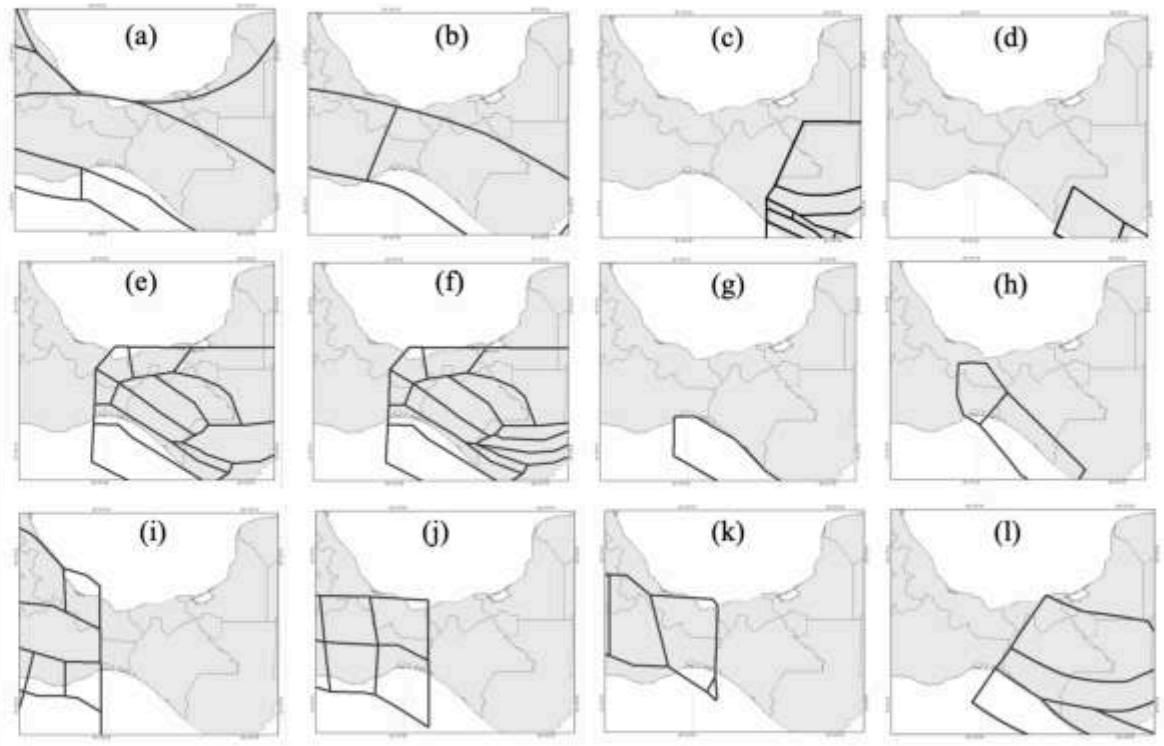

Figure 1.7. Shows the seismic zone models published by previous work for SEM and Caribbean. ***a*** *(shallow seismicity regions),* ***b*** *(intermediate depth) proposed by Zúñiga et al., 2017.* ***c*** *(crustal zones),* ***d*** *(inslab zones) proposed by Alvarado et al., 2017.* ***e*** *(crustal zones model A),* ***f*** *(crustal zones model B),* ***g*** *(interface zones),* ***h*** *(intraslab zones) proposed by Rodríguez-Lomelí and García-Mayordomo, 2019.* ***i*** *(shallow crustal sources),* ***j*** *(inslab intermediate depth),* ***k*** *(inslab deeper sources) proposed by Sawires et al., 2020.* ***l*** *(shallow source macrozonation) proposed by García-Peláez et al., 2023.*

Chapter II. Methodology

2.1 How to create seismic hazard maps?

As previously mentioned, PSHA considers the seismic potential of the seismic sources, the random nature of earthquake occurrence, the random nature of the ground motion produced by earthquakes, the damage potential of the ground motion, the characteristics of the soil in the site, and the epistemic uncertainties involved at different levels. All these elements should be studied individually to enhance the analysis, and the insights of experts in the area will play an important role in the evaluation. The following sections will provide detailed descriptions of each of these elements:

2.1.1 Seismotectonic information: tectonic boundaries

To initiate a seismic hazard assessment, the initial step involves identifying the tectonic setting, which necessitates a thorough reconnaissance of all critical tectonic features. A pivotal aspect of the seismic hazard evaluation entails the delineation of regions within the working zone where a uniform magnitude value can be established and the identification of primary faults. These faults should be modeled as seismogenic sources to assess the seismic hazard, specifically in the context of southern Mexico.

In order to achieve both objectives, a comprehensive methodology has been developed. This methodology commences with the subdivision of the study zone into areas exhibiting similar tectonic and/or morpho-structural characteristics. Within these designated zones, the geometric features of surface tectonics, the evidence of recent activity, and the seismotectonic interactions observed among secondary fault systems distributed throughout the interior, as well as the major faults situated along the periphery. Based on this information the following tasks are performed: estimation of the maximum possible magnitude in each zone, classification of the major faults based on their recent activity, estimation of the maximum magnitude associated with these major faults, and for faults displaying high levels of activity, determination of their temporal recurrence. This systematic approach facilitates a comprehensive assessment of seismic hazard in a region, specifically within the context of southern Mexico.

In the case of crustal zones, the area was subdivided into distinct crustal blocks each of which represent the variations in thickness and structure of the crust in southeastern Mexico. The major faults that limit the blocks were analyzed in each zone. Furthermore, the relationships between the occurrence of seismicity in depth and the crustal layers of each block were studied.

Ultimately, for the subdivision of the deep zones within the study area, the geometry of the Cocos slab in the subduction zone of the Middle American Trench was considered. Various models were taken into account (*e.g.* De Mets *et al.*, 1994; Hayes *et al.,* 2018) as a base for delineating the deep seismic zones. Finally, a preliminary model for defining seismogenic zones was established. This model is regarded as a regional model that incorporates the three potential seismic sources.

2.1.2 Crustal faults: Geological information:

In southeastern Mexico, earthquakes are not limited to subduction and transforming boundaries, they also occur within the North American and Caribbean plates. These events exhibit generally low magnitudes and occur at shallower depths. Many of them show a good correlation with the concentration of quaternary faults. Some crustal earthquakes are associated with continental geological faults. An example is the earthquake of May 30, 1743, with M7.4-8.2 that took place probably in the San Cristobal fault, in Chiapas state (Guzmán-Speziale and Menesses Rocha, 2000).

Recently, Cid Villegas *et al*., 2017, documented a set of active faults in Mexico, where they mention some with quaternary activity, notably the Concordia fault in southeastern Mexico. In a PSHA, it is crucial to identify all earthquake sources capable of generating damaging ground motions. These sources can include individual faults; it is important to bear in mind that if individual faults are not clear enough to recognize these earthquakes, sources can be described by areal regions, meaning earthquakes may occur anywhere inside the selected area. This approach ensures that all potential seismic sources are considered in the seismic hazard assessment.

2.1.3 Seismic catalog: pre-instrumental and instrumental data

To create a unified seismic catalog, three sources of seismic data were employed. Initially, data from the *Servicio Sismológico Nacional* (SSN, Spanish acronym), alongside international database as ISC (International Seismological Center) and CMT (Harvard Centroid Moment Tensor) were used for compilation and catalog development. Additionally, a comprehensive review of published catalogs was undertaken, given the significance of understanding the historical occurrence of high-intensity events.

2.1.3.1 Instrumental period

This work encompasses an area from -89 to -96 West longitude and 14 to 20 North latitude. In order to be able to study the occurrence and characteristics of seismicity in the definition of seismogenic zones, it is first necessary to subdivide the catalog into homogeneous time periods in terms of record completeness, magnitude value variability, and location accuracy. The definition of these periods must be carried out considering the local seismic network's progress and evolution over time and its impact on the data contained in the seismic catalog.

The seismic stations located in southern Mexico, started their operations in 1910, with two seismic stations in Oaxaca, Oaxaca state, and Mérida in the Yucatán state (Figure 2.1)

Figure 2.1. Firsts' two stations located in SE Mexico belonging to the SSN

In 1960, the installation of the first electromagnetic seismograph marked a significant development (SSN, 2023). This allowed for the monitoring of local seismic activity within the study area. However, it is essential to note that the limited coverage of the seismic network during that time did not enable reliable earthquake location and magnitude determination (Figure 2.2).

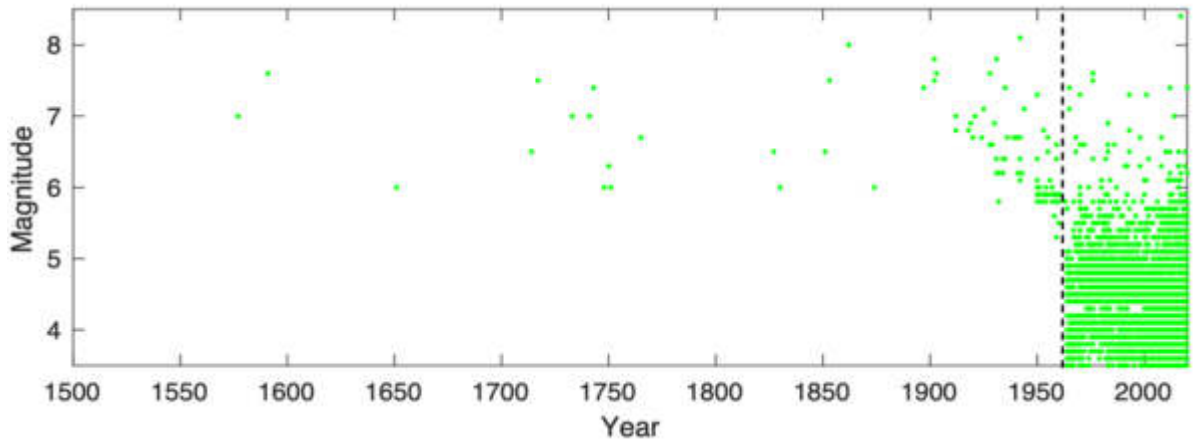

Figure 2.2. Evolution of the unified seismic catalog from 1577 to 2020 period of the catalog generated in this work. It represents the seismicity after the installation of the electromagnetic seismograph, the start of operations of the seismic station is marked by the dashed line.

2.1.3.2 Pre-instrumental period

In regions characterized by low deformation rates, the pre-instrumental or historical seismicity, in conjunction with instrumental data, plays a significant role in the seismic hazard assessment. The record of pre-instrumental information can be used to have an estimate about their earthquake sources often by assessing the impact of significant historical events and the ground shaking effects that may help to confirm the occurrence of past events. Sometimes they can help to know the geographic distribution of the intensity.

An exhaustive revision of pre-instrumental seismicity was made for southern Mexico and Guatemala. In order to know the pre-instrumental or historical seismicity affecting Southeastern Mexico, a wide area has been investigated for large earthquakes that occurred there. This period encompasses from 1533 to 1960 (Table 2.1), representing the time between the oldest information found and the time before the installation of the first seismic station.

The historical earthquakes were compiled from research performed by Kelher *et al.,* 1973; White, 1984; White, 1985; García Acosta and Suárez Reynoso, 1996; Guzmán-Speziale, 1989; Pacheco and Sykes, 1992; White and Harlow, 1993; Ambraseys and Adams 1996; Villagrán *et al.,* 1996; Montero *et al.,*1997; Rebollar *et al.,* 1999; Salgado *et al.,* 2004; White *et al*., 2004; Guzmán-Speziale, 2010; Sawires *et al*., 2019; Suárez, 2021;

those authors show some events that occurred in the states of Oaxaca and Chiapas in Mexico and as well as Guatemala, which had impacts over regional distances. Sawires *et al*., 2019 revealed some pre-instrumental earthquakes near the study area that have evidenced damage by distant earthquakes.

In this work, the composite earthquake catalog was obtained from different sources that might have repetitions of some events of the largest magnitudes. Every event was identified, and their duplicates were removed from the catalog based on location, time, and magnitude. The intensity of these kinds of events may be used to estimate both, their epicentral location and their specific magnitude. However, the geographic distribution of the historic epicenters provides good evidence of the earthquakes' seismic zones and can help to evaluate the rate of recurrence in some seismic areas.

2.1.1.1 Iso-seismals for pre-instrumental earthquakes,

Large and historical earthquakes that occurred in SEM and Guatemala have been associated with large geological structures, some examples are in Table 2.2. Prior to the establishment of the seismic instrumentation in Mexico, the intensities maps were employed to gain initial insights into the effects of earthquakes. Taking advantage of isoseismal maps in the study area, the evidence large events occurred before the installation of seismic stations, exhibits the regions where major damage may happen (Figure 2.3).

In order to show similarities in the effects of a pre-instrumental event and a recent one, with the purpose of having a better understanding of the seismic hazard assessment three events were chosen because their epicenter is almost identical; they are the events of March 22, 1928 (M_s7.5), August 23, 1965 (M_w7.5), and June 23, 2020,(M_w7.4) (Sing *et al.,* 2023).

Table 2.1. Compilation of pre-instrumental events for southeastern Mexico and Guatemala.

Year	Month	Day	Hour	Lat	Long	Mag	Int	De	Source
1577	11	29		14.92	-91.66	>7.0	VIII		White *et al.*, 2004; Montero *et al.*, 1997
1591	3	14		15.2	-92.5	7.2-7.6	VII		GHEA, García Acosta y Suarez Reynoso, 1996, Montero *et al*, 1997, Peraldo y Montero,1999
1651	2	18		14.51	-90.68	6	VII	x	Montero *et al*., 1997, Acosta y Suarez, 1999
1714	5	5		15.4	-92.1	5.5-6.5	x	x	White, 1984, Acosta y Suarez, 1999
1717	9	29		14.4	-91.08	7.5			Villagran, 1996
1717	10	24		14.9	-91.08	7.5			Villagran, 1996
1733	5			14.6	-90.08	7			White, 1984
1741	2	15		15.2	-90.7	6.5-7			White, 1984
1743	5	30		16.75	-92.75	7.4-8.2	VIII	33	White et al, 2004; Acosta y Suarez, 1999
1748	1	6		15.42	-90.42	6	VII		
1750	3	8		15.4	-91.4	6.3-6.7			White, 1984
1751	3	3		14.58	-90.75	6	VII		Montero *et al.,* 1997
1765	6	2		14.6	-89.5	6.7-7.2			White, 1984
1787	3	28		16	-97	8.6			Sawires *et al.,* 2019
1804				16.5	-92.66	6.8 ± 0.3	VII		White *et al.*, 2004
1816	7	22				7.5-7.7			White, 1984
1817	1	30				5.5-6.2			White, 1984
1827	9	1		14.33	-91.08	6.5	VIII		Montero *et al.,* 1997
1830	4	21		14.45	-90.53	6	VIII		Montero *et al.*, 1997
1853	2	9		14.75	-91.75	7.5	VII		Montero *et al.*, 1997
1851	5	17		15.08	-91.83	6.5	VIII		Montero *et al.,* 1997
1858	5	2							Rebollar *et al.,* 1999
1870	5	11							Rebollar *et al.,* 1999
1874	1	19					x	x	García Acosta y Suarez Reynoso, 1996
1874	8	3					x	x	García Acosta y Suarez Reynoso, 1996
1874	9	3		14.5	-90.83	6	VII		Montero *et al.,* 1997
1881	8	13					x	x	García Acosta y Suarez Reynoso, 1996
1887	8	1					x	x	García Acosta y Suarez Reynoso, 1996
1897	6	5		16.3	-95.4	7.4			Rebollar *et al.,* 1999, Salgado *et al*., 2004
1902	4	19	2:23:00	14.9	-91.5	7.5		25	SSN, Ambraseys y Adams, 1996, Abe y Noguchi, 1963
1902	9	23	20:18:00	16.58	-92.58	7.8	VIII		SSN, White et al, 2004. Pacheco y Sykes, 1992, Ambraseys y Adams, 1996, Rebollar *et al.,*
1903	1	14	1:47:36	15	-93	7.6			GHEA, Ambraseys y Adams, 1996, Salgado *et al.*, 2004, SSN
1908	3	26				7.5			Rebollar *et al.,* 1999
1910	9	23	3:32:00	16.77	-95.9	6.9		80	SSN
1911	8	27	10:59:18	17	-96	6.9		100	Sawires *et al.,* 2019
1912	12	9	8:32:00	15.5	-93	7.1			ISC, Salgado *et al.,* 2004
1914	3	30	8:32:00	17	92	7.5		100	Salgado *et al.,* 2004, Rebollar *et al.,* 1999, SSN
1916	6	2	7:59:24	17.5	-95	7		150	SSN
1917	12	29	22:50:20	14.5	-91.75	6.9		33	SSN
1919	4	17		14.8	-92.2	6.8		100	Rebollar *et al.,* 1999, Sawires *et al.,* 2019
1920	1	3	22:21:56	19.27	-96.97	6.4		10	SSN

1920	4	19	15:06:36	19	-97	6.7		110	SSN
1921	2	4	8:22:44	15.68	-91	7	VII	15	USGS, White *et al.,* 2004, Ambraseys y Adams, 1996, SSN
1925	12	10	14:14:25	15.5	-92.5	7		33	SSN, Salgado *et al.,* 2004
1927	5	9				7			Rebollar et al 1999
1928	4	17		17.71	-95.38	6.5	VII		USGS, Rebollar *et al.,* 1999
1928	3	22	4:14:03	16.23	-95.45	7.6			Kellher *et al.,* 1973, Rebollar *et al.,* 1999
1929	2	10		13.9	-91.2	6.7		Sh	Sawires *et al.,* 2019
1931	1	15	1:50:40	16.34	-96.87	7.8			SSN
1933	9	10		14.7	-92.7		VII		White *et al.,* 2004
1935	12	14	0:05:17	14.75	-92.5	7.3		33	SSN, USGS, Ambraseys y Adams, 1996, Rebollar *et al.,* 1999, Rebollar *et al.,* 1999
1937	5	28		17	-93	6.7		150	Sawires *et al.,* 2019
1937	7	25	21:47:13	18.45	-96.08	7.3		80	SSN
1939	12	5	8:30:07	15.33	-92.6	6.8		45	SSN, Sawires et al 2019
1940	7	27	13:32:30	14.25	-91.5	6.7		90	SSN
1941	2	11		15.11	-94.84	7		15	Rebollar et al 1999, USGS
1942	11	11	22:55:34	17.25	-94.25	6.7	VI	33	SSN, USGS
1942	8	6	23:36:29	14.8	91.3	7.7			SSN, Ambraseys y Adams, 1996, Kellher *et al.,* 1973
1943	6	15		14.6	-93	7.2			Rebollar *et al.,* 1999
1943	8	31		15.22	-92.03	6.9		80	Sawires *et al.,* 2019
1943	9	23	16:10:40	15.5	-92.18	6.9		110	SSN
1944	6	28	7:58:44	15	-92.5	7.1		25	SSN, Salgado *et al.,* 2004, Rebollar et al 1999, Ambraseys y Adams 1996, USGS, Sawires *et*
1945	10	27		14.15	-93.38	6.9		100	Sawires *et al.,* 2019
1946	6	15		15.5	-96.7	7.2		0	Sawires *et al.,* 2019
1946	7	11		17.23	-94.61	7.4		70	Rebollar *et al.,* 1999
1946	6	7	4:13:20	16.85	-95.03	7.1		70	SSN, Sawires *et al.,* 2019
1948	8	11	4:36:19	17.75	-95.25	6.9		100	SSN
1949	12	22		15.9	-93	7			Rebollar *et al.,* 1999
1950	10	23	16:13:20	14.3	-91.8	7.2		33	SSN, Kellher *et al.,* 1973, Rebollar *et al.,* 1999
1951	12	11	1:37:34	14	-94.5	7		100	SSN
1953	8	24		14.53	-92.32	6.9		96	Sawires *et al.,* 2019
1953	11	17	13:29:51	13.63	92.16	7.1			Kellher *et al.,* 1973
1954	11	25		15.27	-94.05	5.8		25	USGS
1954	2	5						shal	Guzmán-Speziale y Menesses Rocha, 2000
1955	9	25		15.5	-92.5	6.9			SSN, Rebollar *et al.,* 1999, Salgado *et al.,* 2004
1956	11	9		17.45	-94.08	6.3			Salgado *et al.,* 2004
1957	3	21		14.23	-92.86	6		25	USGS
1957	6	22		16.25	-93.52	6.7		150	Sawires *et al.,* 2019
1959	2	20		15.56	-95	6.5			White and Harlow, 1993
1959	4	28		14.54	-92.31	6.5	VII	25	USGS
1959	8	26	2:25:31	18.22	-94.41	6.4	VI	21	USGS, SSN, Singh *et al.,* 2014
1959	5	24		17.72	-97.15	6.8		80	SSN, Salgado *et al.,* 2004
1959	8	29	8:25	18.26	-94.43	6.4		21	Suarez, 2000

It can be seen that the intensities distribution reported by the 2020 event and the isoseismal of the 1928 event are similar (Figure 2.4). In the case of March 22, 1928 earthquake, that occurred in Oaxaca, the event was reported as strongly felt in Villahermosa. Near the epicenter, a tsunami and underground noises were described (Cornú and Ponce, 1989).

The June 23, 2020, M_w7.4, is a shallow depth event (22.8 km) in the interface region with a thrust fault mechanism. The effects of the event were coastal subsidence, liquefaction, landslides, and tsunami (Velázquez-Bucio *et al.,* 2023) near the epicenter which was expected by large events and moderate intensity. In Tabasco state even with a regional distance (circa 380 km) had intensities up to V.

Table 2.2. Major events felt in Tabasco state and associated with geological structures (events are shown in Figure 2.3)

Date	**Magnitude**	**Associated to**
14/03/1591	M=7.2-7.6	Concordia fault (García Acosta y Suarez Reynoso, 1999; Montero *et al*., 1997; Guzmán-Speziale, 2010)
28/03/1787	Mw 8.6	Rupture mode of interplate earthquake (Suarez and Albini, 2009) Broke 450 km long
22/07/1816	M7.7	Ixcán Fault (Guzmán-Speziale, 2010)
23/09/1902	Mw=7.8	Intraplate in Chiapas (Pacheco and Sykes, 1992; Suárez, 2021)
14/01/1903	Mw=7.4	Subduction earthquake, Tehuantepec Isthmus, (Suárez, 2021)
04/02/1976	Mw=7.5	Motagua fault (Plafker, 1976; Kanamori and Stewart, 1978; Porfido *et al*., 2014). Ruptured 230 km long
08/09/2017	Mw=8.2	Intraplate in Cocos (SSN, 2023; Ramírez-Herrera *et al*., 2018; Suárez *et al*., 2019; Godínez *et al*., 2019). Ruptured 250 km longitude

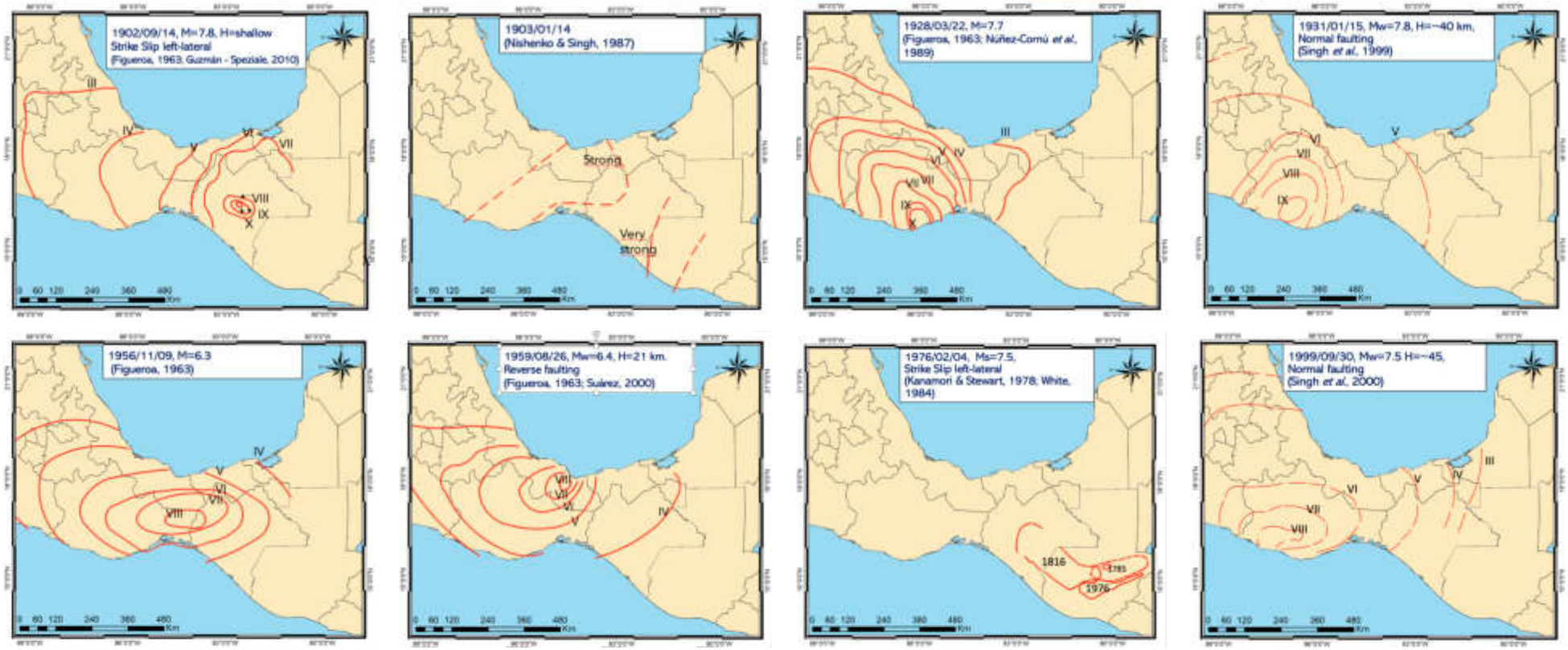

Figure 2.3. Isoseismal maps for pre-instrumental events that occurred in southern Mexico. Red lines are the intensity values.

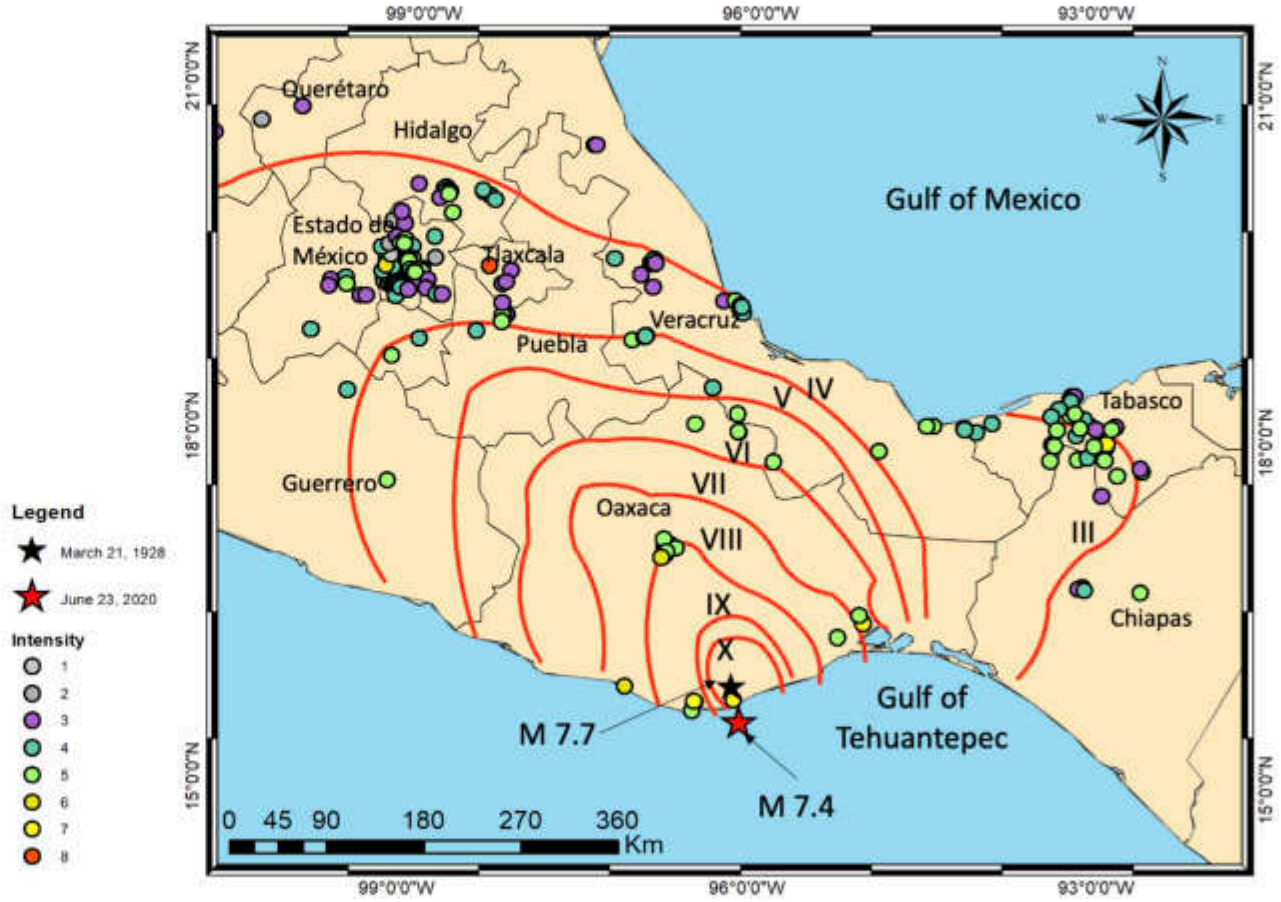

Figure 2.4 Comparison of intensities for one pre-instrumental earthquake (March 22, 1928, M7.7) and an instrumental event (June 23, 2020, M_w7.4).

2.1.2 Focal mechanism solutions

The focal mechanism solutions are another important and essential input in seismic hazard studies. They illustrate the relationship between earthquakes and known faults, the local and global stress field, and their relationships with other possible faults that are unknown. In this work, the definition of the seismic source zone is also based on focal solutions compiled from the Global Catalog of CMT Harvard (Ekström *et al*., 2012), the Moment Tensor Catalog for Mexican Earthquakes, and specific publications like Suárez *et al*., 2000; Guzmán-Speziale 2010; Franco *et al.,* 2012; Sawires *et al*., 2019, and so on.

It is important to keep in mind that, at times, it is advisable to select some representative focal mechanism for each seismogenic zone where the database is complete, which means when a considerable amount of focal mechanism solutions is (*e.g.* Hussaini *et al.,* 2022).

In this study, I collected over 400 focal mechanisms solutions, considering all of them, but assigned the predominant solutions for each seismic zone. These solitions are associated with magnitudes greater than or equal to M_w4.0 and depths up to 180 km, spanning the period from 1959 to 2020.

2.2 Seismic sources zone definition

2.2.1 Identification of seismogenic sources

A seismic source zone can be defined as an area where seismic activity is frequent, and it is typically associated with the coherence between seismicity and the underlying tectonic and geological structures.

The definition of polygons representing seismic source zones is based on the aforementioned data, geological and seismotectonic information available, geophysical data, and seismological characteristics. The seismic classification corresponds with the relationship between the occurrence of seismic events and the location of the tectonic structures. In this context, two seismogenic sources can be defined. Firstly, there is the seismic zones determined by the distribution of the epicenters, and secondly is the active fault. Within this framework, the extremes or boundaries can be defined as the seismotectonic zones.

In the first seismogenic source, the definition of an active fault is linked to the considered criterium depending on the recent deposits, the evidence through the length of the fault, and if there are well-located epicenters with surficial trace or deep structures. In that way, the active faults can be defined in the function of the correlation level of the last parameters mentioned.

An active fault can be classified under different scope:

a) Geological: active faults can be classified from a geological perspective based on their slip rate. For active faults, estimating a representative slip rate for the last 10,000 years is typically enough. In cases of low to moderate seismic activity, estimations might need to extend back up to the last million years (Quaternary time), which can introduce higher uncertainties. The Research Group for Active Faults (1991) categorizes fault activity into three groups: A) faults with slip rates higher than 1 mm/yr, B) faults with slip rates between 1 and 0.1 mm/yr, and C) faults with slip rates less than 0.1 mm/yr. Cid Villegas et al., 2017, presented a classification for Mexican faults based on their geometry, sense of movement and the last known displacement. They mention fault types: A) faults with displacement in Holocene time, B) faults with movement in Pliocene with potential displacement in Holocene, and C) those with displacement in Pleistocene (Table 2.2).

b) Engineering: In the field of engineering, the classification of a fault is typically based on the age of the most recent deposits that it has affected. This classification aims to identify faults with the highest potential of causing new movements within a relatively short timeframe, specifically during the expected lifespan of the structure in question. The California Division of Mines and Geology characterize faults as active if they have experienced displacements in the last 10,000 years, placing them within the which means in Holocene period. time are considered active.

Table 2.2. Comparison between some different active fault classification.

Research Group of Active Faults	**California Division of Mines and Geology**	**Cid Villegas *et al.*, 2017**
A slip rate ≥ 1mm/yr	Holocene	A displacement Holocene
B 0.1 ≥ slip rate ≥ 1mm/yr		B Pliocene and Holocene
C 0.1 mm/yr ≥ slip rate		C Pleistocene

The slip rate of faults serves as an initial indicator for estimating both the potential maximum of the earthquakes that the fault can generate (Figure 2.4), as well as the average time of their recurrence. In general, it is a commonly held belief that faults with higher slip rates are more likely to generate earthquakes more frequently.

Conversely, faults with lower slip rates are less prone to produce earthquakes, but when they do, the events tend to be more substantial, though they occur less frequently.

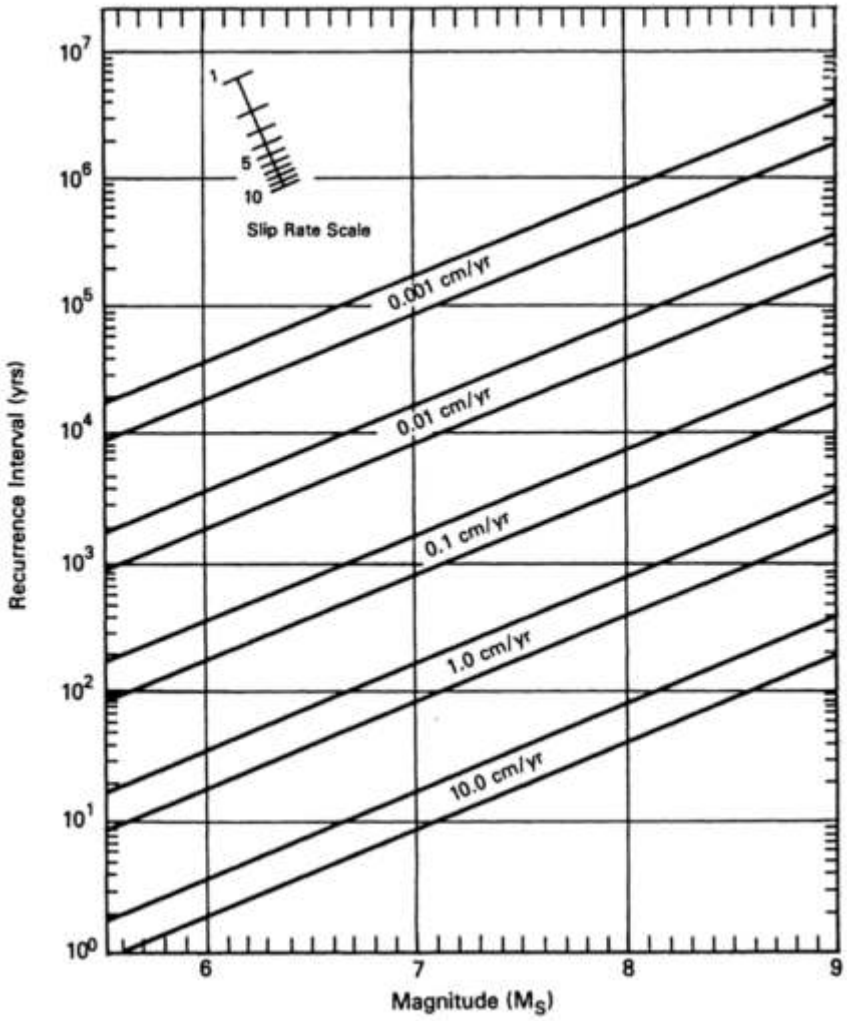

Figure 2.4. Relationship between slip rate and maximum magnitude (Reiter, 1990).

Identifying active faults lies is of paramount importance because it is on these faults that major earthquakes are most likely to occur. In regions within continents, like SEM, faults tend to exhibit a low to moderate slip rate. Consequently, it becomes challenging to discern surface evidence of active faults in such areas.

The identification of surface faults depends on the interplay between the fault's slip rate and the speed at which the landscape is modified, a process influenced by climate (Scott *et al.,* 2023). In regions such as Tabasco, Chiapas, the south part of Veracruz, and Campeche, where rainfalls levels exceed those in other parts of the country, particularly Tabasco which has experienced severe floods in recent decades. Another important issue is the consideration of faults that do not break on the surface. It is a problematic situation, and it is necessary the application of geophysical prospecting techniques.

Lastly, seismotectonic zones are typically characterized as seismic regions where varipus criteria encompassing seismotectonic, geological and geophysical have been taken into account. Consequently, the term 'seismogenetic zones' includes both terms and, it is more used in seismic hazard analysis. The location, size, and geometry of these zones are strongly conditioned by the quantity and quality of the seismic and tectonic information available. Therefore, its final definition will be subject to the analyst's expert criteria. The definition of seismogenic zones constitutes one of the main sources of uncertainty in seismic hazard analysis.

2.3 Seismic source characterization

2.3.1 Recurrence parameters

In each seismic zone, the probability of a specific magnitude value occurring relies on two keys factos: the value of parameter beta (β) and the annual rate of earthquakes occurrence. These two parameters, along with the upper limit of the magnitude distribution, collectively define the seismic potential of a seismogenic source. It is important to consider the uncertainties associated with these parameters. The determination of beta and the annual rate depends on the criteria used in the seismic source definition and the time period that is representative of the recorded magnitudes.

2.4 Seismic waves behavior: GMPE's

Ground motion prediction equations (GMPE) describe the relationship between a ground motion parameter (i.e. PGA, PGV, PSA at different periods, or MMI), earthquake magnitude, source-to-site distance, and uncertainty. Nowadays, there are numerous attenuation functions in the literature generated through different methodologies and data from different regions around the world (*cf.* Douglas, 2021). GMPEs are crucial for engineering seismology and earthquake engineering (*e.g.* civil engineering), and they are used for assessing seismic hazards. They provide estimates of the loading that a structure may be exposed to during a future earthquake.

The characterization of the GMPE from the engineering point of view is made from its three fundamental properties: amplitude, frequency content, and duration. All of them are calculated from the information recorded in the accelerograph stations, which, after noise filtering and correction, makes it possible to obtain the accelerogram, the temporal record in terms of acceleration experienced by the ground. In seismic hazard studies, the most commonly used attenuation function is in terms of peak acceleration. These functions are obtained from the statistical adjustment of the maximum acceleration values that were recorded in a number of accelerographs as a function of the distance and magnitudes of different earthquakes.

2.4.1 Selection of GMPE

Choosing GMPE to use in a seismic hazard analysis is a key decision that will determine the results in a very important way. The attenuation function is the element that exerts the most influence on the results of a seismic hazard analysis. In low-seismicity regions or areas with no representative data for large-magnitude earthquakes, the attenuation functions obtained in other regions are usually adopted, as is the case of the Gulf Plain Coast in SEM. In addition, there are not numerous accelerographic stations that allow for performing GMPE.

On the other hand, data recorded by the accelerographic stations of the II-UNAM (*Instituto de Ingeniería-Universidad Nacional Autónoma de México*) have permitted to obtain some functions, however, due to the scarce seismic stations and the lack of a large amount of large earthquake recorded these relationships give very limited representativeness.

The limitation of these equations is the magnitude and distance among others, as a consequence, is important to consider that attenuation functions not only present a statistical uncertainty comparable to the attenuation functions of ground motion parameters but also carry the added uncertainty inherent in the estimation of the intensity value, especially with the pre-instrumental earthquakes. In addition, the transformation of intensities to engineering seismic parameters through empirical relationships presents the added problem of the strong variability that these relationships present both in relation to the adjustment data and among those obtained by other authors.

2.5 Geophysical information incorporation

In some seismic Hazard studies, a variety of geophysical methods data could be used depending on the availability of the data. Its information can provide evidence or estimations about geological structures in depth. The most common and appropriate for regional interpretations are geomagnetic and gravimetric anomalies. They allow the application of specialized transformations to improve the correlation between the anomalies observed, the geological structure, and the seismological data.

2.6 Uncertainties

The PSHA process, along with the development of its input parameters, accommodates a broad spectrum of interpretations and uncertainties. This probabilistic method addresses the inherent and irreducible variability within the system responsible for generating ground-shaking intensity, treating it as aleatory variability.

One way to represent the aleatory variability is by specifying the standard deviation of a mean ground motion attenuation relationship.

According to Marzocchi *et al.* (2015), uncertainties can be classified into two groups:

1) Aleatory variability: it is employed to characterize the intrinsic and irreducible fluctuations present in the process that generates ground shaking intensity.
2) Epistemological or Inherent: this is associated with the natural variability that exists in any natural process or, with the proximity between the adopted physical model and the observed reality. The reduction of natural uncertainty can only take place with the development of new physical models that better reproduce the phenomenon studied.

The two types of uncertainties are interrelated since the elaboration of a physical model is based on the body observation available on the phenomenon, and in the same way, obtaining new observations is guided by the interest in validating or improving the model.

The epistemic uncertainties are tied to our constrained understanding of the system, encompassing all that can be diminished. In this way, the aleatory variability is the long-term frequency of exceedance for a specific site (*e.g.* the true hazard) while epistemic uncertainty arises from the lack of knowledge regarding what precisely constitutes true hazard.

PSHA calculations include epistemic uncertainties explicitly including alternative hypotheses and models. It can be considered through the evaluation of various individual seismotectonic models or through the formulation of a logic tree that includes multiple alternative hypotheses in a single model.

The logic tree is an integral part of the probabilistic method, it dissects the PSHA into basic components embedded in a hierarchical framework. Its nodes are a logical progression of potential sources of epistemic uncertainties. While their branches represent the possible alternative describing the uncertainty at each node. The final branches depict the complete epistemic uncertainties of the method and they are combined using the probabilistic structures of the classic logic tree.

The attenuation function also presents a significantly associated uncertainty, especially in relation to determining the influence exerted by the phenomenon of seismic site effect in its adequate consideration in the statistical adjustment. In a region with few accelerometric records, as is the case for southeastern Mexico the problem lies in the choice of the attenuation function to be used in the hazard study.

The consecutive application of expert judgment in each of the elements of a seismic hazard analysis allows finally obtaining a probability distribution of the hazard results.

The construction of a Logical Tree starts from the consideration, in each element of the seismic hazard analysis, of the different possible alternatives. In this way, for example, the use of one or other attenuation functions, one value or another one of maximum magnitude, etc., can be considered as alternatives. This technique then makes it possible to effectively organize the sources of uncertainties that will ultimately affect the result obtained and to study its sensitivity in relation to the options considered.

2.7 Results

The results generated through classical PSHA can be categorized into three primary types: hazard curves, hazard maps, and uniform hazard spectra. The most common way of expressing the outcomes of a probabilistic seismic hazard assessment is in a seismic hazard curve. It illustrates the relationship between a ground motion parameter and its exceedance probability.

2.7.1 Hazard curves

The outcome of a probabilistic seismic hazard analysis is a hazard curve, depicting the annual frequency of exceedance *vs* ground motion amplitude. Hazard curves serve as a valuable tool for comprehending how the probability changes, when observing various intensity measure levels and focusing on single sites.

2.7.2 A hazard map

It is a useful tool for understanding the geospatial variation of seismic hazard throughout the region of interest. The hazard curves, acquired for all sites, contribute to the creation of hazard maps. Such a map illustrates the variation of a ground motion parameter (*e.g.* PGA, PGV, SA for a specific period) across the mapped region at a fixed probability of exceedance during an investigation period (e.g. 10%, 5%, or 2% of probability of exceedance in 50 years, Figure 2.5).

In large areas where a seismic hazard has been assessed, it is often depicted through isoline maps representing the value of the parameter for a constant exceedance probability.

The results can be expressed in two ways. The first depends on the exceedance of probability level, which means, risk level as a function of the return period (Table 2.3), and the second depends on ground motion parameters (acceleration, velocity, displacement, spectral ordinates).

The PSHA is often computed in terms of the annual rate of exceedance (annual frequency of exceedance) or probabilities of exceedance for a given time period, which is represented by (*e.g.* Baker, 2008):

$$p(t) = 1 - e^{-\lambda t} \qquad [0 \leq p \leq 1] \tag{2.1}$$

where p(t) is the probability for a given time t and λ is the rate of occurrence of the events.

$$T_R = \frac{1}{\lambda_a} \tag{2.2}$$

T_R is the return period, λa represents the annual probability of exceedance.

The seismic hazard assessment results in this work will be presented through maps corresponding to return periods of 95, 238, 475, 950, 1950, 2475, 4950, and 9950. These maps will analyze different seismic models encompassing in a broad spectrum of possibilities used in the engineering approach. The chosen model, selected to represent the best estimation will be justified.

This type of model will be employed for comparisons with those published by other authors, and in which response spectrum of uniform hazard spectrum will be calculated to compare with seismic criteria proposed for the SEM.

Table 2.3. Typical values used in terms of exceedance probability.

T_R	Exceedance probability	*t* (years)
72	50%	50
95	10 %	10
238	10 %	25
475	10 %	50
950	10 %	100
1950	5 %	100
2475	2 %	50
4950	2 %	100
9950	1 %	100

The commonly adopted return period for the lifetime of a building of 72 years, considering frequent and small earthquakes (*e.g.* Isik and Harirchain, 2022). It corresponds to an exceedance probability of 50% in a time of 50 years. The 475 years return period is often used as a degree of conservativeness, including large events employed for building codes to establish the minimum requirements for seismic design criteria. It is equivalent to a chance probability of 10% in 50 years. For conventional structures, such as hospitals, schools, and so on, is common to consider the same exceedance probability but for 100 years timeframe.

Return periods of 1950, 4950, and 9950 years are assigned to critical seismic design structures, indicating that a malfunction might lead to catastrophic economic and environmental consequences. For these structures, assuming a functional life of buildings of 100 years, the corresponding return period is associated with exceedance probabilities of 5%, 2%, and 1%. Functional life is defined as the time duration from initial use to until the structure is deemed as irreparable or collapses due to hazard-related damage.

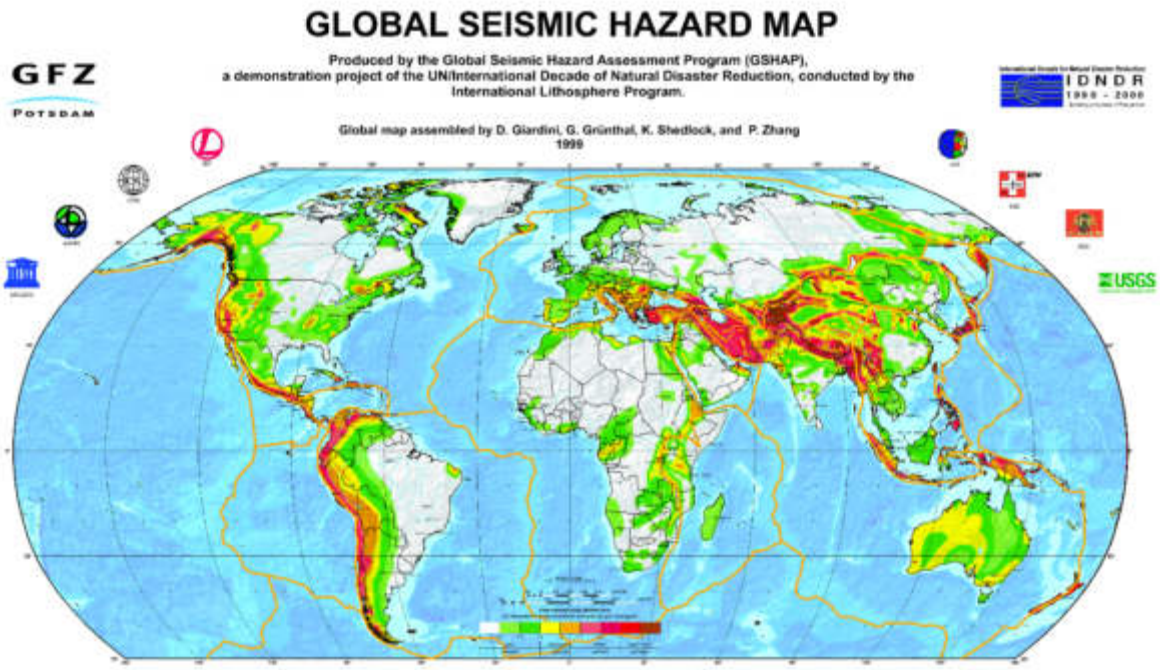

Figure 2.5. Global Seismic Hazard map showing the distribution of PGA of 10% chance of exceedance to be exceeded in 50 years. The return period of 475 years. (GSHAP)

2.7.3 Uniform Hazard Spectra

A UHS (Uniform Hazard Spectra) is the combination of different periods of hazard curves into a uniform hazard spectrum, which shows, for a certain probability value, the shaking intensity expected on buildings with different resonant periods. UHS corresponds to a probability of exceedance for a specific interest period (Figure 2.6).

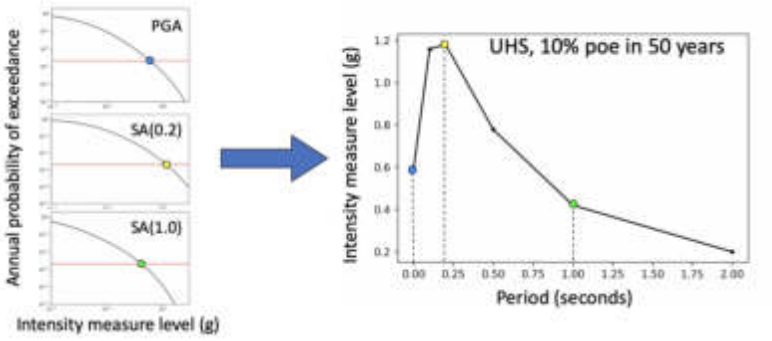

Figure 2.6. Example of a UHS. Left: hazard curve for different periods. Right: UHS shows the same periods.

2.8 Building a seismic hazard map

Modeling a seismic source can be made as points, lines, areas, rectangular faults, slabs, grids, and ruptures, depending on the identified seismic source and the software employed (Figure 2.7). The significance of the spatially modeling seismogenic sources lies in the control exerted by their geometry in the probabilistic analysis of the random variable distance-to-site. This is due to the consideration of earthquakes occurring in the entire area or line that the zone occupies as equiprobable events. In deterministic analysis, the problem is simplified to the maximum, considering only the shortest distance, which means, the most unfavorable location.

The construction of seismic maps needs a software code to represent the ground motion parameters visually. Platforms have been developed for this aim. Due to the importance of its results, seismic hazard calculations have led to the creation of numerous software allowing this kind of calculation.

Seismogenic zones can be modeled as areas in a three-dimensional calculation, it is when the source deep is taken into consideration.

Based on Cornell-McGuire methodology, currently exist some programs to compute the probabilistic seismic hazard. Among them are EQRISK, R-CRISIS, SEISRISK I, II, III, EQRAM, etc. Three of the most popular are explained as follows:

2.8.1 SEISRISK

SEISRISK I (Algermisen *et al.,* 1976), SEISRISK II (Bender and Perkins, 1982)., and SEISRISK III (Bender and Perkins, 1987) are computer programs for seismic hazard analysis. The programs allow the modeling of the seismic zones first as lines and in the latest versions as areas (or volumes).

Concerning the source geometry, the most substantial seismic hazard gradients, and the distance, and in order to produce more smoothed results, the SEISRISK III program, for example, allows incorporating variations in the limits of seismogenic zones into the calculation, considering that the uncertainty in its layout follows a normal distribution with a particular standard deviation. One disadvantage is that if some modification in the input parameters is needed, it must be made in the program code.

2.8.2 EQRISK

The first code to compute PSHA was released by, EQRISK (McGuire, 1976), they model seismogenic zones as quadrangular areas. EQRISK computes seismic hazard in terms of exceedance probabilities versus earthquake intensity measures, such as peak ground acceleration. The program allows the use of the results for a given site for up to eight different return periods. Even if there are many advantages, such as computing the seismic hazard over a grid, some are missing, such as it has a fixed attenuation model and another one is that only computes a single structural period for which is needed to run the program many times if the aim is to work on it.

2.8.3 R-Crisis

R-Crisis is a program to perform probabilistic seismic hazard analysis, which works with exceedance probabilities. It was developed by Ordaz 1991, and is based on the approach proposed by Esteva, 1967 and Cornell, 1968. R-Crisis requires as input a set of seismic sources, frequency-magnitude distributions, to evaluate the chance probability of the intensity values of interest given that an earthquake of known magnitude an occurrence probability has occurred.

2.8.4 Seismic hazard software justification

The similarities between the three programs are that they are freely available, and they compute seismic hazard in a probability way. However, the main difference between the three presented software lies in the geometric characterization of the seismic sources (Figure 2.7). A significant variant in R-Crisis program concerning the other ones is that it is a helpful tool to compute a complete PSHA within an entire approach. Its strategy lies in that the program considers earthquake recurrence parameters and allows using the ground motion prediction equations. They are visible in each area, allowing a better and quicker understanding by the user.

In R-Crisis, the seismic hazard map and UHS are the program's results. They are computed in a complete zone through a grid of sites and not through a single site. However, they are obtained for each site in terms of probabilities of exceeding but also in non-exceeding probabilities. It means that the annual probability of exceedance can be obtained for a given site.

In the study area, there is not a detailed seismic hazard assessment; some have been carried out in neighborhood places; however, with all the seismic parameters incorporated in R-Crisis software, such as a complete catalog, updated recurrence parameters, and GMPE, the software will allow good modeling in a regional zone such as southern Mexico, allowing to know different seismic hazard parameters in a specific site through a regional map. It is because it will be used in this work.

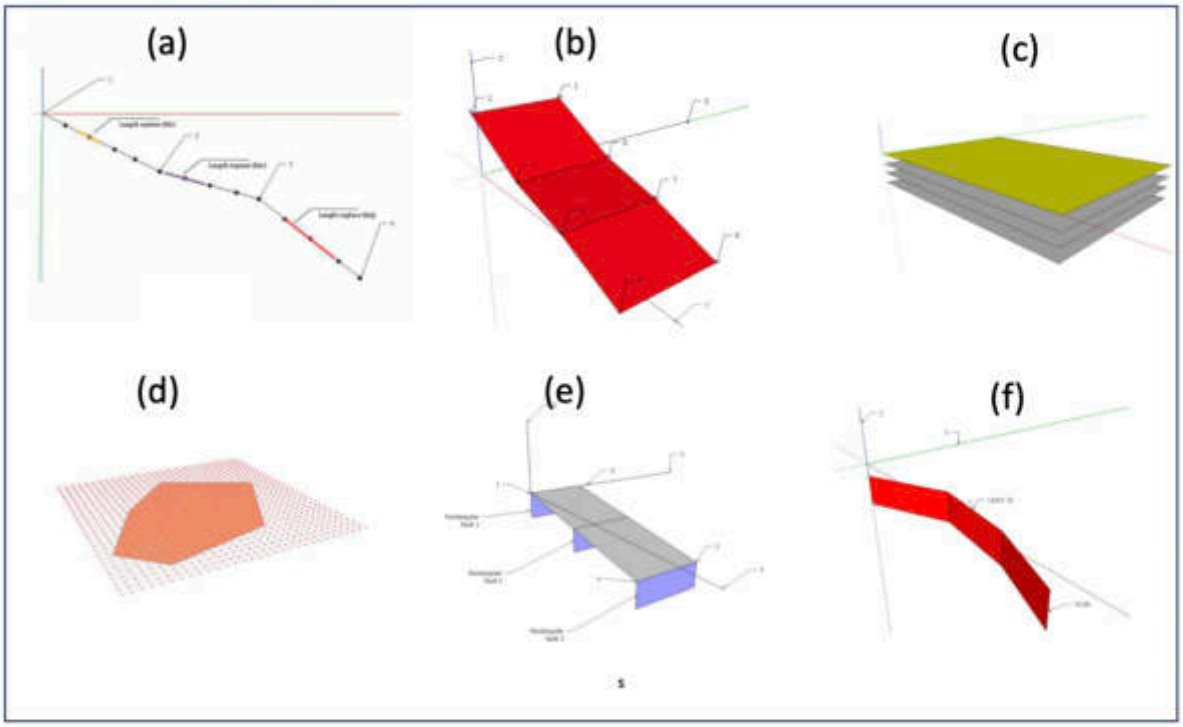

Figure 2.7. Some examples of geometric models are available in R-CRISIS. In this program can be chosen between eight different types of source models. (a) Lines, (b) areas and virtual faults, (c) volumes, (d) grids,(e) slabs, and (f) rectangular faults (taken from Ordaz et al., 2021).

2.9 Local site conditions: Vs_{30} values

Local site effects are generally treated as a site parameter, such as Vs_{30}, which is the value of the shear wave velocities on the top of the 30 meters of the subsoil. A global map of Vs_{30} was compiled by U.S. Geological Service USGS (Heath *et al.*, 2020), showing a first approximation for seismic hazard analysis and seismic codes.

Although there is controversy about whether to use or not the parameter because values may differ in small areas, its advantages and disadvantages are yet in question. However, in areas with evidence of a considerable thickness of sedimentary material, as in southern Mexico, global values of Vs_{30} give a good estimation.

In situ measurements of shear wave velocities using different techniques, for example, MASW (Multichannel Analysis of Surface Wave), ReMi (Refraction Microtremors), SPAC (Spatial Autocorrelation), etc., that have been obtained with the correct instrumentation allow obtaining values with greater certainty. In Tabasco state, there is a municipality that has data of the Vs_{30} parameter; in this work, it can help us to know a clear idea of the behavior of the subsoil in the entity and after being used in the GMPE to perform the seismic hazard evaluation.

3.1 Seismotectonics and Geology

3.1.1 Tectonic setting

Tectonic and geologic features for SEM have been collected through a detailed literature review, maps, and seismological and remote data. The principal mechanisms of the region are represented by the convergence between the Cocos-North American boundary, which subducts with approximately 7 cm/yr (DeMets *et al*., 1994).

In this region, a drastic change in subduction geometry is present in the western portion; the Cocos slab is subducting with 20°-25°, which coincides with the younger part of the slab (19 My), while in the east, an angle of 40°-45° change occurs in the Isthmus region where the slab age becomes older (27 My) (Figure 1.2). The region where the change occurs at the Tehuantepec ridge is a transforming fault trending NE-SW generated in the Pacific East. It accommodates the convergence rate in the subduction zone.

In the easternmost part of the study area is the left lateral strike-slip fault system. It is a tectonic boundary with a 2 cm/yr slip rate. This fault system is formed mainly by Ixcan, Chixoy-Polochic, Motagua, and Jocotán-Chamelecón faults. These structures have been the source of large and damaging earthquakes, except the last one without seismic activity documented (Guzmán-Speziale and Molina, 2022). Near the Tehuantepec Isthmus is the possible triple junction between Cocos, North American, and Caribbean plates. Its ambiguity lies in the unclear definition beyond its surface trace; it means the diffusivity increases to the west of the junction and inland with both overriding plates (*e.g.*, Guzmán-Speziale, 2010; Authemayou *et al.,* 2011; Manea *et al.,* 2013).

3.1.2 Crustal faults in SEM

In the North American plate, a series of crustal faults are present (Figure 3.1). In the south of the study area, Polochic-Motagua fault system is lying. It encompasses Polochic, Motagua and, Ixcán faults. These faults are active with Quaternary displacement documented (*e.g.,* Guzmán-Speziale, 2010). The actual displacement is accommodated by North American and Caribbean boundary (Guzmán-Speziale 2001).

Another morphotectonic region is the Gulf of Mexico, which is part of a large sedimentary basin containing carbonates, detrital, and salt that were affected by different tectonics processes. Within this basin province are lying Salina del Istmo, Macuspana, and Comalcalco sub-basins and Reforma Akal uplift (Pindel and Miranda 2011). The last structures were formed by Chiapaneca orogeny in the Middle Miocene. Macuspana basin is a Middle Miocene basin formed by a series of normal faults dipping landward, while the Comalcalco basin shows Pliocene ages with normal faults dipping basinward (Padilla y Sánchez, 2007). Comalcalco basin has an average rate of displacement of 3.84 mm/yr.

The Reforma-Akal uplift is formed by fold and thrust structures and is an extension of the Chiapas fold a thrust belt offshore, this is perpendicular to the basins, it has a displacement of 2.6 mm/yr. The formed faults of the basins are mainly normal and reverse, however, there is not a clear definition of the fault age and recent slip activity.

Sierra Madre de Chiapas is composed of two main subprovinces, first, the fold and thrust belt formed by faults of Neogene in age. And second, the strike-slip provinces, a series of left-lateral strike-slip faults. The strike-slip deformation is present with 5-8 mm/yr (Witt *et al.,* 2012) of lateral accommodation, it may have occurred contemporary to folds (Graham *et al.,* 2021). Yucatan Platform (YP) is located on the easternmost which borders *Sierra Madre de Chiapas*. Normal faults are representative of this area with NNE trending. There is no evidence of large earthquakes, and it is considered the lowest seismicity area (Andreani and Gloaguen, 2015). It has a displacement of 0.7 mm/yr.

Chiapas massif complex is a physiographic unit of the *Sierra Madre de Chiapas* that domains the pacific coastal plain, which mostly consists of Permian igneous rock; it is bounded by the Tonalá shear zone. Is suggested that the uplift of the complex began in the Oligocene (Witt *et al.,* 2012). This is considered the termination of the Polochic fault trace. Tuxtla-Malpaso fault is one of the major crustal faults, with strike-slip motion and with late Miocene age and activity involving 5-8 mm/yr of left lateral movement (Andreani *et al.,* 2008a,b).

Veracruz fault is a left-lateral structure that makes a junction with strike-slip province of Chiapas; some authors suggest that is the source of the August 26, 1959, M_w6.4, earthquake (*e.g.* Andreani *et al*., 2008). On September 6, 1997, an earthquake with M_w4.5 occurred (Singh et al, 2015) which was linked to a stress regime in the lower crust of the Comalcalco basin. Shallow seismicity with focal mechanism solution strike-slip suggests some events as afore-mentioned, March 11, 1967, M_w5.7, and October 29, 2009, M_w5.7 may be related to this structural phenomenon (Franco *et al*., 2013).

The Concordia fault in Chiapas state is recognized as a significant left-lateral strike-slip fault, exhibiting seismic activity and a displacement rate of 2.5 mm/yr. This fault has experienced two periods of activity: extensional activity in the Late Triassic – Early Jurassic and reverse faulting in the Late Cretaceous – Early Eocene (Meneses-Rocha, 2001).

While some authors such as Meneses-Rocha, 2001; Guzmán-Speziale, 2010; Witt *et al.*, 2012, have classified it as a left-lateral strike-slip, a recent study by Cid-Villegas *et al.*, 2017 suggest it may be a Class B dextral fault. This classification implies possible Holocene displacement as proposed by Crone and Wheeler, 2000.

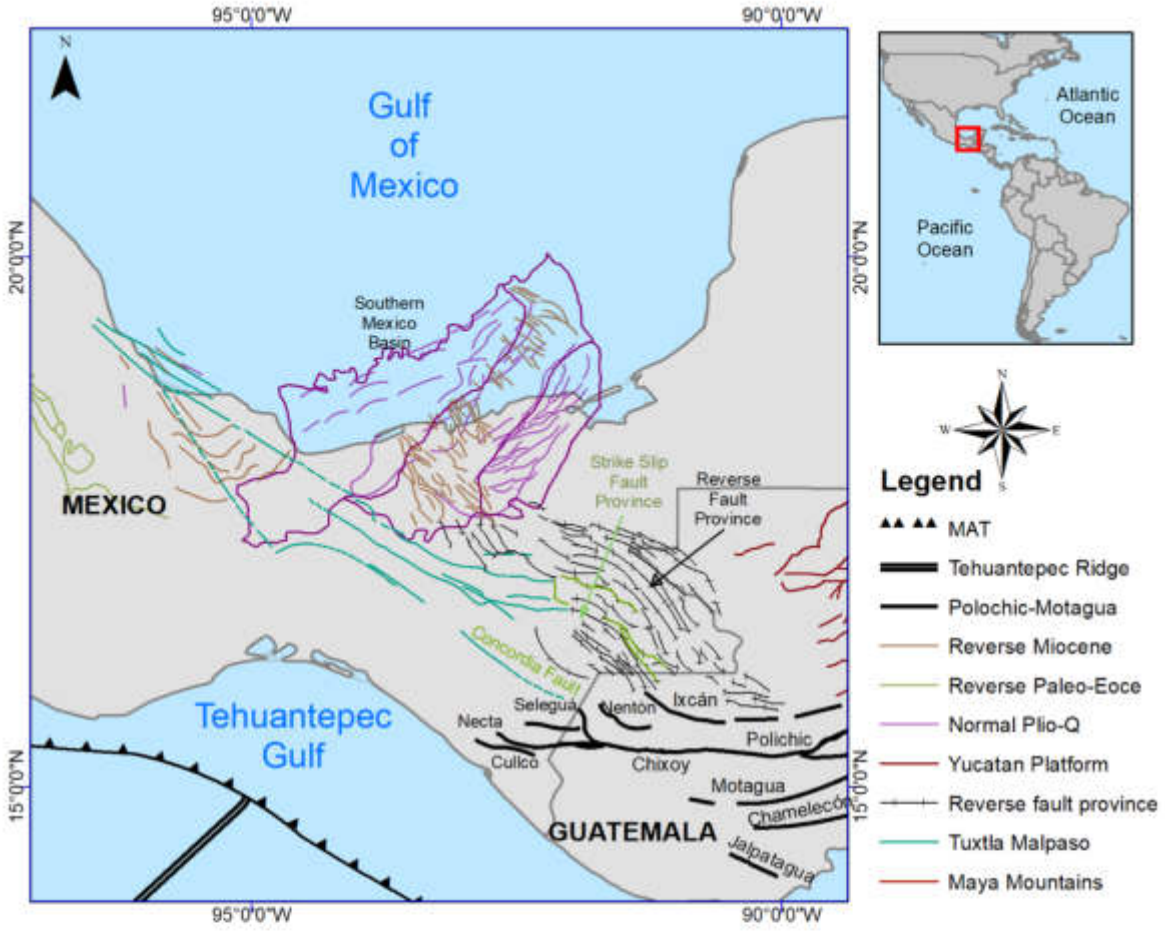

Figure 3.1. Shows an updated spatial distribution of the main crustal and shallow faults in southern Mexico. Offshore of the Gulf of Mexico and in Tabasco state are quaternary faults of southern Mexico basins (Padilla y Sánchez, 2013). Reverse and strike-slipe fault provinces (Guzmán-Speziale, 2010). Red lines show the normal fault of the Maya mountains (Andreani and Gloaguen, 2015). Polochic-Motagua Fault system taken from Guzmán-Speziale and Molina (2022).

3.2 Pre-instrumental seismicity

Considering the seismicity of a pre-instrumental period could lengthen the observation span for seismic hazard studies. In this work, the non-instrumental period is considered from 1577 to 1959 (Figure 3.2), the time before the first seismic station was installed in SEM, including earthquakes that were compiled by published catalogs from historical documents and books (*e.g.* Abe and Noguchi, 1983; White *et al.,* 1984; Pacheco and Sykes, 1992; White and Harlow, 1993; Ambraseys and Adams 1996; Montero *et al.,* 1997; Peraldo and Montero, 1999; Rebollar *et al.,* 1999; García Acosta y Suarez Reynoso, 1996; Sawires *et al.,* 2019)

A total of 83 events with a magnitude equal to or greater than 6 ($M \geq 6$) have been compiled. These events could provide valuable insight into potential future earthquakes, especially if they appear to be linked with geological or tectonic structures. Notable, strong historical events are related to the MAT at shallow and intermediate depths. The largest and most destructive was by the San Sixto earthquake, with M_w8.6 (*e.g.,* Suárez and Albini, 2009, Sawires *et al.,* 2019; Solano-Hernández *et al*., 2022). Other pre-instrumental events have been associated with geological structures. March 14, 1591, July, 22, 1816, earthquakes were related to the Concordia fault. September 23, 1902, correlated at the beginning to Tuxtla-Malpaso and Concordia fault, newly defined as an intraplate earthquake (Suárez, 2021). The August 26, 1956, earthquake was the largest event in the South of the Gulf of Mexico with M_w6.4; it damaged some buildings in Coatzacoalcos and Minatitlan, two hub cities of Veracruz state, a state also important by their petroleum activity. This event occurred on the border of Tabasco and Veracruz. It was caused by sediment loading and salt tectonics (Franco *et al.,* 2013). Some events have been updated continuously; their epicentral location has been obtained through microseismic data (*e.g.,* Suárez, 2021).

3.3 Seismic Catalog

3.3.1 Databases used.

The study area covers southeastern Mexico and the westernmost part of Guatemala, and a regional catalog has been compiled up to December 2020 based on different seismic sources. Within the catalogs analyzed are SSN, ISC, CMT NEIC-USGS, and research from published papers.

A total of 62965 events from the mentioned agencies were reviewed across various periods (Table 3.1). The seismic catalog spans the instrumental period from 1961 to 2020. Data for this study were sourced from both international and local agencies.

In this region, the SSN there is a seismic network belonging to and operating by the *Universidad Nacional Autónoma de México*. The SSN is a Mexican institution that has been operating since 1910. However, the available information is from 1970 to 2020 for southeastern Mexico. The earthquake magnitude used was $3.5 \leq M \leq 8.2$ for the events obtained from SSN; it was formed by 40788 events checked individually.

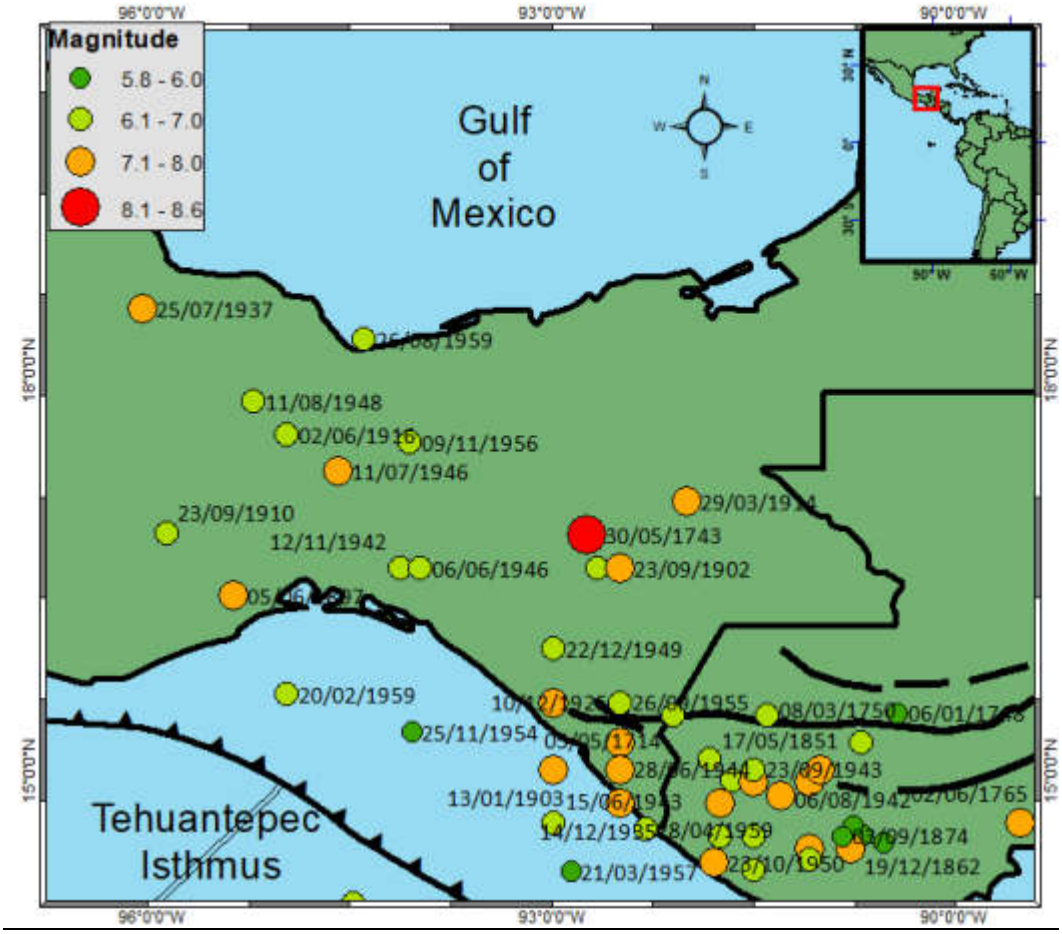

Figure 3.2. Pre-instrumental seismicity in southern Mexico. Covering a period from 1577 to 1959 (White, 1984; Montero et al., 1997, White et al., 2004; Sawires et al., 2019).

The SSN conducts information on local and regional earthquakes through its website, http://www.ssn.unam.mx. The location solutions offered by SSN for local events have been regarded as the best due to its superior seismic station coverage. Preliminary seismological parameters for low and some moderated events are reported in coda magnitude (M_c) a magnitude related to the duration of the seismic record.

The second-best solution considered was ISC (http://www.isc.ac.uk/ web page). It has the advantage of long-term coverage. It aims to provide the best earthquake parameters from published data by other agencies. ISC reports locations since 1900 but started operating with its solutions in 1964. The Global Centroid Moment Tensor CMT was the third considered, which reports focal mechanism solution and, therefore M_w values.

It was used for moderate and large earthquakes (https://www.globalcmt.org) and has reported solutions since 1976.

The National Earthquake Information Center (NEIC), operated by the US Geological Survey, was the last one considered. This decision was based on the number of seismic stations in the study area owned by the USGS.

Concerning to focal mechanism for Mexican Earthquakes, the work performed by Franco *et al.*, 2020, was considered. They analyzed more than 20,000 database events from SSN with magnitudes higher than 4.0. The CTMTM (*Catálogo de Tensor de Momento para Terremotos Mexicanos*, Spanish acronym) that was used covers the 2000 to 2018 period (132.248.6.13/~cmt web page). After checking out the last catalogs and considering the minimum magnitude of 3.5. or low-magnitude events, the priority order was given to the results from SSN, because of the local network in the SEM. For moderate earthquakes, the solution and M_w values reported by the tensor moment solution for CMT were chosen.

3.3.2 Moment magnitude homogenization

The aim of merging data is to obtain an instrumental catalog regarding the data sources available.

The first step to generating a homogeneous catalog was identifying the same event in the different databases. If distinct databases are used, it is necessary to avoid duplication of earthquakes reported by different agencies, it is solved by checking one by one of the selected events. In this work, the procedure was made manually as follows: the events that might be similar were first identified and inspected in their origin time, depth, latitude, longitude, and magnitude to choose the one with the best result. It was checked over the international and local databases available if one event was recognized with different values, the local agency was chosen.

The collected catalog was initially from local and regional institutions, which contained 62965 earthquakes reported with m_b, M_S, M_L, M_w, M_c, and *non-defined* magnitude, by the four different agencies in a range magnitude $3.3 \leq M \leq 8.2$.

The conversion process to the different reported magnitudes has been obtained by several empirical relationships used worldwide. Setting an equation for magnitude conversion might have different effects on the final catalog. Bearing this in mind the conversion equations were chosen with the premise that could be applied if (a) come from a similar setting tectonic, (b) have a valid range of magnitude of this work catalog, (c) have valid depth values, (d) type of magnitude and (e) type of data used (global or regional).

Adding, GMPE will be used in the following steps, and they need a magnitude characterized in the same terms; all events were converted to the same magnitude type, M_w, or equivalent. M_w is well-defined; its benefit is that does not become saturated for different magnitude ranges. It is a good parameter to represent the earthquake size because it is based on the rupture area and medium stiffness. However, calculating M_w for low and moderate events can be a difficult task because of the kind of seismographs used by different institutions; as a consequence, it can cause under/overestimation in the size of the earthquakes (Hanks and Kanamori, 1979).

Zúñiga *et al.,* 2017 pioneered in developing equation conversion from m_b to M_s, for Mexican earthquakes, which can be used as a first instance to reach an M_w value.

In this work were analyzed equations performed by Scordillis *et al.,* 2006, Das *et al.,* 2011, Gasperini *et al*., 2013, Beauval *et al.,* 2013, DiGiacomo *et al.,* 2015, Sawires *et al.,* 2019 to convert directly between the different type of magnitude reported to a M_w scale. The first step was to check out the setting tectonic for which were prepared and the magnitude range for which they are valid (Table 3.1). Those with similar tectonics characteristics and global settings were selected. In Figure 3.3 can be seen the differences between the conversion using the chosen equations. In the case of Das, DiGiacomo, and Sawires with the ISC catalog, an overestimation is presented for m_b>6. While for M_s data Sawires and Scordillis showed a good one-to-one fit; however, Sawires has a wider magnitude range.

Most of the data used in this catalog are in M_L/M_c and M_D magnitude. The earthquakes with low magnitudes usually reported by the SSN are in magnitude type M_D. In the conversion with Sawires' equation is seen that data are similar to one-to-one line. It is because the Sawires *et al.,* 2019 equations were used in this work to homogenize the final seismic catalog performed (Figure 3.4); they are shown as follows:

$$Mw = \begin{cases} (5.58 \pm 0.29) - (0.68 \pm 0.10)Ms + (0.13 \pm 0.01)Ms^2 & valid\ for \quad 4.0 \leq M_S \leq 7.9. \quad (3.1) \\ (-1.36 \pm 0.13) + (1.35 \pm 0.15)mb & valid\ for \quad 4.0 \leq m_b \leq 7.1. \quad (3.2) \\ (-0.31 \pm 0.26) + (1.06 \pm 0.21)(M_D \text{ ó } M_L) & valid\ for \quad 4.0 \leq M_D/M_L \leq 6.6. \quad (3.3) \end{cases}$$

Table 3.1.-Empirical equations analyzed to select the magnitude conversion equation.

Autor(s)	Type magnitudes	Magntiudes ranges	Equation	Depth ranges	Period	Data used	Setting tectonics
Scordillis *et al* (2006)	Mb → Mw	3.5 ≤ mb ≤ 6.2	$M_w = 0.85(\pm 0.04)m_b + 1.03(\pm 0.23)$	h ≤ 70 km	1976-2003	Global	Global
	Ms → Mw	3 ≤ Ms ≤ 6.1	$M_w = 0.67(\pm 0.05)M_S + 2.07(\pm 0.03)$				
		6.2< Ms ≤ 8.2	$M_w = 0.99(\pm 0.02)M_S + 0.08(\pm 0.13)$				
Das *et al.* (2011)	Mb → Mw	2.9 ≤ mb ≤ 6.5	$m_b = 0.65(\pm 0.003)M_w + 1.65(\pm 0.02)$	h ≤ 70 km	1976-2007	Global	Global
	Ms → Mw	3 ≤ Ms ≤ 6.1	$M_w = 0.67(\pm 0.00005)M_S + 2.12(\pm 0.0001)$				
		6.2 ≤ Ms ≤ 8.4	$M_w = 1.06(\pm 0.0002)M_S - 0.38(\pm 0.0006)$				
Beauval *et al.* (2013)	Mb → Mw	4.5 ≤ mb ≤ 6	$M_w = 0.93 * m_b + 0.6$	No included	1900-2012	Ecuador	SC, S, Ecuador
Gasperini *et al.* (2013)	Mb-Mw		$M_w = 1.39 * m_b - 1.75$	--	1900-2009	Europe, Global	Global
DiGiacomo *et al.* (2014)	Mb→ Mw	4 ≤ mb ≤ 7.5	$M_w = 1.38 * m_b - 1.79$	h ≤ 60km	1900-2009		Global
	Ms → Mw	3.5< Ms ≤ 6.47	$M_w = 0.67 * M_S + 2.13$				
Zúñiga *et al.* (2017)	Mb → Ms	5.5 ≤ Ms ≤ 8	$M_S = 1.7(\pm 0.057)\mathrm{m_b} - 3.38(\pm 0.2)$	h<200 km	1904-2014	Mexico	SI, SC

Sawires *et al* (2019)	Mb → Mw	4 ≤ mb ≤7.1	$M_w = (-1.36 \pm 0.13) + (1.35 \pm 0.15)m_b$	h <700 km	1787-2018	Mexico	S, SC, I
	Ms → Mw	4 ≤ Ms ≤ 7.9	$M_w = (5.58 \pm 0.29) - (0.68 \pm 0.10)M_S + (0.13 \pm 0.01)M_S^2$				
	MD/L → Mw	4 ≤ Md/Ml ≤ 6.6	$M_w = (-0.31 \pm 0.26) \pm (1.06 \pm 0.21)(MDMl)$				

SC: Shallow Crustal
SI: Subduction Inslab
S: subduction
I: Inslab
S: Subduction

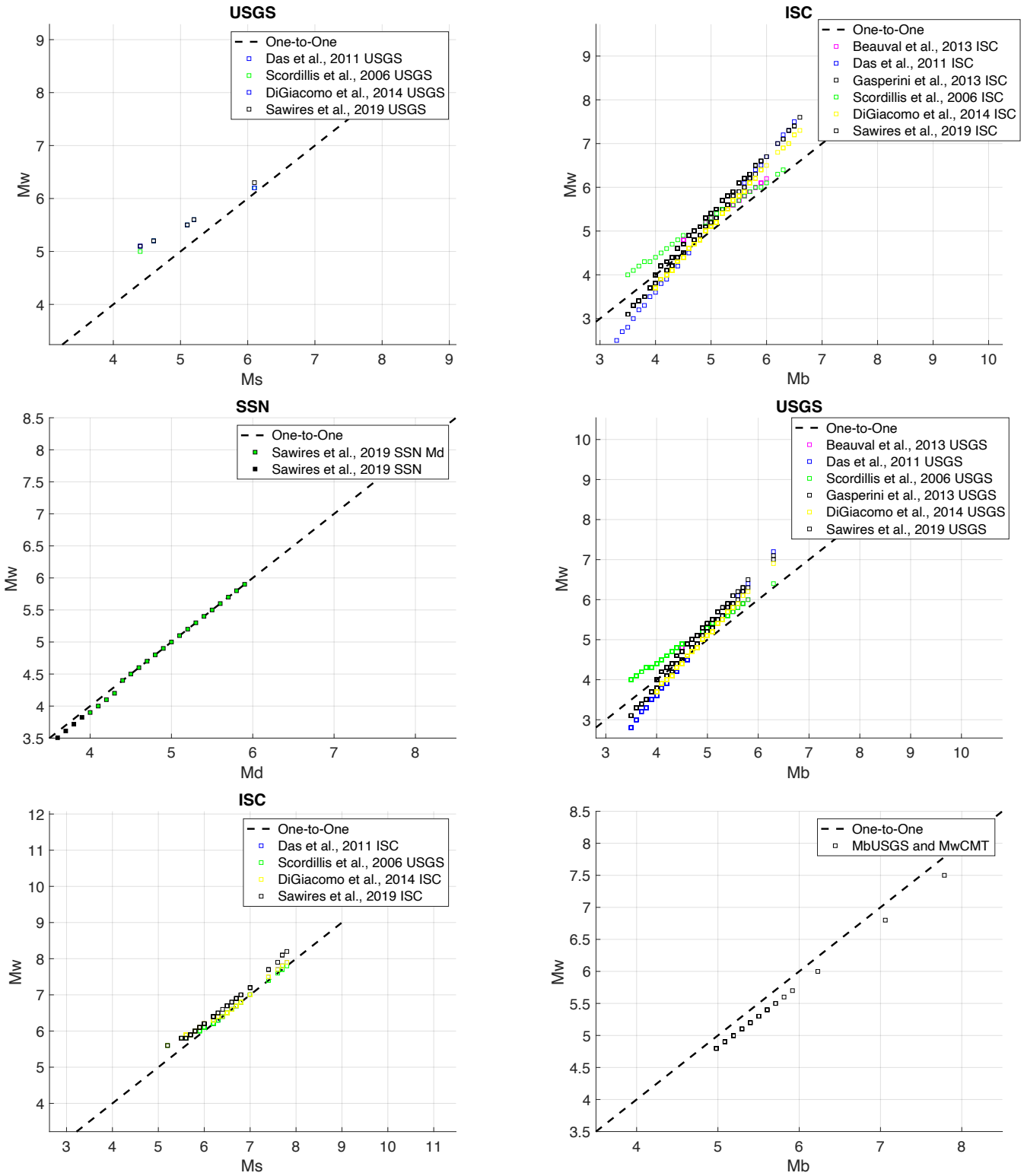

Figure 3.3. Correlation between the magnitudes of the four agencies used, taking into account all events described by all magnitude types available in each one. The dashed blue line represents one-to-one relation.

3.3.3 Declustering of the catalog

Any seismic hazard study necessitates declustering seismicity rate involving the removal of dependent events. Declustering is the process of eliminating events within a cluster, such as aftershocks and sequences of swarms, which are identified based on their proximity and temporal correlation. Various declutering techniques are available (*c.e.* VanStiphout *et al.,* 2012). However, for probabilistic seismic hazard studies, commonly employed methods include Gardner and Knopoff (1974) who utilize magnitude-dependent spatial and temporal windows to filter out aftershocks in a catalog. The size of the window is specified in Table 3.2. Another widely used method is the algorithm by Reasenberg (1985), which incorporates an interaction zone considering Omori decay aftershocks. This algorithm assumes a circular cracks radius for the events and searches within the vicinity of the aftershocks. In context of this study, the southeastern Mexico catalog was declustered using the Reasenberg algorithm, a process carried out with ZMAP (the seismicity analysis package by Wiemer, 2001).

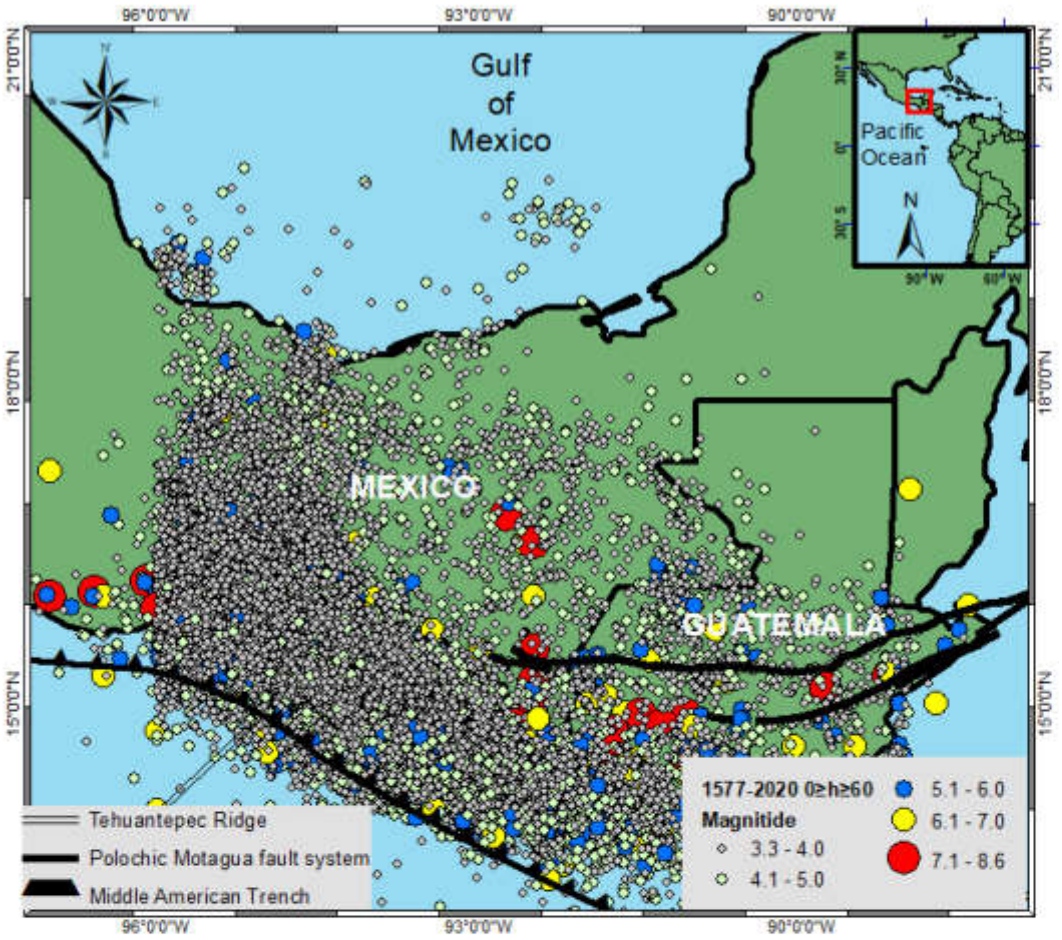

Figure 3.4. Black lines show the tectonic setting for the study area. Circles are the total events that represent the seismic catalog performed in this work, covering the pre-instrumental (1577 to 1960) and instrumental periods (1961 to 2020).

3.3.4 Induced seismicity in the Gulf of Mexico

Southern of the Gulf of Mexico has been widely studied because of the oil and gas reserves found there. However, there is a lack of seismicity and seismotectonic studies. This is a region located far from a tectonically active boundary. Nevertheless, the SSN has reported seismicity of low magnitude. Looking at the seismic catalog in this work, together with structural geology in southern Mexico basins is clear some clusters of seismic activity near oil and gas reservoirs (Figure 3.5).

In the last decades, the moment tensor has been used to describe seismic sources; it can be described as decomposed by means of a DC (double couple) and CLVD (compensated linear vector dipole). A characteristic of tectonic events is their small isotropic component and low CLVD component.

It is known that human activities, such as mining and reservoir exploration, are capable of inducing seismicity; however, specific rules to discriminate between natural and induced earthquakes are missing yet. Due to the low magnitude values and the lack of seismic stations, there is no focal tensor moment information for all events.

Only two earthquakes occurred near the places where the oil reservoirs and oil wells are located and have moment tensor solutions. They are (1): February 09, 2007, M_w4.8 and (2): October 20, 2013, M_w 3.8. The first event shows normal faulting, while the second one has a strike-slip solution.

Another essential characteristic is that the of focal mechanics of the first event (M_w 4.8) match well with the geological faults of the area, corresponding to an extensive region of the Macuspana basin. The event occurred at shallow depth and in proximity to where Padilla and Sánchez (2007) proposed normal faults. Adding the information that the CLVD is 9%, it can be defined as a natural event. The second event, M_w 3.8, exhibits a strike-slip focal mechanism, a CLVD of 56%, and a depth of 18 km, also falling under the category of natural seismicity. Consequently, all seismic events were treated as natural events in the catalog compiled for this work. However, it is acknowledged that more detailed studies are warranted to gain a better of the remaining seismicity.

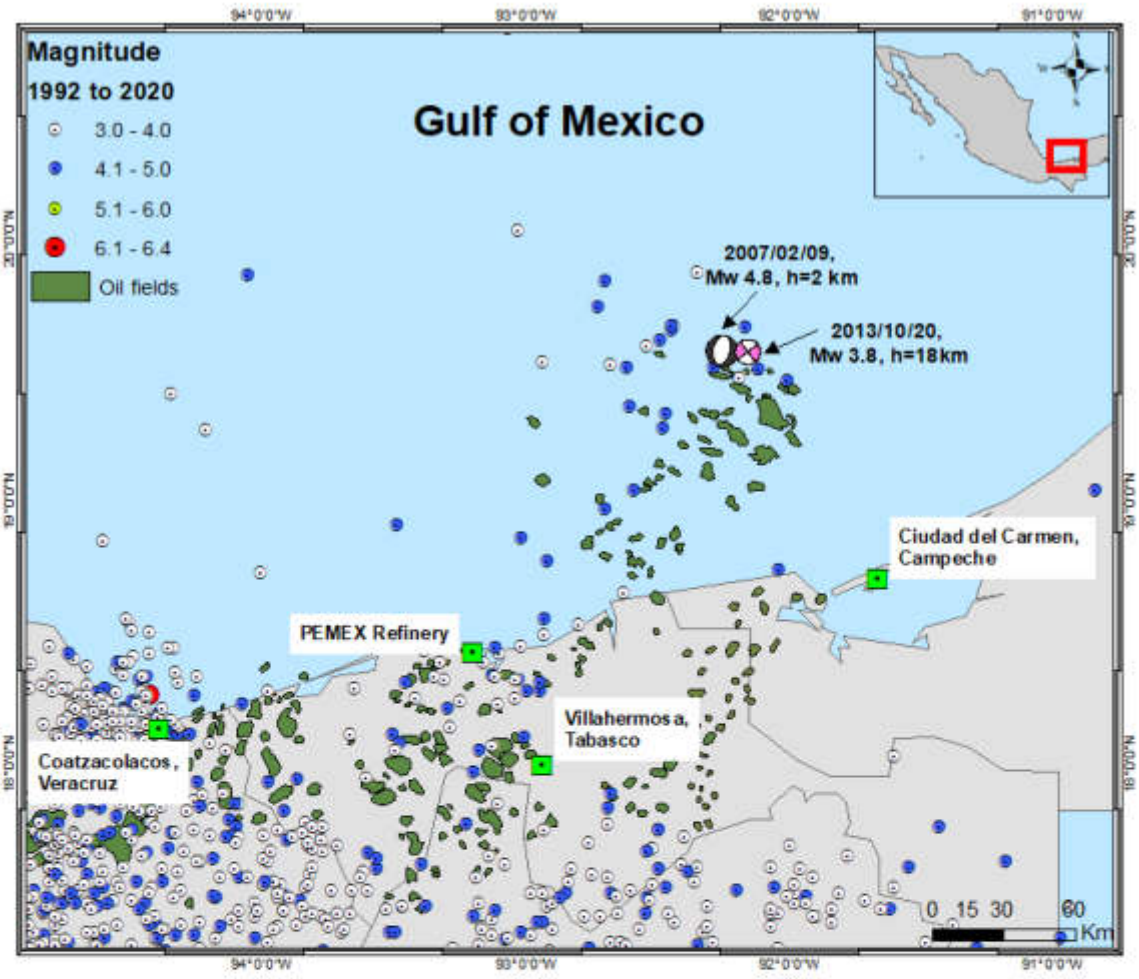

Figure 3.5. Green polygons represent the oil reservoirs and the circles of the epicenters for the 1992 to 2020 period. Two focal mechanisms of events in the Gulf of Mexico are shown: Black for M_w4.8 earthquake and Magenta for M_w3.8.

Table 3.1. Compilation of different agencies for the period of 1910-2020. This period comprises since the available data in the four agencies considered in this work.

	Md	**Periodo**	**Mag**	**M_C/ M_L**	**Period**	**Mag**	**M_S**	**Periodo**	**Mag**	**m_b**	**Period**	**Mag**	**M_w**	**Period**	**Mag**	**ND**	**Period**	**Mag**
SSN	40798	1974-2020	3.5 - 5.9										40	1902-2017	6.0 – 8.2			
ISC	12317	1990 - 2020	3.5 - 6.9	57	1982-1987	3.5 - 6.0	69	1902-1963	5.2 – 7.8	5515	1912-2020	3.3 - 7.1	4	2014-2016	3.5 – 3.8	137	2019-2020	3.5 – 4.8
USGS	1224	2000-2020	3.5 - 5.0	5	2016-2019	3.5 - 3.9	5	1973-2000	4.6 – 6.1	2284	1973-2020	3.5 – 7.5	227	1902-2020	4.0 - 8.2			
CMT													283	1902-2020	4.7 – 8.2			
Total	54339			62			74			7799			554			137		62965

ND: No defined magnitude

Table 3.2. Space and time window of Gardner-Knopoff, 1974 decluttering.

Magnitude	L (km)	T (days)
2.5	19.5	6
3.0	22.5	11.5
3.5	26	22
4.0	30	42
4.5	35	83
5.0	40	155
5.5	47	290
6.0	54	510
6.5	61	790
7.0	70	915
7.5	81	960
8.0	94	985

3.4 Focal mechanism catalog

An important element in the seismic hazard assessment is a catalog of focal mechanism solutions. The complex setting tectonics of southeastern Mexico can be better managed by a database containing solutions of the event of Cocos, Caribbean, and North American plates.

A catalog of focal mechanism solutions that contains a database from Global CMT, CTMTM, and a series of solutions published by individual papers (Guzmán-Speziale, 1989; Guzmán-Speziale and Meneses Rocha, 2000; Guzmán-Speziale, 2001; Andreani *et al,* 2008a,b; Guzmán-Speziale, 2010; Suárez, 2000; Rodríguez-Pérez, 2014; Sawires *et al,* 2019) were used (Figure 3.6).

Most of the focal mechanisms in the Middle American Trench are inslab and interface events. Along the coupling zone in the subduction zone, *T* axes are oblique to the interface and parallel to the subducted slab (Bravo *et al*, 2004). Some normal events in and close to the subduction zone are interpreted as tensional stress, they are generally between 0 and 50 km deep. A good example is the normal-inslab event with M_w8.2, showing the stress is dominated by down-dip tension. Deeper earthquakes between 50 and 180 km have different patterns of stress. In this zone, on October 21, 1995, M_w=7.2 occurred. It responded to the down dip tension of subducted Cocos plate.

3.4.1 Crustal model

In the northern part of the study area lies the Gulf of Mexico characterized by a low to moderate seismicity. Two focal mechanisms in this region show shallow normal and strike slip seismicity. Moving towards the center of the study area, there are the reverse faulting and strike-slip provinces demonstrating significant being seismic activity.

In the first province, focal mechanisms with a reverse solution revel compressional stress pattern, particularly in moderate and shallow events. In the second province, fault plane solutions exhibit sinistral solutions aligning with the prevailing stress field. The *T* axes and *P* axes are oriented horizontally, with the *T* axis in the NW-SE direction and *P* axis oriented NE-SW (Guzmán-Speziale and Meneses Rocha, 2000).

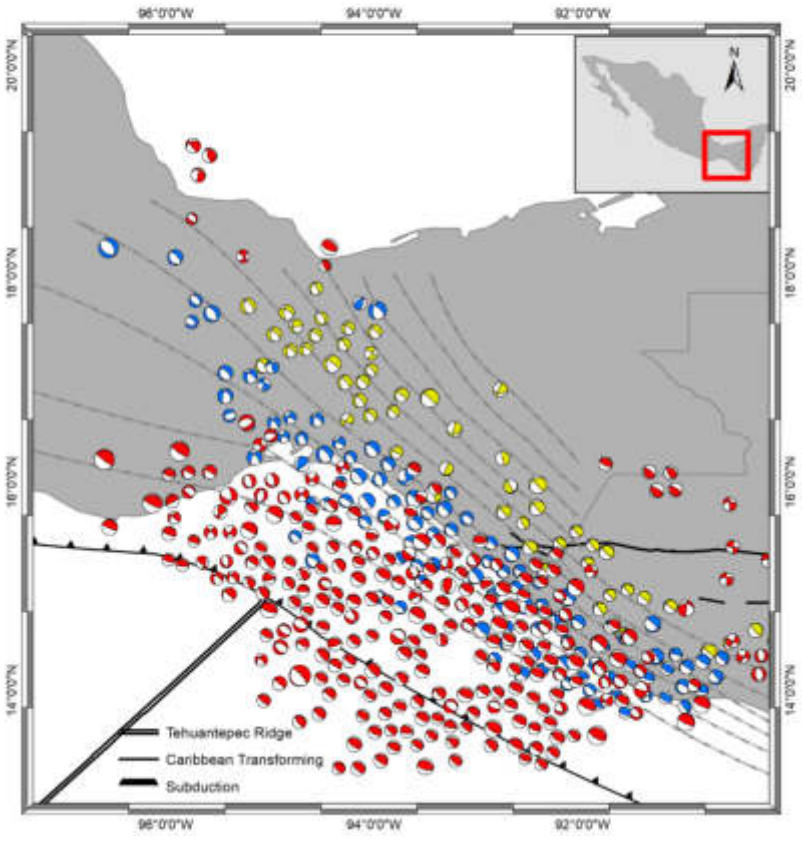

Figure 3.6. Focal mechanism solution from 1959 to 2020 with a magnitude range of 4.6 ≤ M_w ≤ 8.2 Red color represents depth of 0 to 60 km. Blue colors are solutions with 61 to 120 km of depth, and yellow colors are mechanisms with a depth of 120 to 283 km. Source: CMT, SSN, Guzman-Speziale, 1989; Andreani et al., 2008ab; Franco et al., 2013; Rodríguez-Pérez, 2014; Singh et al., 2015.

3.4.2 Deep model

Isodepth values of Hayes *et al.*, 2018 and focal mechanism solutions for deep greater than 60 km allowed making a delimitation of the inslab seismicity (Figure 3.7). The division of the two polygons is where a drastic change in the angle of subduction of Cocos plate is present. Most of the focal mechanisms in the Middle American Trench are inslab and interface events. Along the coupling zone in the subduction zone, *T* axes are oblique to the interface and parallel to the subducted slab (Bravo *et al*, 2004). Some normal events in and close to the subduction zone are interpreted as tensional stress.

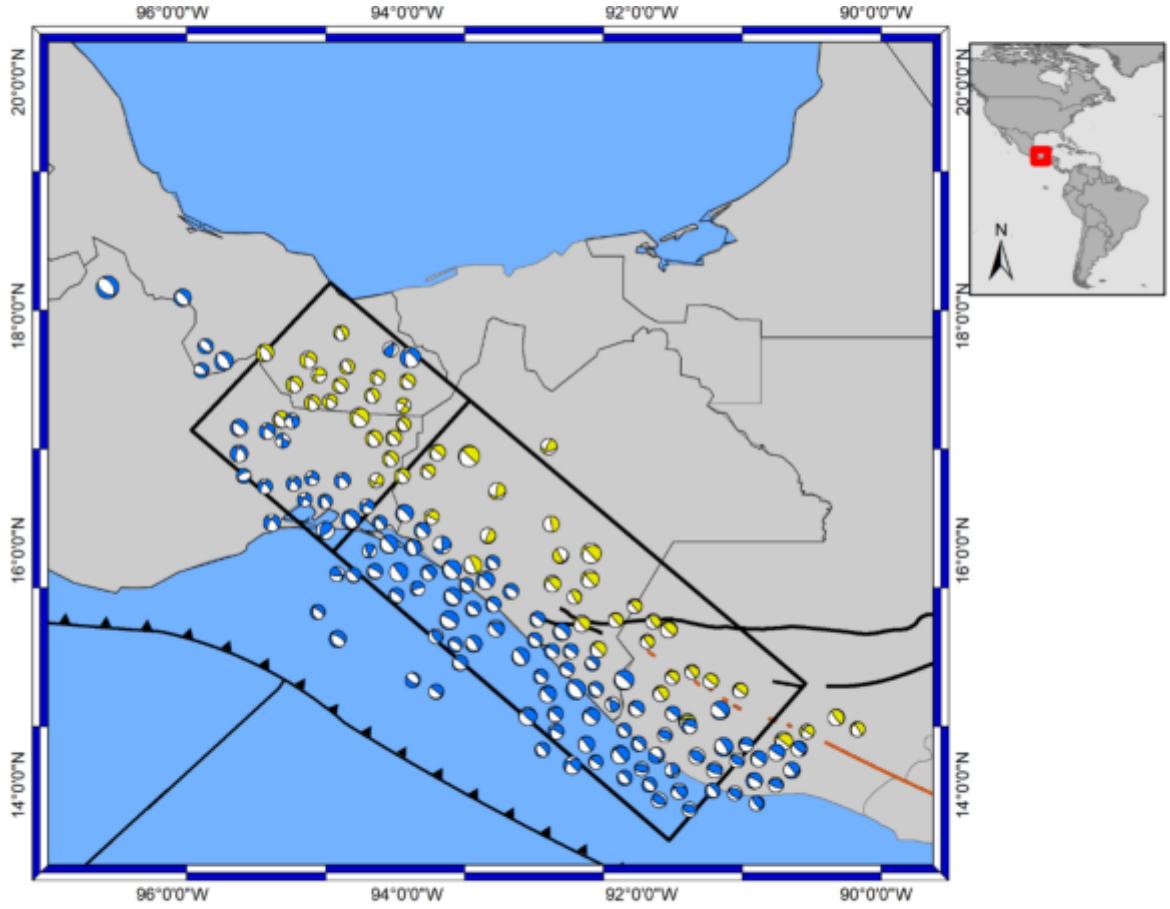

Figure 3.7. Focal mechanism solution for deep greater than 60 km. Blue colors are solutions with 61 to 120 km of depth, and yellow colors are mechanisms with a depth of 120 to 283 km.

3.5 Seismic Regionalization in Southern Mexico

The integrations of findings from tectonics, geology, seismicity, and geophysics facilitates the delineation of seismotectonic provinces, with due consideration given to seismic sources zones. Subsequently, the outcomes from the preceding section will be applied in this context.

A crucial factor in establishing seismogenic sources lies in outlining polygons that represent potential seismic origins. This delineation, as presented herein, forms the basis for seismic hazard assessment. The model considers three disctinct types of seismic sources: crustal, interface and inslab. The latter is further categorized into shallow inslab and depth inslab. This comprehensive classification serves as a foundation for seismic hazard evaluation.

Correspondence of crustal source is related to faults in the upper crustal. Most seismicity of crustal faults is in the brittle crustal, this seismicity is an answer to internal deformation through minor faults present in the crustal block. The occurrence of seismicity obeys a Poissonian in time. The size of the earthquakes is distributed according to an exponential law following Gutenberg-Richter relation, it means the maximum boundary will be the maximum magnitude possible of the block that encompasses the seismogenic source.

Most part of the faults in the SEM are not clearly identified, their age is not defined, and do not show clear evidence of activity in recent time. Is because in this work, has been decided treat the model as seismic areas.

3.5.1 Defining seismic sources

The delineation of seismic sources has been meticulously defined through a model that elucidates the occurrence of seismicity. This model takes into account their coherence with the tectonic and crustal characteristics inherent in the territory, along with the pertinent geophysical information available, such as gravity data within the study area. Within this framework, a comprehensive source model is proposed consisting of 21 zones (Table 3.3).

Table 3.3. Location parameters of the seismic sources models proposed in this work.

Name SZ	Source name							
1	Salina del Istmo Basin North	Longitude (°)	-96.4	-96.4	-94.31	-94.4		
		Latitude (°)	20.03	17.87	18.03	20.11		
		Depth (km)	30	30	30	30		
2	Tabasco's basins	Longitude (°)	-94.4	-92.27	-91.45	-90.87		
		Latitude (°)	20.11	17.28	18.08	20.22		
		Depth (km)	20	20	20	20		
3	Salina del Istmo Basin South	Longitude (°)	-96.4	-96.4	-94.23	-94.3		
		Latitude (°)	17.87	17.39	16.04	18.03		
		Depth (km)	30	30	30	30		
4	Chiapas complex	Longitude (°)	-94.26	-94.22	-93.2	-92.16		
		Latitude (°)	17.26	15.53	15.63	17.69		
		Depth (km)	30	30	30	30		
5	Strike slip fault province	Longitude (°)	-94.26	-92.16	-91.19	-92.73		
		Latitude (°)	17.26	15.53	15.63	17.69		
		Depth (km)	30	30	30	30		
6	Reverse fault province	Longitude (°)	-92.73	-91.18	-90.85	-89.75	-91.44	
		Latitude (°)	17.69	15.63	15.66	16.06	18.07	
		Depth (km)	30	30	30	30	30	
7	Yucatan platform	Longitude (°)	-91.44	-89.75	-88.19	-89.34	-90.86	
		Latitude (°)	18.07	16.06	16.59	18.15	20.23	
		Depth (km)	30	30	30	30	30	
8	Polochic Motagua fault system	Longitude(°)	-93.22	-92.34	-89.96	-87.71	-88.2	-90.85
		Latitude (°)	15.41	14.87	14.67	15.81	16.58	15.66
		Depth (km)	30	30	30	30	30	30

Name SZ	Source name					
9	Central American volcanic arc	Longitude (°)	-92.34	-90.3	-89.96	
		Latitude (°)	14.87	13.62	14.67	
		Depth (km)	40	40	40	
10	Interface I	Longitude (°)	-96.4	-97.48	-96.16	-95.16
		Latitude (°)	17.39	15.67	14.97	16.6
		Depth (km)	40	40	40	40
11	Interface II	Longitude (°)	-95.16	-96.16	-94.8	-93.88
		Latitude (°)	16.6	14.97	14.25	15.82
		Depth (km)	40	40	40	40
12	Interface III	Longitude (°)	-93.88	-94.8	-93.78	-92.93
		Latitude (°)	15.82	14.25	13.71	15.24
		Depth (km)	40	40	40	40
13	Interface IV	Longitude (°)	-92.93	-93.78	-92.6	-91.78
		Latitude (°)	15.24	13.71	13.08	14.53
		Depth (km)	40	40	40	40
14	Interface V	Longitude (°)	-91.78	-92.6	-91.21	-90.3
		Latitude (°)	14.53	13.08	12.34	13.62
		Depth (km)	40	40	40	40
15	Inslab I	Longitude (°)	-96.4	-97.48	-96.16	-95.16
		Latitude (°)	17.39	15.67	14.97	16.6
		Depth (km)	60	60	60	60
16	Inslab II	Longitude (°)	-95.16	-96.16	-94.8	-93.88
		Latitude (°)	16.6	14.97	14.25	15.82
		Depth (km)	60	60	60	60

Name SZ	Source name					
17	Inslab III	Longitude (°)	-93.88	-94.8	-93.78	-92.93
		Latitude (°)	15.82	14.25	13.71	15.24
		Depth (km)	60	60	60	60
18	Inslab IV	Longitude (°)	-92.93	-93.78	-92.6	-91.78
		Latitude (°)	15.24	13.71	13.08	14.53
		Depth (km)	60	60	60	60
19	Inslab V	Longitude (°)	-91.78	-92.6	-91.21	-90.3
		Latitude (°)	14.53	13.08	12.34	13.62
		Depth (km)	60	60	60	60
20	Depth inslab I	Longitude (°)	-94.64	-95.82	-94.62	-93.46
		Latitude (°)	18.24	16.99	15.96	17.24
		Depth (km)	180	180	180	180
21	Depth Inslab II	Longitude (°)	-93.46	-94.62	-91.76	-90.59
		Latitude (°)	17.24	15.96	13.5	14.83
		Depth (km)	180	180	180	180

3.5.1.1 Gravimetric map and focal mechanism

Gravimetric data available in Southern Mexico allow a relationship with the seismicity and focal mechanism to improve the delimitation of polygons. In a general way, some anomalies and setting tectonic were compared spatially to have a better constraining in the definition of the seismic sources, as follows:

In the north of the study area, near the coast and Tabasco, Campeche, and Veracruz state, two anomalies with ~+50 mGal, its trending coincides with Reforma-Akal uplift faults. For the Southwestern Gulf of Mexico area, close to the Tuxtlas volcanic field where the Veracruz fault is also positioned, the Bouguer anomaly has values of +146mGal. Near the last province mentioned, October 09, 2001, M_w4.9, h=22 km, November 14, 2005, M_w4.4, h=28 km, August 26, 1959, M_w6.4, h=21 km, March 11, 1967, M_w5.7, h=26 km, October 29, 2009, M_w5.4, h=16 km, October 29, 2009, M_w5.7, h=17 km, earthquakes occurred (Franco *et al.,* 2013).

Near the Polochic-Motagua boundary, there is a variation of Bouguer anomaly of -200 mGal. This region has experienced seismicity of moderate to higher magnitudes. (*e.g.,* Suárez, 2000, Suárez and López 2015, Franco *et al*., 2013).

In the area of the Middle American Trench (Figure 3.8), there is an anomaly that coincides with the change in the age of the Cocos plate; it also coincides with the high coupling of the slab area of the Tehuantepec Isthmus, which shows a high seismicity region.

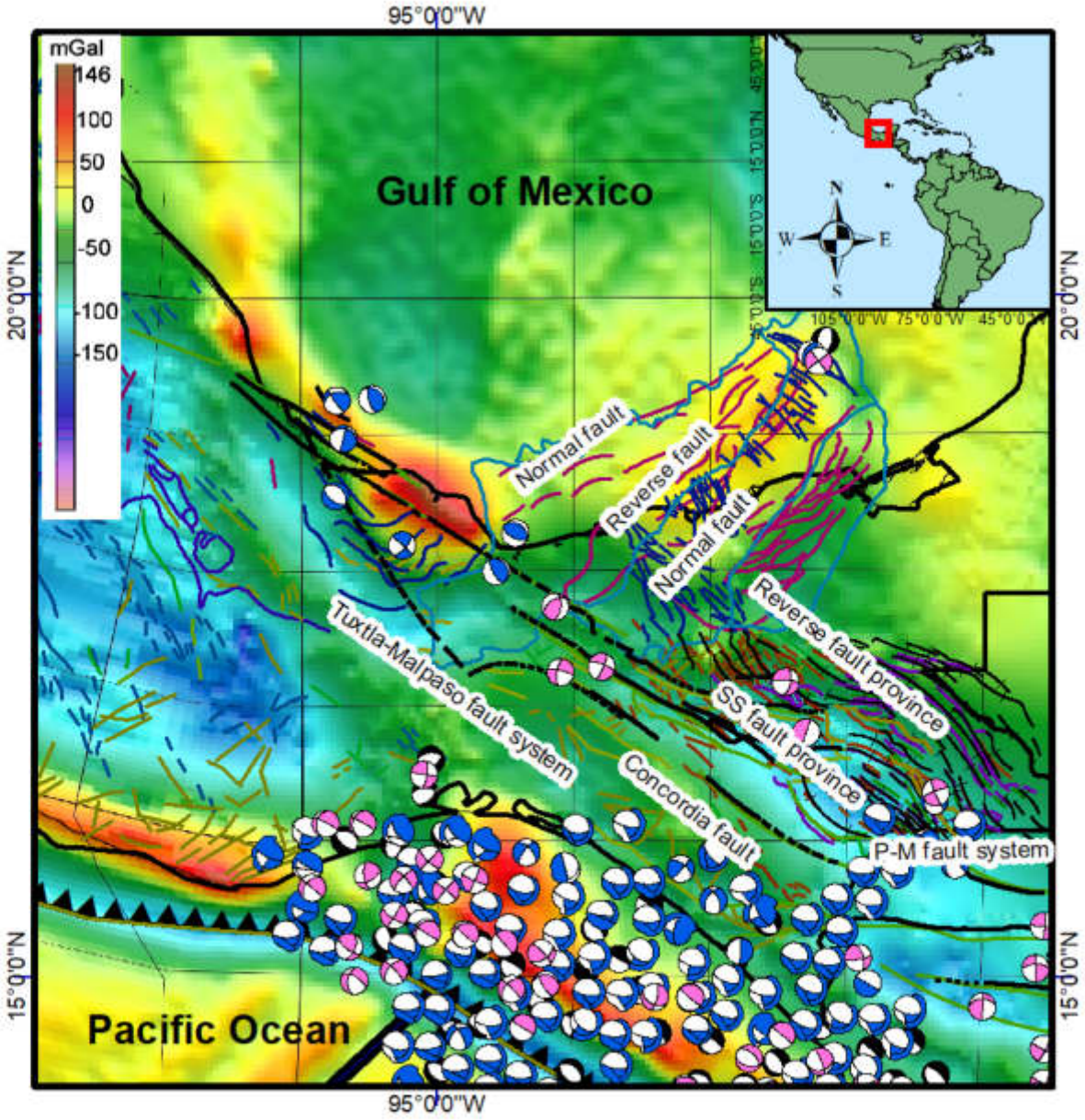

Figure 3.8. Bouguer anomaly map (INEGI, 2023). Color lines depict the main crustal faults of the provinces in Southern of Mexico. Red and green lines show the faults of the southeastern Mexico basins. Blue lines represent the main faults of the strike-slip province. Black lines are the main faults of the fold and thrust belt of the reverse province in Chiapas.

3.5.1.2 Shallow sources model

Another input parameter for PSHA is the modeling of the seismogenic potential of active areas. The relationship between seismicity and setting tectonic is a challenge for the study area because some of the occurred earthquakes are not linked to geological structures.

Due to, the large earthquakes occurring during the pre-instrumental period and macroseismic data does not allow a good certainty in the epicentral location. Even if for the study area, there is scarce information about (a) the faults with quaternary activity, (b) paleoseismic data that allow identifying fault activity in the past, (c) surface rupture lengths of faults on the surface that allows their complete identification, (d) the geodesic information that only is present for scarce and small areas and, (e) the absence of a dense seismic network is giving as result uncertainty in the epicentral location of a certain type of events; as a consequence, the definition of the seismogenic sources has been a demanding task, because there is no specific method to delimitate the polygons that represent the potential seismic sources. The seismic zones in this work were treated as area sources, which means that each region has experienced seismicity in the past and can be treated as potential seismic sources for future earthquakes.

3.5.1.3 Crustal zones

Shallow crustal zones represent a model with uniform seismicity throughout the tectonic or geologic region with constant geologic or strain characteristics. The study area is divided into nine regions. The zones are (1) Isthmus North, (2) Southern Mexico Basins, (3) Isthmus South, (4) Chiapas Complex, (5) Strike Slip Province, (6) Reverse Faults Province, (7) Yucatan Platform, (8) Polochic Motagua Fault System, and (9) Central American Volcanic Arc. Next, they are described (Figure 3.9).

1) Isthmus North (IN) is lying in the Veracruz basin with a thickness of the continental crustal is 34 km (Román-Ramos *et al.*, 2008), this zone shows a dense clustering of epicenters, the largest earthquake is Jáltipan August, 26, 1959, M_w6.4, h=21 km, and reverse faulting, which caused several damages in Veracruz with an intensity IMM of VIII. The thickness of the sedimentary layer can reach 10 km (Manea *et al.,* 2019).

2) Southeastern Mexico basins (SEMB), encompasses Macuspana, Comalcalco (driven by gravity tectonics and salt withdrawal), Salina del Istmo basins and Reforma-Akal uplift (a continuation of Chiapas fold-and-thrust belt), this region has a set of normal and reverses faults trending NE-NW (Menesses Rocha, 2001). Salt deposition encompasses Jurassic and Cretaceous accumulation. Seismicity clustering is low with a recorded

earthquake with M_w5. The SEMB is a prolific basin containing rocks from Jurassic to Pliocene, highlighting the opportunities for future hydrocarbon explorations. Even with the absence of recorded great earthquakes, this zone has experienced intensities up to VIII from regional events. Two focal mechanism solutions Normal and strike-slip show the differences in the stress present in the zone.

3) Isthmus South (IS) shallow and low magnitude seismicity. However, most of the low seismicity activity is related to salt tectonics although some of it may be related to transforming faulting (Melettti *et al*., 2008).

4) Chiapas complex (CC) has a crystalline basement is Precambrian and Paleozoic granite and gneiss, this is the termination of Polochic fault (Andreani and Gloaguen 2015).

5) Strike Slip Province (SSP) is represented by shallow seismicity with left-lateral strike-slip motion oriented NW-SE, the SZ present quaternary activity with basement-involved structures (Graham *et al.,* 2021), Focal Mechanism are consistent with faulting, showing shallow depth. This zone has been related to historical earthquakes.

6) Reverse Fault Province (RFP) faults with Neogene displacement, it is part of the fold-and-thrust belt, the motion between NorthAmerican and Caribbean plates is caught by RFP and SSP regions (Andreani and Gloaguen 2015). The seismicity is low to moderate, and the largest earthquake recorded is M_w7.

7) Yucatán platform (YP) is the region with the lowest seismicity, but a historical earthquake with M_w 7.1. This region covers a part of the Maya Mountains which are the northernmost part of the Polochic-Motagua fault system

8) Polochic-Motagua Fault System (PMFS) is formed by the set of Ixcán, Polochic, and Motagua faults which delineate the Caribbean-North American plate boundary and has Quaternary displacement. A destructive earthquake occurred on February, 24 of 1976 with M_s7.5 and, historically 1591, 1816, and 1902 earthquakes took place in this zone, strike-slip and shallow focal mechanism solutions may describe the relationship between faults and pre-instrumental events

9) Central America Volcanic Arc (CAVA) is a region characterized by recent volcanic activity, CAVA may be understood as a mix of continental and oceanic crust (Gazel *et al*, 2021) with shallow and moderate seismicity, their focal mechanism show thrust solutions. Destructive earthquakes occurred in this narrow zone. The Moho depth is 30-40 km. It has a rate of 12 to 14 mm/yr.

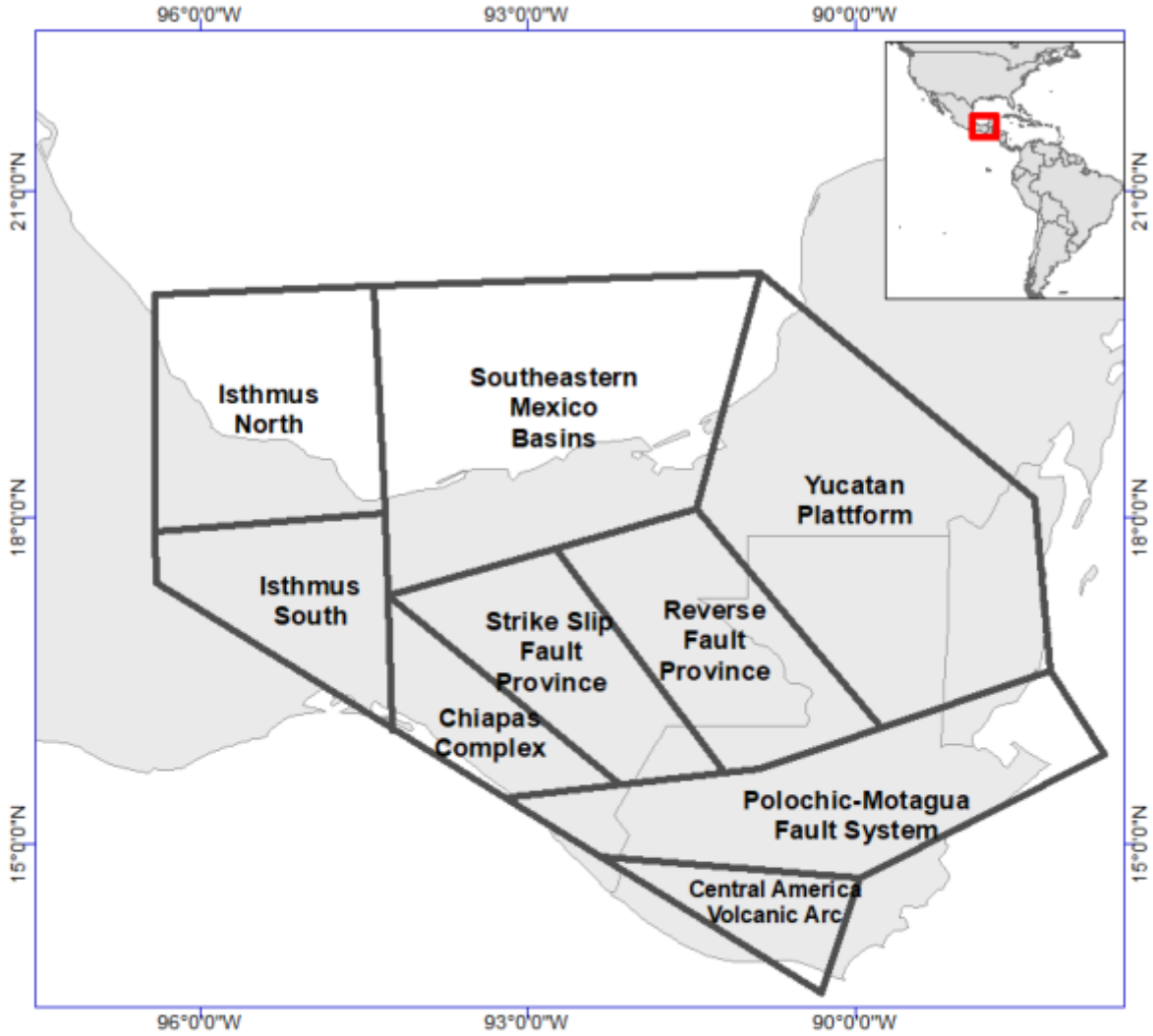

Figure 3.9. Crustal zone model defined in this work. It covers a depth of up to 60 km.

3.5.1.4 Interface regions

The interface seismic sources (named here I1-I5) are related to the regions between the Cocos-North American plate and encompass regions with more coupling. Reverse focal mechanism solutions represent it, and the depths considered are h<60 km (Figure 3.10):

1. Interface 1 (I1) the contact between Cocos and the North American plate that gives, as result interface earthquakes with depth up to 50 represent I1. The zone with the highest coupling between the Cocos-NA plate. The most significant event in Mexico occurred in this zone with M_w8.6 (*e.g.* Sawires *et al.,* 2019; Suárez *et al.,* 2020), this zone has the potential to generate a tsunamigenic earthquake.

2. Interface II (I2) this region is the second with high mechanical coupling (Franco *et al*., 2012) and encompasses the northernmost part of the Tehuantepec Ridge.

3. Interface III (I3) in this region can be seen a drastic change in the age and dip of the Cocos plate. In this region, the low coupling is present (Lyon-Caen *et al.,* 2006).

4. Interface IV (I4), focal mechanism solutions show a combination of reverse and normal events. Historical earthquakes have placed in this region (*e.g.,* October 23, 1950, M_w7.2). Previous studies have shown that in this area.

5. Interface V (I5), this region covers the subduction interface seismicity of southern Guatemala. Large and pre-instrumental earthquakes hosted here (*e.g.,* August 06, 1942, M_w7.7)

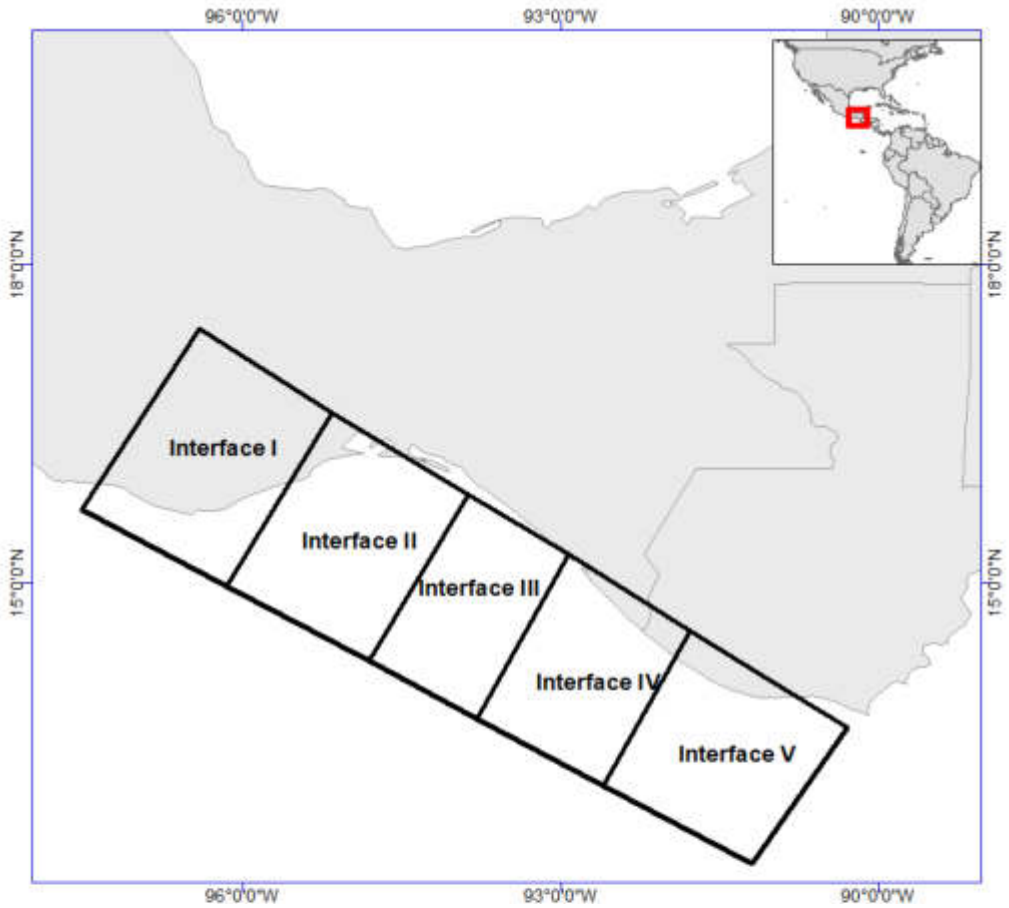

Figure 3.10 Interface-subduction model. This zone represents the major coupling between Cocos-North American plate, and the Caribbean plates.

3.5.1.5 Shallow inslab

Shallow inslab (or intraslab) regions have depths between 41 $\leq h \leq$60 km; this seismic zone geographically has the same distribution as interface regions but different depths (Figure 3.11). This region encompasses inslab events by releasing downdip stresses within the Cocos plate. Another characteristic of these events, apart from normal faulting, is that they can cause strong ground motions, for example, the well-known Chiapas, 2017, earthquake, M_w8.2.

1. Shallow inslab 1 (SI1), the Cocos plate may create large earthquakes related to the sinking process of the slab, in this region. The maximum recorded magnitude for the seismic zone until now is M_w6.0.

2. Shallow inslab 2 (SI2) in this region the change in the seismicity can be shown through focal mechanism solutions, and ought to be related to the change in the subduction angle. This zone encompasses the Tehuantepec ridge and is related to the seismic gap for some authors. A *Mmax* earthquake *with* M_w6.9 has been recorded.

3. Shallow inslab 3 (SI3), this region hosts the largest recorded event, on September 08, 2017, the M_w8.2 earthquake had its epicenter here. It event is linked to downgoing of Cocos plate. The frequency of large and tensional earthquakes show the deformation in the Cocos plate that is under tensional stress (Suárez, 2021).

4. Shallow inslab 4 (SI4) in this region the dip of Cocos plate is higher, the largest earthquake recorded has M_w7.3. The limit between high and low coupling of the Cocos-NA plate occurs in this zone.

5. Shallow inslab 5 (SI5) the focal mechanisms of these events show tensional solutions, indicating down-dip extensional faulting. In this region, Cocos plate has a steep dipping going from 20 to 80 km in a narrow zone.

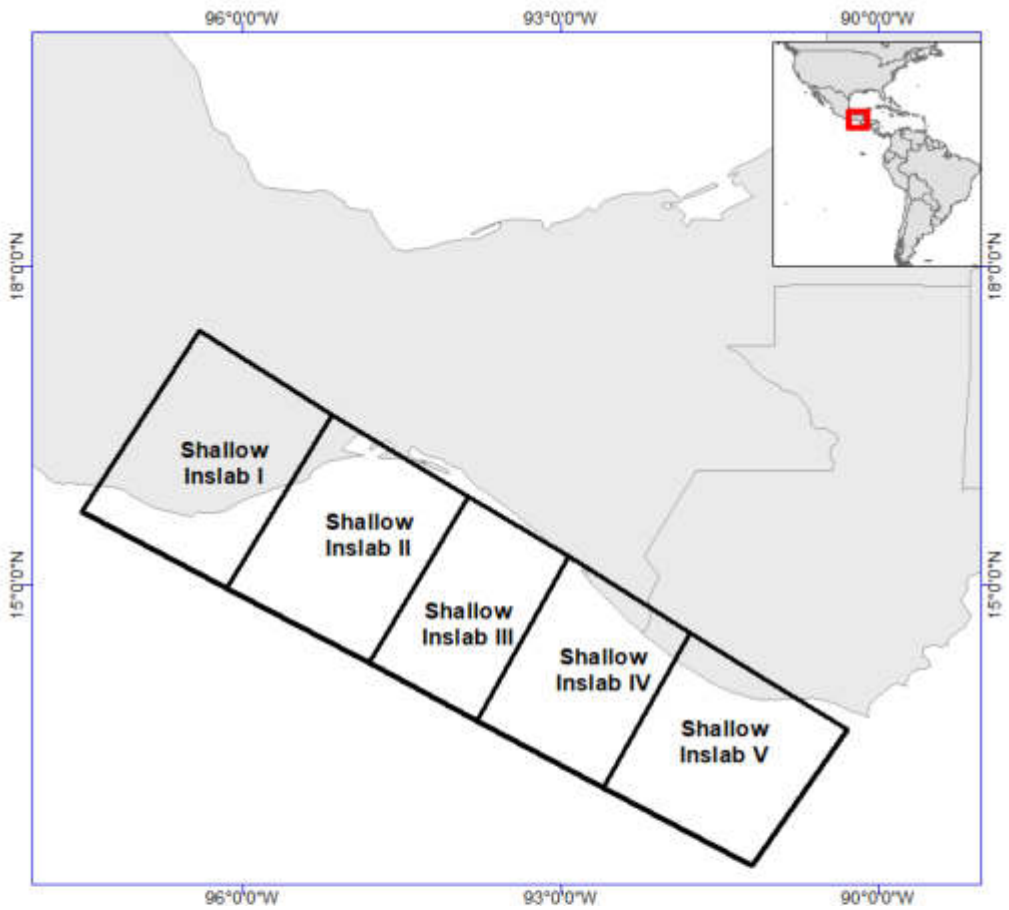

Figure 3.11. Shallow inslab model proposed in this work.

3.5.1.6 Deep sources model

The depth seismogenic zones encompass earthquakes with $60 \leq h \leq 180$ km (Figure 3.12). The largest event that occurred in these areas corresponds to M_w7.4. Among the most important items to define the depth source model was the geometrical analysis defined by Hayes *et al.,* 2018, their study modeled the subduction of the Cocos plate taking into consideration the seismicity, and the geometry of the Mexican subduction zone called *slab2*.

The geometry of the Cocos plate plays an important role defining a seismic depth model, joined to the available seismological information and focal mechanism solutions. In southeastern Mexico, a change in the dip of subduction increasing in Central America. Another thing considered for the delimitation of the depth seismic zones was the Tehuantepec fracture zone separates the Cocos plate

into two parts (1) the North, a region with a slip rate velocity of 6.35 cm/yr, and the youngest age plate of 19 My, and (2) a change in the slip rate of 7.45 cm/yr and age plate 27 My (*e.g.,* Caló, 2022).

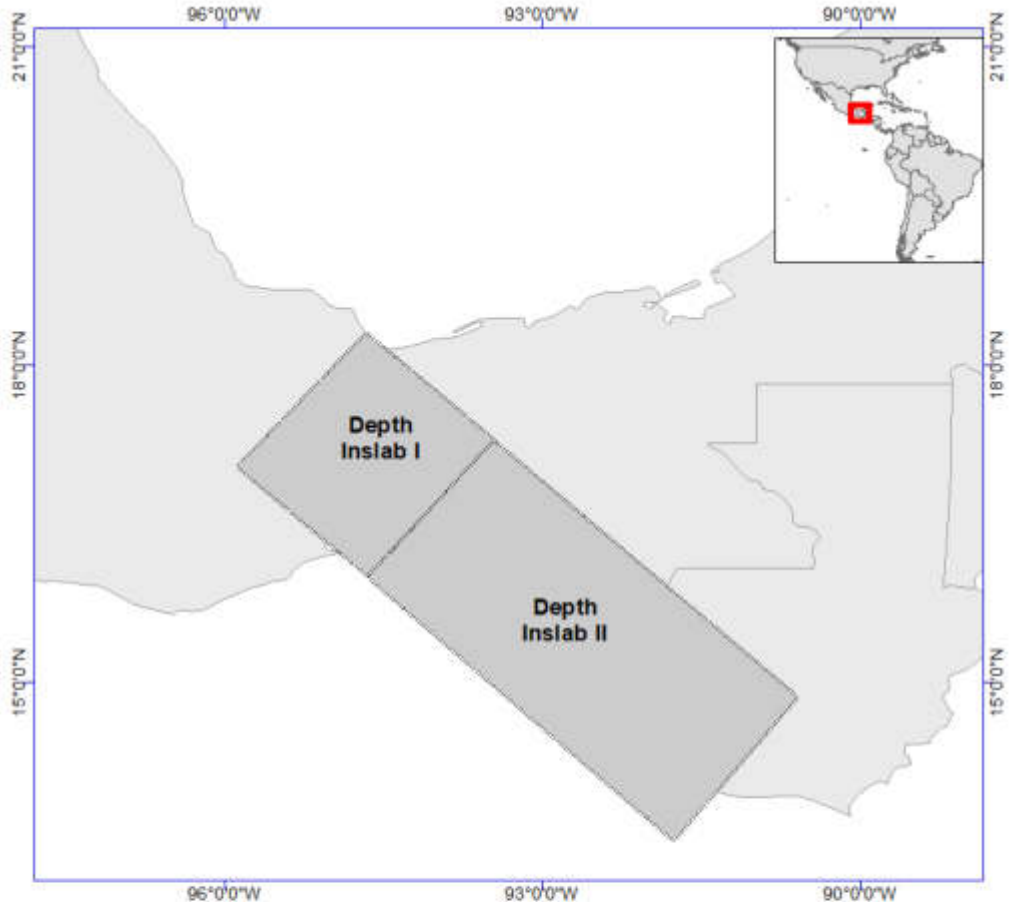

Figure 3.12. Deep inslab model proposed by this work.

3.6 M_{max} estimation

M_{max} depicts the maximum earthquake magnitude for a given seismogenic region; it is applied in seismic hazard studies. In regions with low-seismicity rates such as the case of southern Mexico basins and Yucatan Platform, sometimes is complicated because to establish the value of the largest event the frequency-magnitude *G-R* relation is used.

Well and Coppersmith's relationship can be an indication of the expected magnitude. Even if getting a magnitude versus displacement has a great uncertainty, they are generally used when seismic data of large events do not exist.

Other equations developed to get a magnitude estimation are Johnston *et al.* (1994a,b), authors mention that for Stable Continental Regions (SCR) such is the case of southern Mexico basins and Yucatan Platform, where there are low local observations the M_{max} estimation might be critical. In their research, they propose an increment of 0.5 above the maximum magnitude of the recorded earthquake.

Another way to establish a maximum magnitude is the extrapolation for a specific region (Kijko, 2004); he assumes that the maximum magnitude is related to an increment according to the penultimate event in magnitude recorded.

In SCR the maximum magnitude value sometimes is imposed with a maximum value of M_w7.9 (Vanneste *et al.*, 2016)

In the study area are the southern Mexico basins and the Yucatan Platform, two seismic sources with low seismicity and no evidence of large and destructive earthquakes; however, in the first one, even if there are no evidence of large magnitude earthquake recorded, regional event have caused considerable damage.

In southern Mexico basins, there is some documented line of faults by Padilla y Sánchez (2013) in its tectonic map for Mexico, where most parts of those structures have a length average of 20 km. In agreement with the relationship mentioned of Wells and Coppersmith (1994) between length fault and magnitude, a M_w~6.6 may happen in this region (Table 3.4).

Table 3.4. Principal shallow and crustal structures in southern Mexico. M is the magnitude estimated with length faults measured with satelital images and afer using Well and Copersmith. (1994) and Papazachos et al. (2004) relationships.

Structure	Segment	Earthquake	Type	Class USGS	Average Long.	M (Well and Copersmith,1994)	M (Papazachos *et al*,. 2004)
Tuxtla-Malpaso-Aztlán system	North: Malpaso fault		SS LL (Strike Slip left-lateral)	B	100	7.40	7.29
	Center South: Tuxtla fault		SS LL	B	100	7.40	7.29
	South: Tuxtla fault	1592, M7.2	SS LL	B	52	7.07	6.81
Malpaso-Aztlán	North		SS LL	B	70	7.22	7.03
	South		SS LL	B	55	7.10	6.85
High Sierra fault system	North: Tectapan-Ocosingo fault		SS LL	-	49	7.04	6.76
	Center: Tenejapa fault		SS LL	A	53	7.08	6.82
	South: San Cristobal fault		SS LL		60	7.14	6.91
Falla Concordia	North		SS LL	A	54	7.09	6.83
	South: inferred		SS LL	B	60	7.14	6.91
Grijalva-La Venta fault	North: La venta fault		SS LL	-	70	7.22	7.03
	South: Grijalva fault		SS LL	-	-		
Reverse Fault Province	Northwest		Reverse fault	-	-		
	Southeast		Reverse fault	-	-		
Ixcán fault	West: reverse fault		reverse fault	-	88	7.34	7.61
	Middle: Infered		SS LL	-	42	6.96	6.97
	East		SS LL	-	80	7.29	6.65

Structure	Segment	Earthquake	Type	Class USGS	Average Long	M (Well and Copersmith,1994)	M (Papazachos *et al*,. 2004)
Polochic-Motagua	Polochic fault West	1816, VII	SS LL	A	200	7.75	7.12
	Polochic fault East		SS LL	A	200	7.75	7.80
	Motagua fault West		SS LL	A	84	7.31	7.80
	Motagua fault East	1975, Mw7.5	SS LL	A	220	7.80	7.16
SS Fault Province	North		SS LL	-	-		7.87
	South		SS LL	-	-		
Macuspana-Comalcalco basin	-		Normal fault	-	20	6.6	
Veracruz fault system	-		SS LL	-	-		
Jaltapagua	-		SS RL (Strike Slip right-lateral)	-	-		

3.7 Recurrence parameters

One important input in the evaluation of the seismic hazard is that the seismic zonation allows for depicting each seismic zone as a region that has similar seismological and tectonic characteristics (Figure 3.13). This seismic activity can be represented with G-R magnitude-frequency relationship $log_{10}N(m) = a - bm$. (Gutenberg and Richter, 1954). The recurrence parameters, such as G-R values for all seismic zones, were calculated, and their spatial distribution was also estimated; this value (b-value) shows a good correlation with the tectonic setting in the area and a good agreement with previous studies. The a value is an indicator of the seismicity level in each seismic source; in the current study, they have values from 5.02 to 10.7, while b value gives an indication between low and large magnitude earthquakes; in this study is from 0.67 to 1.96 (Table 3.5).

Table. 3.5. Earthquake recurrence parameters for the proposed zones.

Source zone	**Source depth**	**b-value**	**λ Mw>3.5**	**Mmin**	**Mmax**	**Mc**
Salina del Isthmo Basin North	0-40	1.39±0.12	7.583/5.796	3.3	6.4	3.8
Southeastern Mexico basins	0-40	1.42±0.11	7.602/5.856	3.4	5.5	3.9
Salina del Istmo Basin South	0-40	1.57±0.03	8.926/6.959	3.4	6.6	3.5
Chiapas complex	0-40	1.17±0.11	6.546/4.513	3.4	7.1	3.7
Strike slip fault province	0-40	1.15±0.08	6.560/4.809	3.4	5.1	3.7
Reverse fault province	0-40	1.13±0.07	6.719/4.719	3.4	7.0	3.7
Yucatan platform	0-40	1.37±0.93	7.114/5.081	3.4	7.0	4.4
Polochic-Motagua fault system	0-40	0.73±0.03	5.253/2.606	3.4	7.6	3.4
Central American volcanic arc	0-40	0.68±0.03	5.021/2.453	3.4	8.0	3.4
Sub 1/Interface 1	0-30	1.33±0.04	8.066/5.698	3.4	8.6	3.6
Sub 2/ Interface 2	0-30	1.79±0.02	10.763/8.860	3.4	6.7	3.7
Sub 3/ Interface 3	0-30	1.31±0.02	8.574/6.674	3.4	7.3	3.7
Sub 4/ Interface 4	0-30	1.01±0.02	7.316/5.244	3.4	7.6	3.8
Sub 5/ Interface 5	0-30	0.73±0.03	5.364/3.403	3.4	7.3	3.5
Shallow Inslab 1	40-60	1.96±0.07	9.950/8.126	3.4	6.0	
Shallow Inslab 2	40-60	1.58±0.04	9.055/7.301	3.4	6.9	
Shallow Inslab 3	40-60	1.30±0.06	7.636/5.703	3.4	8.2	
Shallow Inslab 4	40-60	0.77±0.02	5.753/3.907	3.4	7.3	
Shallow Inslab 5	40-60	0.56±0.02	4.549/2.700	3.4	6.7	
Deep Inslab I	61-180	0.7±0.12	9.445/7.552	4.9	7.4	5
Deep Inslab II	61-180	0.67 ± 0.06	5.360/3.346	4.7	7.2	5

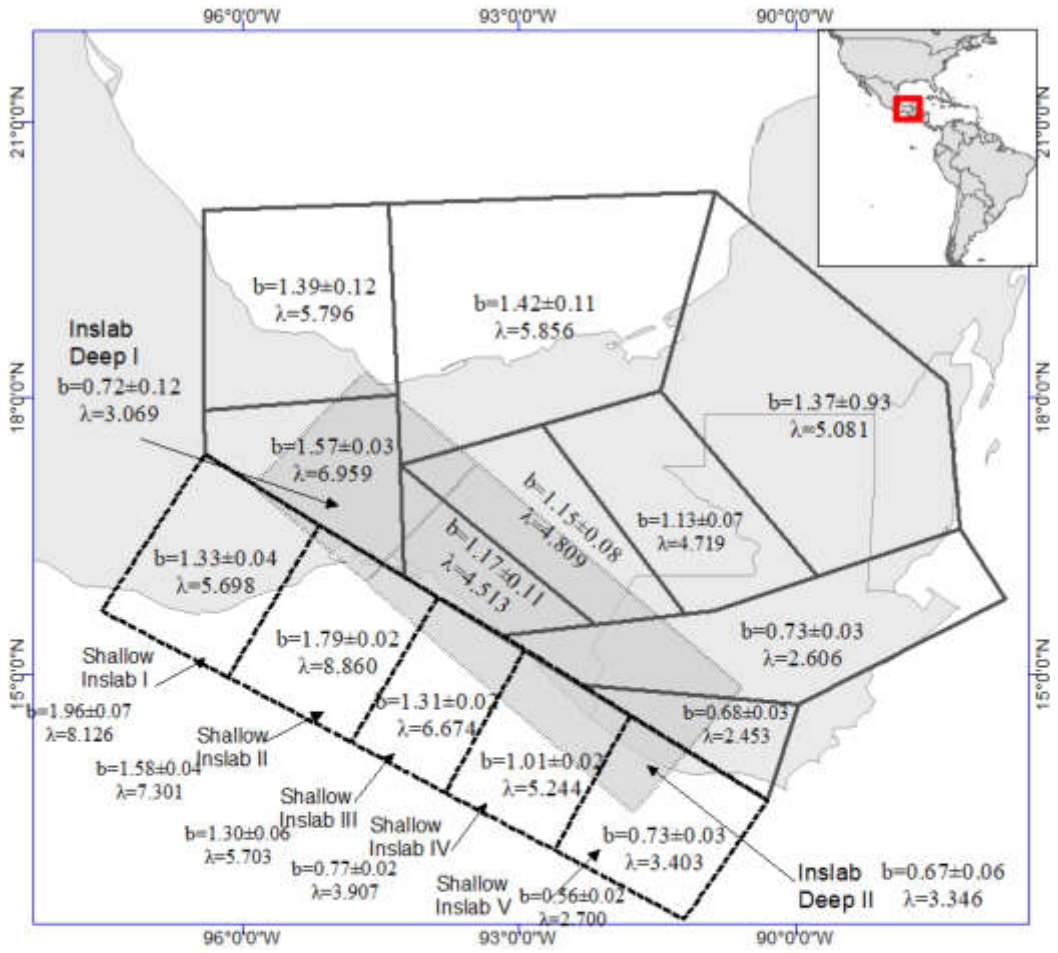

Figure 3.13. Earthquake recurrence parameters for the seismic sources model. Black lines represent the seismic zonation model proposed for crustal, interface, and shallow inslab; the gray zone is the deep inslab zone.

3.8 GMPE selection

Another important stage for the seismic hazard assessment is the selection of the Ground Motion Prediction Equations (GMPE), based on the specific parameters of a region. These equations are related to motion parameters and seismological parameters (*e.g.,* PGA, M_w, Strike, Slip, Rake, etc.).

There are some criteria for selecting the most appropriate GMPE (*e.g.,* Cotton *et al.,* 2006). Among the characteristics to consider in the selection are: the setting tectonic for which the equations were created, the magnitude, depth, distance, and if the authors consider the seismic site effect. Next, we present GMPEs used to assess the Seismic Hazard in southeastern Mexico.

3.8.1 GMPE used for earthquakes in SEM

Different GMPEs have been used in southeastern Mexico and Central America, among them, are Beauval *et al.,* 2013, Chiou and Youngs, 2008, 2014, and so on. There are some developed for earthquakes in the Mexican Subduction zone, for example, García *et al.,* 2005, Arroyo *et al.,* 2010. Others developed worldwide can be applied in the region, *e.g.,* Youngs *et al*, 1997; Abrahamsom and Silva, 1997; Zhao *et al.*, 2006; Campbell and Bozorgnia, 2008; Chiou and Youngs, 2014.

The selection of GMPE in this work was carried out by analyzing those created for global and regional earthquakes, considering a similar setting tectonic and the type of earthquake (crustal, interface and, inslab, Figure 3.14). Also, the magnitude range, type of distance, and depths were considered.

However, some GMPE curves are unavailable for distances greater than 300 and 400 km, and Tabasco state is lying approximately 360 km of distance from the Middle American Trench (Figure 3.15). It is important to mention that GMPEs for southern Mexico focusing on the Gulf of Mexico region are missing in some equations. To solve this issue, instrumental data from recent earthquakes were tested, which means that available data for some earthquakes were used to extrapolate the curve. In that way, the GMPE can be trusted for distances greater than the initially proposed (Figure 3.15 and 3.16).

The *Instituto de Ingeniería* belonging to UNAM *(II-UNAM)*, has an accelerometric seismic station in Tabasco state, in which some events that occurred at different distances and with different magnitude and depth were selected to compare with the acceleration values estimated by the GMPEs studied. These events are shown in Table 3.6:

Table 3.6 Some events used to superimpose the observed values in the GMPEs curves. Stations are: CHPA: Arriaga, Chiapas, TGBT: Tuxlta Gutiérrez Chiapas, HUAM: San Pedro Huamemula, Oaxaca, MIHL: Minatitlan, Veracruz. NITL: Santiago Niltepec, Oaxaca. VHSA: Villahermosa, Tabasco, SCCB: San Cristobal de las Casas. Amax, maximun acceleration recorded in te horizontal component.

Earthquake and source parameters	Station	Source-station distance	Amax recorded
September 23, 2017 M_w6.1, Depth: 10 km, Normal faulting, S254/D30/R-80	CHPA	134	20.18
	TGBT	221	4.95
	HUAM	76	28.56
	MIHL	177	5.99
	NILT	56	109.06
September 08, 2017 M_w8.2, Depth: 45km, Normal faulting, S315/D81/R	NILT	207	488.63
	HUAM	219	251.73
	MIHL	360	56.25
	VHSA	377	2.19
	SCCB	259	72.12

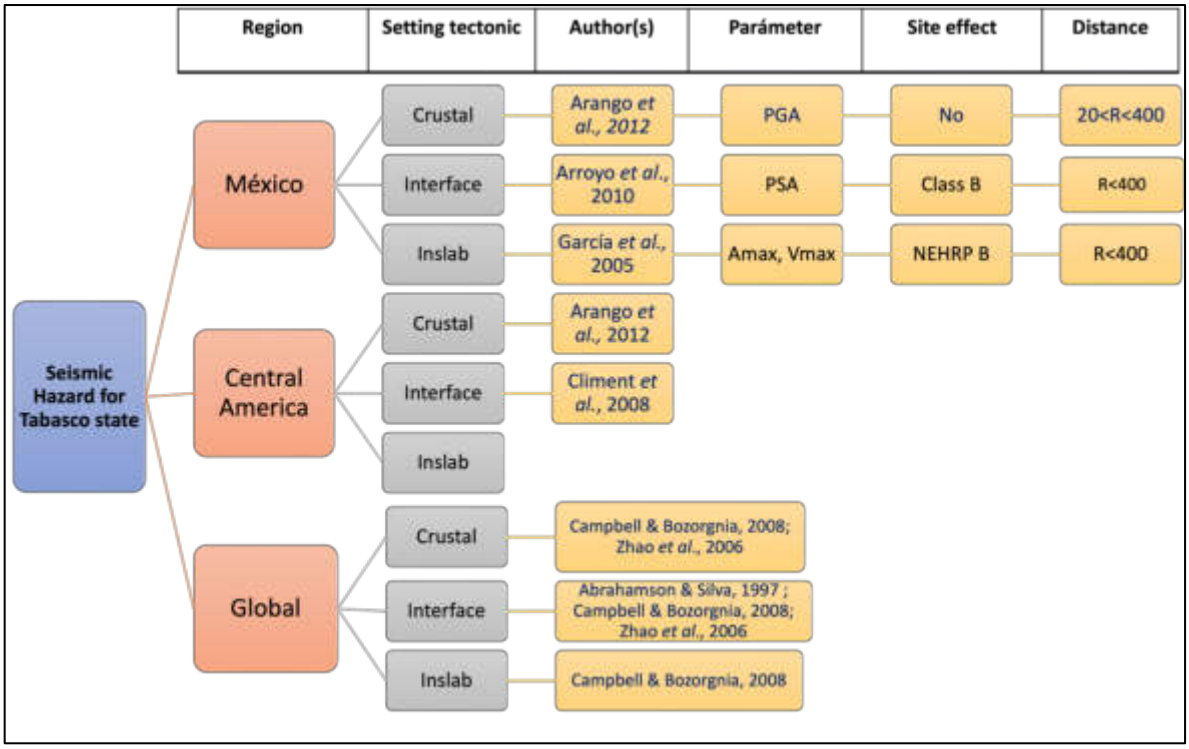

Figure 3.14. Showing the GMPEs and their characteristics analyzed in this work.

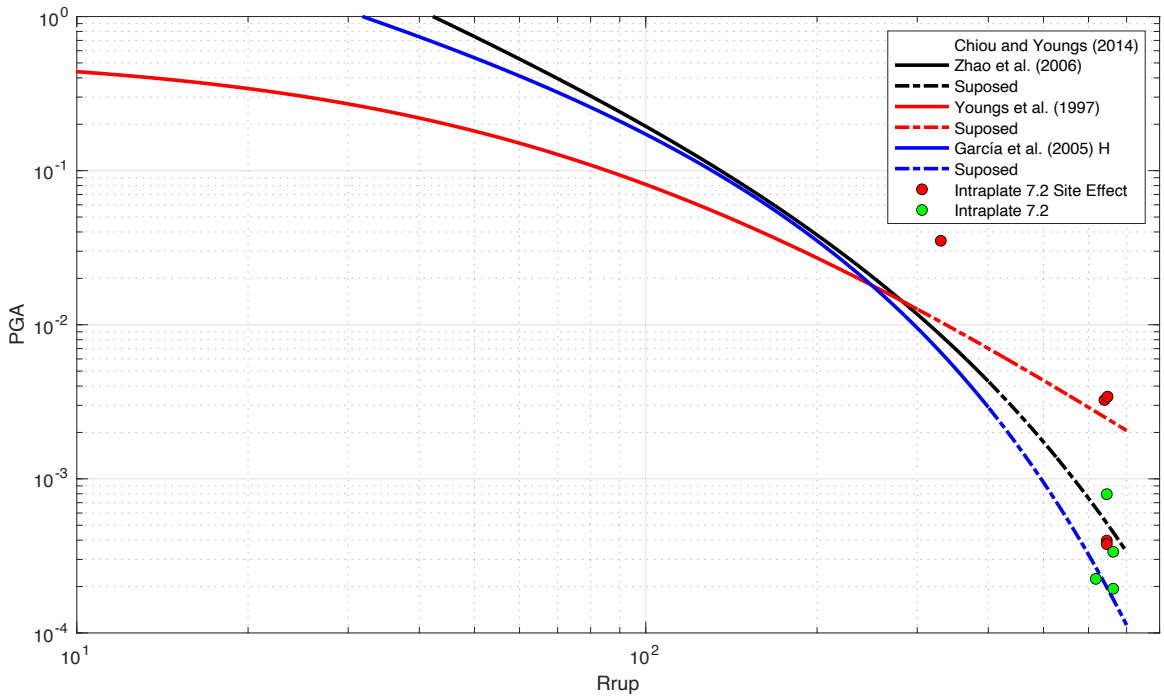

Figure 3.15. GMPEs available for distances up to 400 km for intraplate earthquakes. The extension of the curve was made following its tendency and rectified with earthquake data that occurred in southeastern Mexico.

3.8.1.1 GMPEs considering site effect

One of the influential factors, aside from the frequency range, is the type of soil in the study area. Soils have a tendency to amplify the movement of the elastic waves. Given this perspective and considering that Tabasco state is situated in a sedimentary basin where Quaternary sediments predominate, seismic site effect become a crucial that must be taken into consideration. A couple of GMPEs that account for the site effect were selected (Figure 3.16).

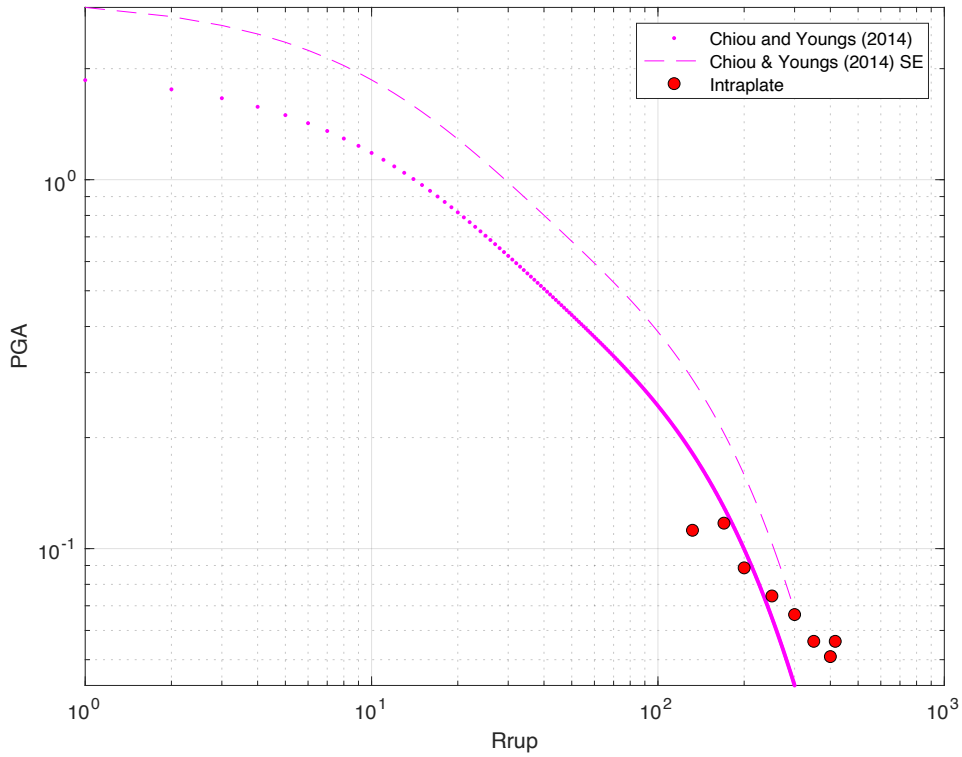

Figure 3.16 Comparison between GMPE curve of Chiou and Young, (2014) with site effect and without it.

Ultimately, considering the range of the elements range and characteristics specified in the GMPE, the selected equations were those developed by Chiou and Youngs. (2014) for crustal earthquakes. For interface events, Arroyo *et al.* (2010) and Zhao *et al.* (2006) were utilized, while Garcia *et al.* (2005) and Zhao *et al.* (2006) were applied for deep inslab events. The specified curves are effective for a range of 1<R<300 km. The chosen GMPEs will be employed to compute the seismic hazard maps for southeastern Mexico, which will be presented in the next chapter.

3.9 Discussion

While seismic models have been developed for southern Mexico and Central America to study seismic hazard assessment, there is a notable absence of focus on Tabasco state. In this work, we address this gap by developing an updated seismic model.

The data used to create a seismic zonation model encompass a seismic catalog, incorporating both pre-instrumental and instrumental databases compiled for the region.

The proposed model exhibits significant differences from previous models that encompass the study area (Zúñiga *et al*., 2017; Alvarado *et al*., 2017; Rodríguez-Lomelí and García-Mayordomo, 2019; by Sawires *et al*., 2020; García-Peláez *et al*., 2023). In this study, the Middle American Trench in the southern Mexico Basins has been subdivided into smaller zones compared to prior works. This subdivision takes into consideration the rupture area for large earthquakes and the coupling of Cocos-North American plates. Additionally, a broad zone has been defined in the Gulf of Mexico, accounting the basin's faults and offshore seismicity.

A gravimetric map proves instrumental in establishing precise correlations between geological and tectonic structures, thereby enhancing our capacity to delineate seismogenic zones. In the southern regions of Mexico, particularly north of the Tehuantepec Isthmus, a noticeable uptick in the Bouguer anomaly is discernible in the Tuxlas zone compared to the Salina del Istmo, Comalcalco, and Macuspana basins. The opposite happens in the Strike-Slip and Reverse faults provinces, where a low anomaly is present. It allows for complementing the outline of the seismic zones.

The southern Mexican basins are situated within the interior of the North American plate, hosting numerous small-to-moderate seismic events concentrated in a relatively compact area. This area is also scattered with oil wells and fields, reflecting the critical role of oil exploration and production in Mexico's southeast basins. Recent research has empashizes that various methods of oil and water extraction can induce alterations in the subsurface, attributed to factors such as fluid injection and pore pressure changes. As a result, its effects may result in low to intermediate-magnitude events. Consequently, these alterations may lead to seismic events of low to moderate magnitudes (SSN, 2022). In the southern Gulf of Mexico, moderate earthquakes have been recorded, falling within magnitudes range of $3.5<M<5$ and depths ranging from $3.5<h<5$ km. Noteworthy seismic events include those on February 9, 2007 with a magnitude (M_w) of 4.8 and a depth of 2 km, and on October 20, 2013 with a magnitude (M_w) of 3.8 and a depth of 18 km. The locations of these events were reported by SSN, with normal and strike-slip solutions for their focal mechanisms, respectively.

Most of these seismic events in the southeastern Mexico basins have predominantly occurred offshore. However, a detailed analysis becomes necessary due to the sparse distribution of seismic stations and the considerable epicentral distance of the sole seismic station in the Gulf of Mexico's southern states. This analysis may involve procedures such as re-location and determination of source parameters to establish a meaningful link between industrial activity and reported seismicity. The lack of a dense seismic network in the southeastern basins introduces significant uncertainty regarding the locations and magnitudes of earthquakes near oil wells in the Gulf of Mexico. Consequently, establishing a clear relationship between seismicity and oil production has proven challenging so far.

Two zones in southern Mexico are considered stable continental regions; they are the southern Mexico basins and Yucatán platform, where low to moderate seismicity is present. The presence of local faults in those regions with average lengths of 20 km, were used in Well and Coopersmith's relationships to estimate a M_w6.6 earthquake. In the south of the Gulf of Mexico, highlighting that the Jaltipán event had a M_w6.4 in the same area.

Several empirical relationships used for the homogenization catalog to M_w as the unified magnitude were analyzed to compare one-to-one plots. Sawires *et al.,* 2019 were chosen because most data sets were from SSN catalog and because their equations were generated for Mexican earthquakes. The different conversion relations between *mb* and M_w showed similar tendencies for a magnitude range of ~ $4.5 \leq M_w \leq 6$, nevertheless, the proposed for Mexican earthquakes was chosen.

The *G-R* parameters were obtained for the 21 seismic zones proposed. In crustal regions, *b*-values were from 0.73 to 1.96; considering the maximum expected magnitude, they are a little higher than those previously published for the westernmost part of the study area concerning crustal areas, maybe because of the seismic catalog and the of M_{min}>3.5 used. The estimated values for interface/subduction regions are 1.33, 1.79, 1.31, 1.01, and 0.73 in regions I, II, III, IV, and V respectively. In previous work (Zúñiga *et al.,* 2017; Rodríguez-Lomelí and García Mayordomo, 2019), a regional seismic zone was defined for the subduction Mexican area; the average value was estimated to be 1.23 compared with previous work. When the results are compared with some published values, they are higher than this work; it may be attributed to a study in a smaller area.

In the subduction region I, the value is similar to the proposed by Zúñiga *et al.,* 2017 and Sawires *et al.*, 2021; the result was compared only with this zone because their research encompasses the westernmost part of our work. Finally, in the shallow inslab I, II, III, IV, and V, the values are 1.96, 1.58, 1.31, 0.77, and 0.56; a little different from the previous one. The highest *b* values are related to shallow events and their type of faulting (Rodríguez-Pérez and Zúñiga, 2018).

4.1 Maps

A representation of a Probabilistic Seismic Hazard Analysis is through a seismic hazard map. This chapter shows the results of a probabilistic seismic hazard analysis map in terms of PGA (peak ground acceleration) and UHS (Uniform Hazard Spectra) for some important cities in southern Mexico. The first figures show the values for rock sites and different return periods. The second part considers the local site effect where data on shear wave velocities are available.

The seismic hazard maps were computed using R-Crisis software (see Chapter II). This program allows us an input different source geometry, recurrence values, and different parameters of the GMPEs. Maps of PGA were generated for seven return periods: 95, 238, 475, and 950 years. The iso acceleration maps were performed using the information from the latest chapters such as recurrence values obtained from the seismic catalog, the source geometry proposed, and some of the mentioned GMPEs, checking if those results are in the same units (cm/s^2, m/s^2, and g). All those maps were constructed with a grid spacing of 0.1° in Latitude and 0.1° in Longitude.

4.1.1 Seismic hazard map on rock

This chapter shows the maps obtained from applying the GMPEs of Chiou and Young (2014), Abrahanson *et al.* (2014), and Parker *et al.* (2022), with return periods, approximated 95 (10% probability of exceedance in 10 years), 238 (10% probability of exceedance in 25 years), 475 (10% probability of exceedance in 50 years), and 950 (10% probability of exceedance in 100 years). They are shown in Figure 4.1.

This map corresponds to a seismic hazard for rock sites. The highest hazard level is present in the southern region how it was supposed, which corresponds to Chiapas and Oaxaca states and the western part of Guatemala. In the Tabasco state, the values in PGA are of 0.2, 0.3 and 0.4 g.

These maps clearly show the effect of the distance: the longer the distance from the subduction zone, the lowest the seismic hazard level displayed in the contour lines. The lines of the highest values are parallel to the subduction zone and near the Gulf Coastal Plain are the lowest ones. The isoacceleration lines are similar to the isodepth lines of the Cocos plate subducting in North American plate

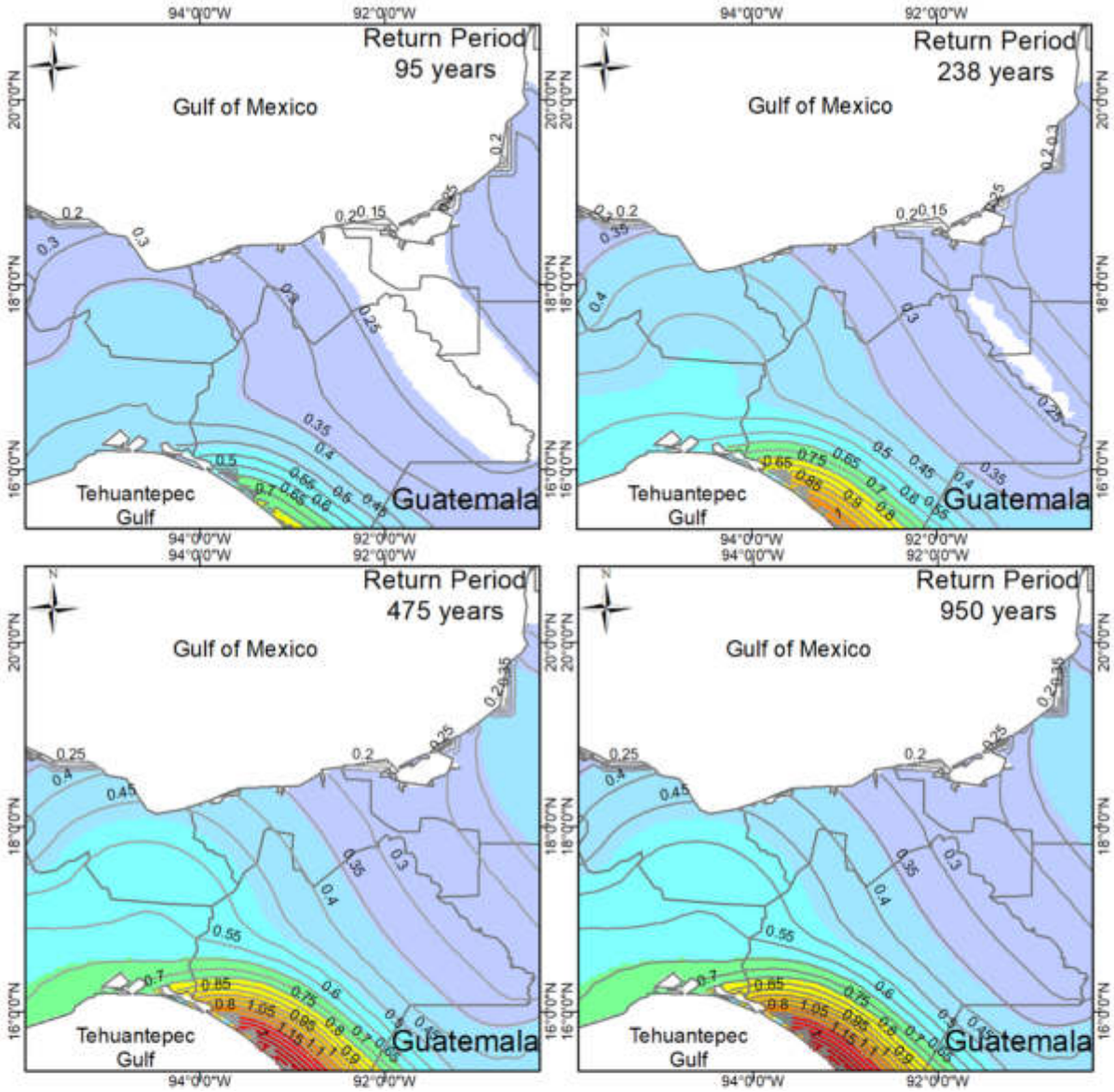

Figure 4.1.-Seismic Hazard Map for different return periods computed on rock

4.1.2 Seismic hazard map considering site effect

Local site effects strongly influence almost all seismic characteristics such as acceleration, amplitude, and ground motion frequency during an earthquake. In seismic hazard studies considering the local conditions can result in differences between the seismic hazard maps. Assessing seismic hazard maps in rock generally shows low seismic wave amplification, while in the evaluation in sedimentary basins higher amplifications are expected. Tabasco state is lying in quaternary material, some studies of shear wave velocities were carried out in the same place by Rodríguez-Vázquez (2018) and Alejandro Almeida (2020). The average shear wave velocity of the first 30 meters of subsoil, known parameter Vs_{30} obtained from surface profiles by Multichannel Analysis Surface Wave (MASW) test, shows range values lying in C, D, and E class according to NEHRP classification (Building Seismic Safety Council, 2003) for some Tabasco's municipalities. The classes were considered when computing seismic hazard maps.

The levels of seismic hazard for the southern part of the study area that were obtained in this work are similar to those published by other authors who studied tectonic zones in adjacent states; however, for Tabasco the comparison is possible only with the global Vs_{30} model (Heath *et al.,* 2020) where values coincide with those acquired in the two Tabasco's municipalities. This work presents the results of a seismic hazard map considering site effects.

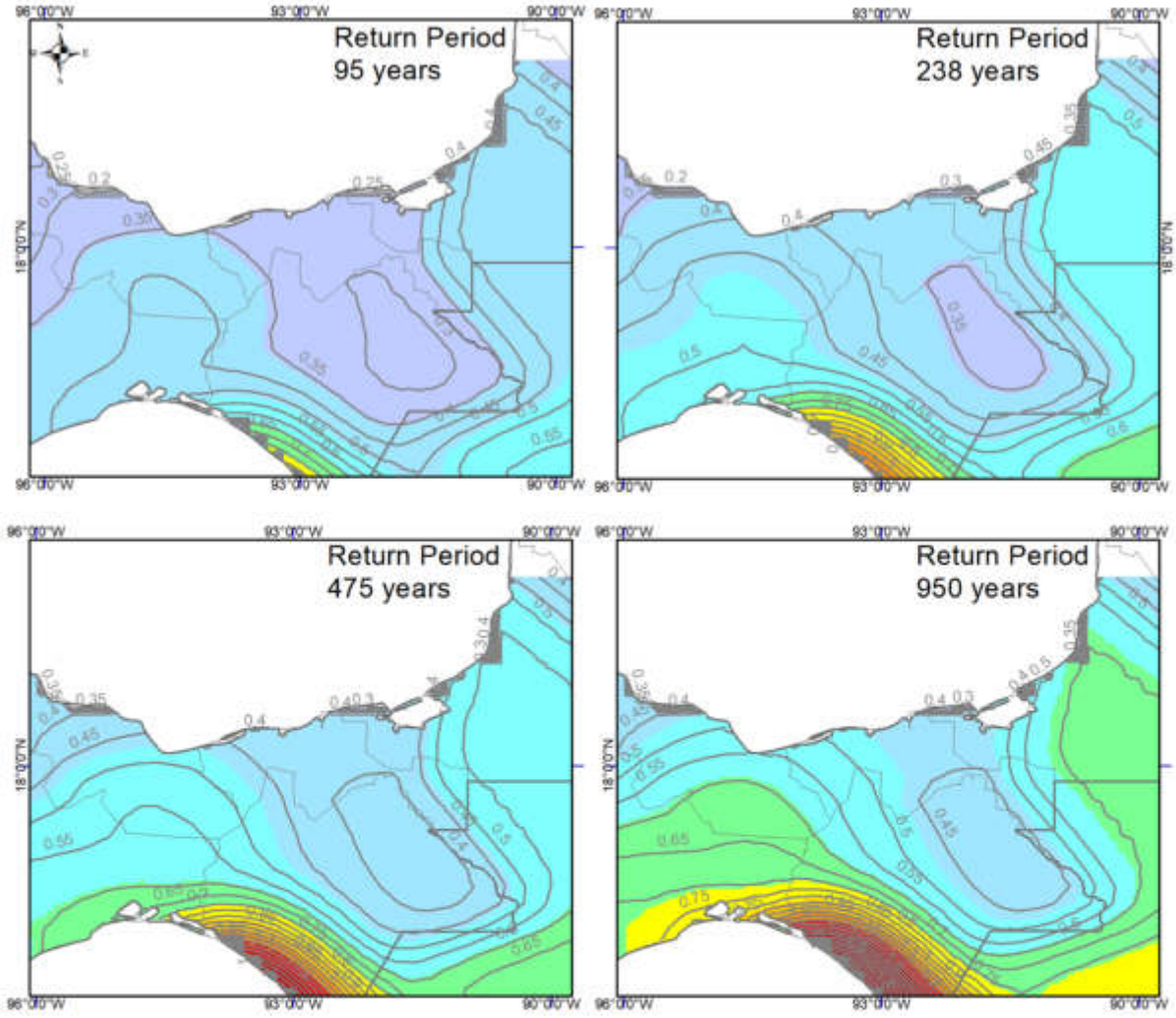

Figure 4.2.- Seismic hazard maps taking into consideration site effect of Vs_{30} values.

4.2 Discussion

The main purpose of this work was to obtain the seismic hazard map, that was estimated using R-Crisis software. An updated seismic catalog, homogenized to M_w using the magnitude conversion equation by Sawires *et al.* (2019), was used. The seismic hazard maps were performed using a grid of size 0.1° x 0.1° and were evaluated first on rock and second considering site effect for different return periods of 95 (10% probability of exceedance in 10 years), 238 (10% probability of exceedance in 25 years), 475 (10% probability of exceedance in 50 years), 950 (10% probability of exceedance in 100 years).

The results obtained in this work and those presented by Prodisis (*Comisión Federal de Electricidad, 2008*) are similar in the sense that the seismic hazard is decreasing toward Northeastern. However, the values of seismic hazard are different. Results show that the most hazardous zones in southern Mexico are close to the MAT, and they are dominated primarly by three main seismic sources, the first one is related to the interface of the subduction zone in Cocos and North American plates, the second is related with Strike-slip movement between Caribbean and North American plates, and third one with the in-slab events of the Cocos and North American plate. All those sources have a distance larger than 300 km from Tabasco state, and even if it can be seen that PGA decreases with the distance in direction to the Gulf of Mexico where Tabasco state is located, there is a considerable PGA value.

Some seismic hazard maps were published near or in the study area, such as Zúñiga *et al.* (1997 2017), which proposed a seismic regionalization of Mexico for seismic hazard purposes. They used several seismic catalogs for moderate and large earthquakes to obtain *a* and *b* values for the Gulf of Mexico, an interface region, and an intraplate zone. Compared with this work, there is wider seismic zonation. Benito *et al.,* 2012, prepared a seismic hazard map for Central America, covering the westernmost part of the study area showing PGA up to 610 cm/s^2, for a return period of 500 years. Rodríguez -Lomelí and García Mayordomo (2019), found that the most hazardous zone show PGA values of 600 and 750 cm/s^2, for a return period of 500 and 1000 years. The hazard maps performed by the CFE (2015), have results with lower values than this work and even with those documented in other works, maybe because they use a more general seismic zonation among other different input parameters. Recently, Sawires *et al*. (2023), show seismic hazard maps computed on rock and considering local site effect. Their maps present a decrease in PGA while far away from the trench. However, it does not cover southern Mexico; only the easternmost part of their study can be compared with this work.

The results obtained in this work are supported by an earthquake catalog up to 2020 including the M_w8.2 instrumental Chiapas event and *M*8.6 pre-instrumental Oaxaca earthquake, it is because the PGA values are higher than those published in other work.

Chapter V. Seismic site effects in Centro, Tabasco

5.1 Seismicity in Tabasco state

Southern Gulf of Mexico where are Tabasco, Veracruz, and Campeche states, is a region that has been exposed to shallow small earthquakes (M<4.5) and dense deep seismic activity related to the subduction of the Cocos plate.

Nevertheless, seismically speaking, this area has been damaged by earthquakes of moderate and large magnitudes that occurred in the surrounding states that are located near the Middle American Trench. A recent and large magnitude example is the 2017 Chiapas earthquake (M_w8.2, Sarlis *et al*., 2018; Suárez *et al*., 2019) with an epicenter of 360 km from Centro town (Figure 5.1) and having an intensity MMI of II-VI in Tabasco (SSN 2023). The event caused damage to buildings and civil structures (IPCET 2020, Figure 5.2). In the pre-instrumental epoch, a regional earthquake that occurred on September 23, 1902, had isoseismal values of V-VII in Tabasco state, looking similar in intensity to recent events.

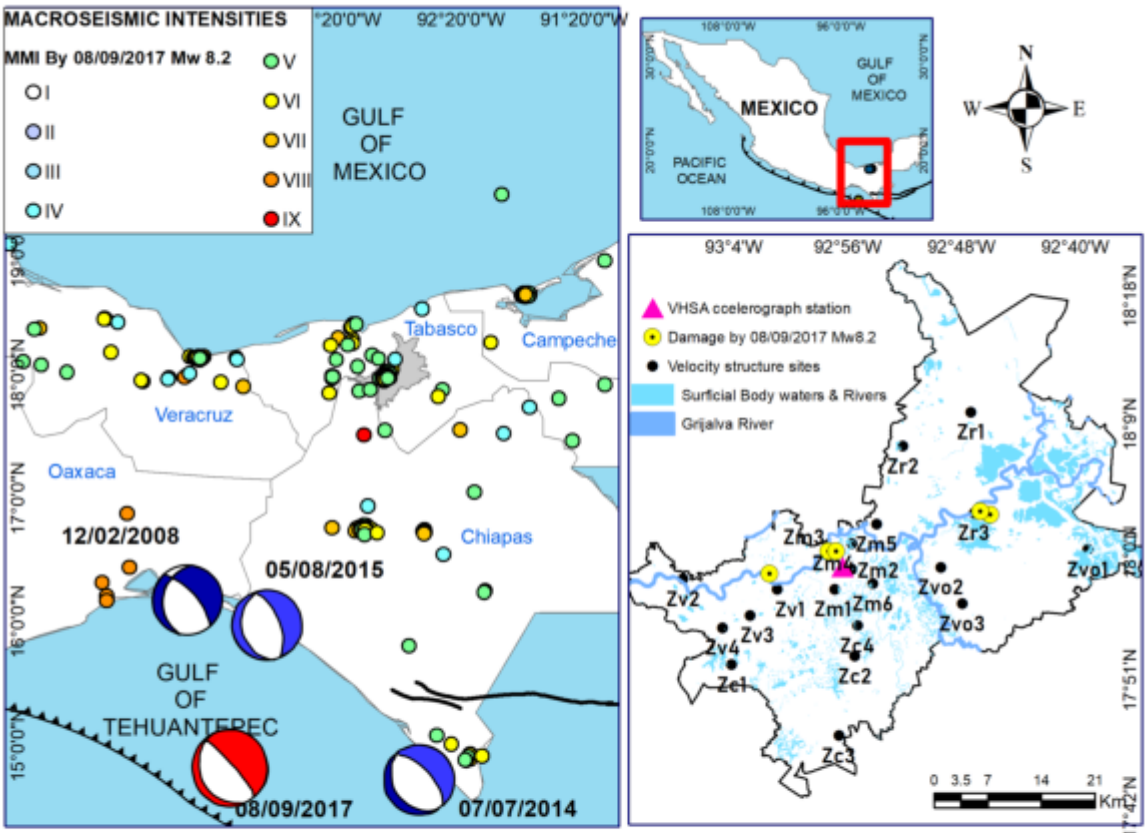

Figure 5.1. Left, setting tectonic of Southeastern Mexico; focal mechanism are from three events related to the subduction zone. red is the focal mechanism solution for M_w8.2 Chiapas earthquake. The intensity values were obtained from ¿Sintió un sismo? (www.sismos.uanl.mx webpage). Bottom right, principal hydrogeological systems crossing Centro municipality. Black dots indicate the location where seismic profiles were acquired.

Figure 5.2. Evidence of major damage caused in Centro, by September 8, 2017, M_w8.2 earthquake.(a) and (b) failure of sediments, landslides and liquefaction process, (c) shows the structural damage observed in the Zafiro Tower a building 16 stories high, (d) the roof of the catholic church de Nuestra Madre de Asunción de María, (e) failure of sediments and liquefaction process in a elementary school, (f) The Hotel Fairfield Marriot tower damaged during the event, and (g) the roofing of the Sendero mall collapsed.

5.1.1 Tabasco as a region of low-seismicity

The location of Tabasco state in a stable continental such as the Gulf of Mexico Coastal Plain region turns into the entity as a low seismicity region, characterized by low seismicity and a lack of strong ground motion (Schulte and Mooney, 2005). The Federal Power Commission (CFE in Spanish), generated a seismic regionalization where Tabasco state is classified as a *B* zone, which means that is a region with infrequent earthquakes (Franco *et al*., 2013; Suárez and López 2015; CFE 2015).

This state is located at 350 km from a tectonically active region configured by the subduction zone between Cocos and North American plates, the strike-slip boundary between Caribbean-North American plates, and the triple junction Cocos-Caribbean-North American (Figure 5.1).

Nevertheless, as was mentioned in earlier chapters, damages were reported in Tabasco state by M_w8.2, Chiapas´ earthquake. Considering that the epicentral distance was *c.a.* 350 km, the evaluation of local site effects was considered.

5.2 General setting of Centro, Tabasco

Centro municipality is the most economically significant area in Tabasco state, it covers approximately 1612 km^2. Villahermosa City is in this region, the state's most populated and urbanized area. The population has grown by 28% in the last 10 years (INEGI 2023). Industrial buildings, residential structures, and new avenues have taken place.

Geologically, Centro municipality is sitting on sedimentary deposits of recent ages. The urban zone is growing on old lake zones, quaternary soils, and sedimentary rocks (Larios-Romero and Hernández 1992, Figure 5.3) belonging to Neogene. These soft soils may be prone to significantly amplify seismic waves, trigger subsequent liquefaction, and cause remarkable damage, especially in urban areas built with no consideration of seismic criteria. Under this scope, a local site effect evaluation was carried out to determine the actual contribution of soil conditions to seismic site amplification in the municipality. This aims, to try to understand why some parts of the damage caused by the M_w8.2 earthquake were concentrated in certain areas of the city.

Figure 5.3. Villahermosa City at two different times. Left: Color green polygons represent Lagoons at Villahermosa, Tabasco in 1884. Right: grays regions are urbanized nowadays in the same city.

5.3 Seismic data acquisition

5.3.1 Seismic refraction

As a complement to the surficial wave technique, seismic data refraction was acquired at the same places. The process consisted of deleting bad signals and assigning a geometry of 5 meters between each geophone and in each profile. Other moduli of *SeisImager*, *Pickwin*, and *Plotrefa* were used to pick the first break on each seismic trace. Under the assumption that the waves were refracted in the same interface, the first-arrival phases were picked. The curves of distance versus time were made considering the source location, offset, profile length, and first break time. The software allowed the estimation of the *P*-waves velocity in the time-distance curves for each profile. Next, modeling velocity-depth profile given an initial model as input and iteratively ray traces with the aim of reducing the *rms* error between observed and calculated travel times. A feasible fit was obtained with values less than 6 meters/second. The P velocity got with this method and those obtained by MASW were very similar in the deep of the interfaces.

5.3.2 Surface waves data

A total of 20 seismic profiles of surficial waves were performed using the MASW technique. It determines the 1D velocity structures of the 2D velocity distributions of shear waves (Park *et al.* [1999] 2007). The distribution of the acquisition points is in Figure 5.1, right. *Seisimager* software (Park *et al.,* 1999) was used to process data where in each site and was obtained the dispersion curve through the *WaveEq* module where the fundamental and higher modes can be visualized (Aki and Richards 2002), to obtain the fundamental mode. The Fourier transformation was computed with a range of 0-40 Hz and with a phase velocity range of 0-800 m/s with interval values from 0.5 s. The pre-processing of the 20 profiles consisted of killing bad traces, assigning the offset of 5 meters between each trace, and setting up the shot to gather records 5 meters at the beginning and at the end of the profile.

Because of dispersion curve picked represents the velocity structure below the dispersion point, it is dominated by the velocity and the effects caused by lateral variations in the received spread, these spreads give as a result a greater resolution in the 1D approximation model.

The different colors in the spectrum show the phase velocity, the signal, and the amplitude which is a function of the wavelength.

5.4 Vs_{30} parameter and well data

V_{S30} is a parameter easily obtained by means of a geophysical test with low cost. It is a parameter that summarizes the behaviors of the soil, adding to it is considered a representative quantity by NEHRP (National Earthquake Hazards Reduction Program (NEHRP, 2020) and IBC (International Building Code (IBC 2006) that is used for the site classification in earthquake hazards studies. The time-averaged shear-wave velocity in the upper 30 m (Dobry *et al.,* 2000) is calculated with the following expression:

$$V_{S30} = \frac{30}{\sum_{i=1}^{N} d_i / v_i} \qquad (5.1)$$

where d_i and v_i denote the thickness (in meters) and the shear-wave velocity in m/s of their formation or layer, respectively. N_i indicates the number of layers within 30 m. V_{S30} was introduced by Borcherdt (1994) to provide unambiguous definitions of site effect to estimate spectra response. The new building code assigns one of six soil profile types to a site, from hard rock defined as A-type up to soft soils defined as E-F types (Table 5.1).

The aim of this study is to generate a model of 30 meters in depth, which is obtained by the dispersion curve. Figure 5.4 shows three examples of records of the measurements, they are the dispersion phase velocity *vs* frequency in the sites Zr2, Zm5, and Zvo1. The interval of the separation was 5 meters in each geophone. The next step in the process was the inversion of the dispersion curves, aiming to get the shear wave velocity models and depths carried out to get 1D shear wave velocity.

This processing stage involves different subsoil properties such as *P* and *S* wave velocities, the thickness of the layers, and density. An initial parameters model was used as input to get the theoretical shear wave velocity from the dispersion curve. The goal of this section was to get the model of shear wave velocity average between the theoretical and observed model until the error is minimized by iterating.

Some models were used as input derived from SPT (standard penetration test) that were near the locations where seismic profiles were performed. All the *rms* were less than 6%, which means a good fit between models.

The V_{S30} values of the 20 sites were determined resulting as follow: $V_{S30} \geq 539$ m/s are Zvo2, Zm6, and Zr3, according to NEHRP which corresponds to soil class C characterized by a very dense soil. Sites class D with $181 < V_{S30} < 345$ m/s corresponds to the locations Zm1, Zm2, Zm3, Zm4, Zvo3, Zr1, Zr2, Zv1, Zv2, Zc1, Zc2, Zc3, and Zc4, are correlated with stiff soil. The lowest values of $V_{S30} \leq 180$ m/s were located in the sites Zm5, Zvo1, Zv3, and Zv4. The site with small values are nearby surface water bodies (Figure 5.1, bottom right). It can be correlated with strong ground motion amplification.

Near those study points, outcropping is the high compressibility of silts and inorganic and organic clays. The Zv3, Zv4, Zm5, and Zvo1 sites were classified as class E. Here, the geotechnical basement is located under 25 m depth.

Most V_{S30} sites in Centro town correlate to classes D and E of NEHRP (Figure 5.5). The V_{S30} in the study area varies from 124 to 570 m/s. Low V_{s30} values cover most parts of Centro while the highest values ranging between 480-570 m/s were found in the central part of Centro town.

Table 5.1. Site categories in NEHRP Provisions (BSSC 1997).

Soil Profile Type	**Rock/Soil description**	**V_{s30} m/s**
A	Hard rock	>1500
B	Rock	760-1500
C	Very dense soil/soft rock	360-760
D	Stiff soil	180-360
E	Soft soil	<180
F	Special soils requiring site-specific evaluation	

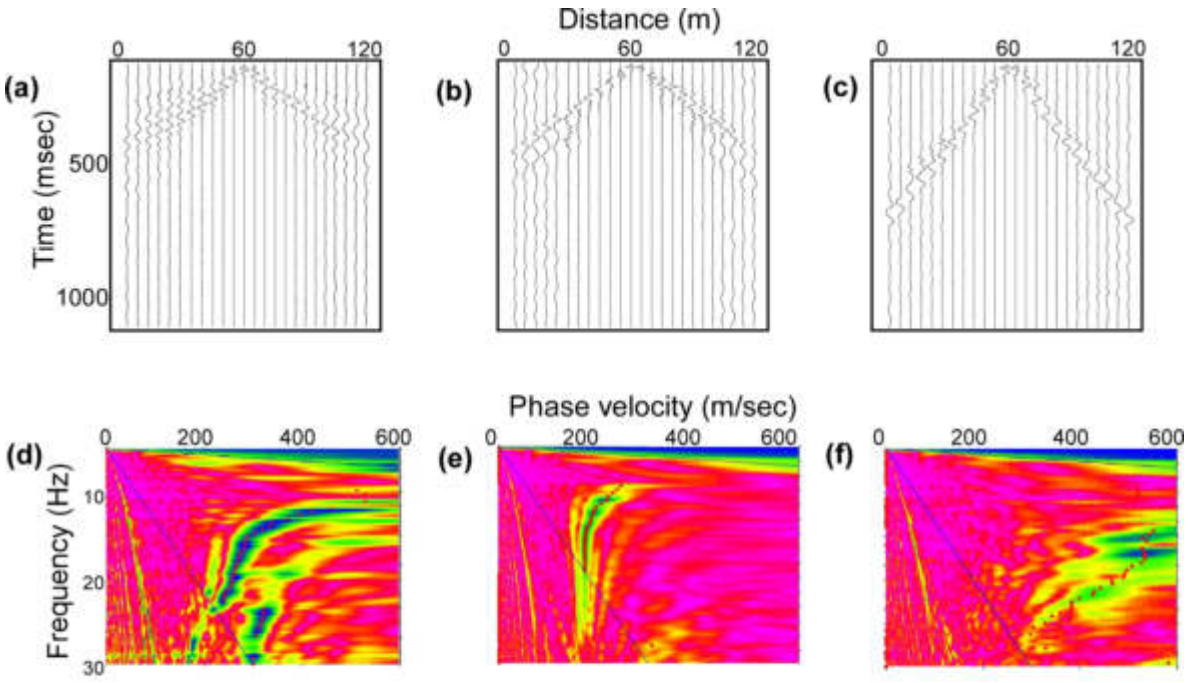

Figure 5.4. Up: seismic profiles got from some studied points. Down: Dispersion curves computed by the Seisimager of Zr2 (a and d), Zm5 (b and e), and Zvo1 (c and f).

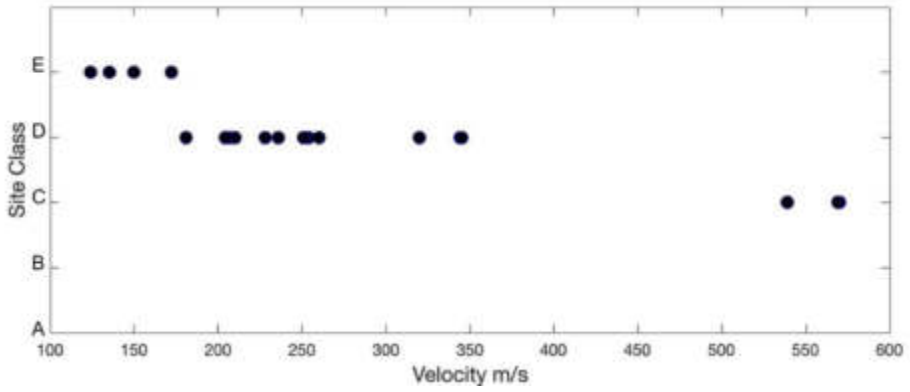

Figure 5.5. Site classification for Centro Municipality was obtained in this work. The most part of the measurements in the study area corresponds to C and D class according to NEHRP classification.

An important stage in assessing a seismic hazard study is the site characterization, which is performed to aim a near-surface shear wave velocities values in the first meters deep. Vs_{30} parameter is accepted to this site classification. A shear wave velocity study allows a classification such as NEHRP (National Earthquake Hazard Risk Program) and IBC (International Building Code, Table 5.1). With this approach, a series of linear profiles of MASW (Multichannel Analysis of Surface Wave) were carried out in Centro municipality.

Regarding geotechnical available data in the study area, three seismic study points were correlated to. Zr2, Zvo2, and Zvo3 are close to geotechnical boreholes P1, P2, and P3 (Figure 5.6). The geotechnical data include Standard Penetration Test (SPT) information and a detailed description of the thickness and lithology of each well. The deep reached was 10 m for P1 and P2, and 25 m for P3 boreholes. The distances from Zr2, Zvo2, and Zvo3 were 500, 300, and 200 meters respectively. Zr2, Zvo2, and Zvo3 sites have the lowest values of shear wave velocities, which correlate according to Palma-López *et al.* (2017) with unconsolidated soils in Centro.

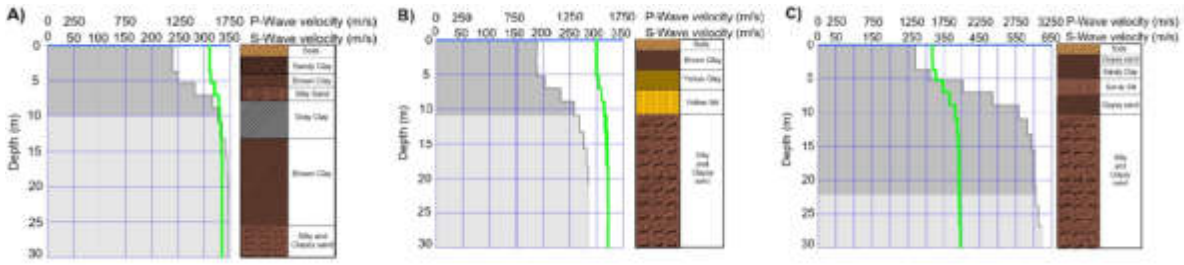

Figure 5.6. Data correlations between the velocity structures of this work's Zr2, Zvo2, and Zvo3 sites, and the thickness and description of the P1, P2, and P3 Borehole lithology obtained by Ovando-Arias (2019).

5.5 Transfer functions

An important parameter to bear in mind is the regional geology, for this case Centro municipality is on the Macuspana basin, which is a Quaternary structure with soft horizontal deposits without significant spatial variability, which can be modeled as 1D, that is why we obtained the transfer functions (TF) of each site by means of the Thomson-Haskell method (Aki and Richards 1980) and considered a vertical propagation of *SH* waves. Those (TF) obtained, had resonance frequency (f_0) values ranging $0.92 \leq f_0 \leq 2.6$ Hz for the sites Zr1, Zr3, Zvo1, Zm1, Zm2, Zm3, Zm4, Zm5, Zv1, Zv2, Zv3, Zv4, Zc2, Zc3 and Zc4. It corresponds to soft soils. On the other side, the highest values are greater than $f_0 \geq 4.1$ Hz and they are located at sites Zm6, Zc1, Zr2, Zvo2, and Zvo3 (Figure 5.7). As can be seen, the maximum amplitudes of the transfer functions are located where the V_{S30} values are less than 150 m/s. The sites Zv4 and Zm5 present $f_0 < 1.0$ Hz, and amplitudes of 4.2 and 4.3 respectively.

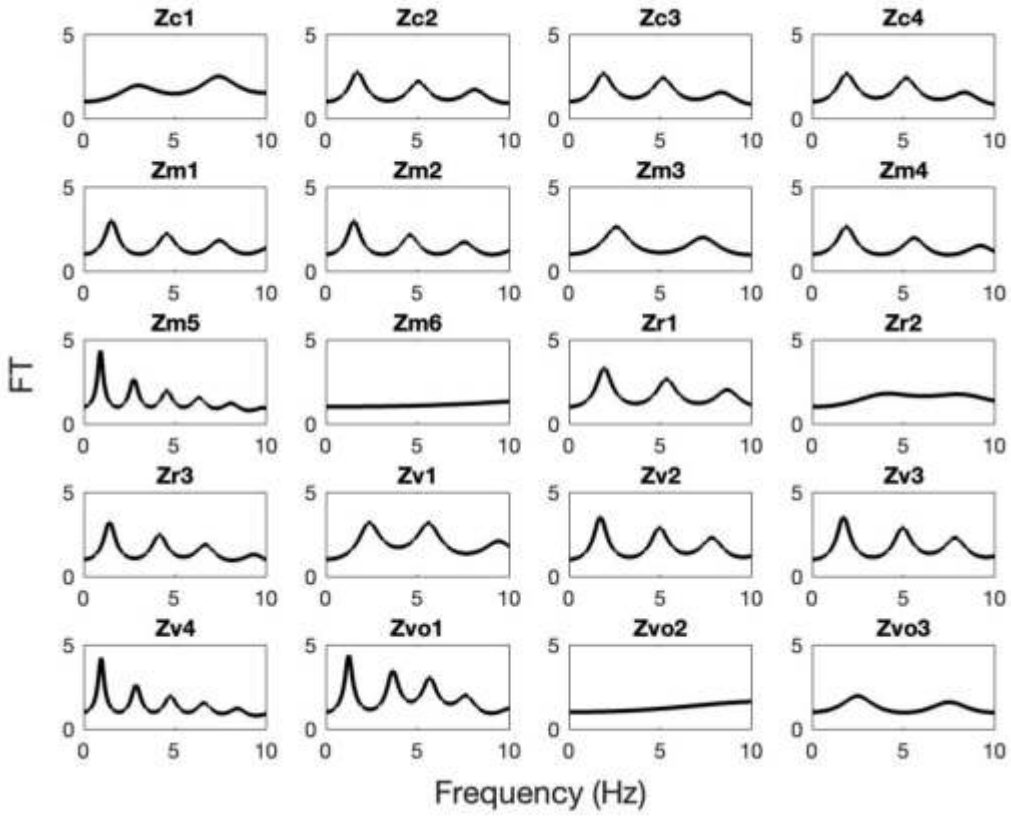

Figure 5.7. Transfer functions of the 20 studied points.

5.5.1 Regional earthquakes and transfer functions

In Tabasco state there is one accelerometric station is installed. This is VHSA station located in Villahermosa city, which is part of the national accelerograph network operated by the *Instituto de Ingeniería* of UNAM. VHSA is a station located on soft sediments. To estimate the spectral ratio horizontal/vertical (H/V) of the site, three seismic records in the same station and with good quality were selected, corresponding to the February 12, 2008 (M_w6.6), July 7, 2014 (M_w6.9), and August 5, 2015 (M_w5.8) earthquakes. Figure 5.8 represents the *H/V* ratio for NS/V and EW/V components for the three events, and the transfer function of the VHSA site. It can be seen that the transfer function reproduces the resonance frequency (f_0 = 0.9 Hz) in both *H/V* ratios and the second vibration mode near 3 Hz. It I important to highlight that the TF of the VHSA site is similar to the Zm5 point.

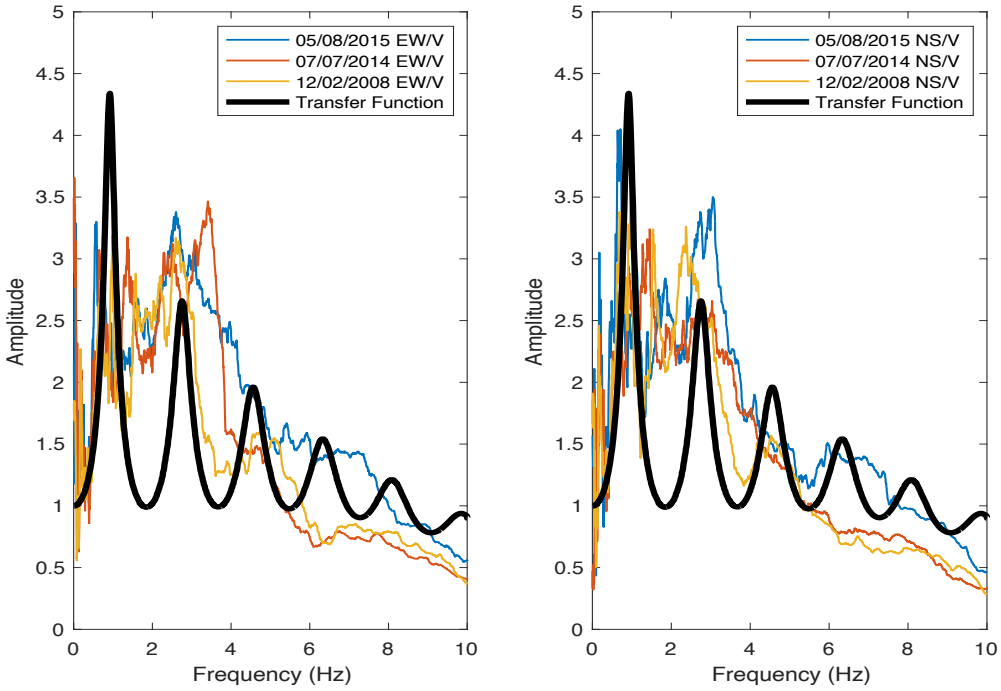

Figure 5.8. H/V ratio for NS/V and EW/V components for the February 12, 2008 (M_w6.6), July 7, 2014 (M_w6.9), and August 5, 2015 (M_w5.8) earthquakes, and the transfer function of the VHSA site.

5.6 Synthetic strong motion accelerograms

The TF obtained reproduces the *H/V* spectral ratio of VHSA. Under this scoop and to extract the site response of the VHSA site. Its TF was deconvolved and the accelerogram deconvolved of the July 7, 2014 earthquake was used as the input signal at the base of the velocity structures performed by MASW technique and seismic refraction in the study area.

The synthetic strong motion accelerograms for the July 7, 2014 earthquake (M_w6.9) for the sites Zc1, Zc2, Zm5, Zr1, Zvo1, Zvo2, Zvo3, Zv1, and Zv4, are depicted in the Figure 5.9.

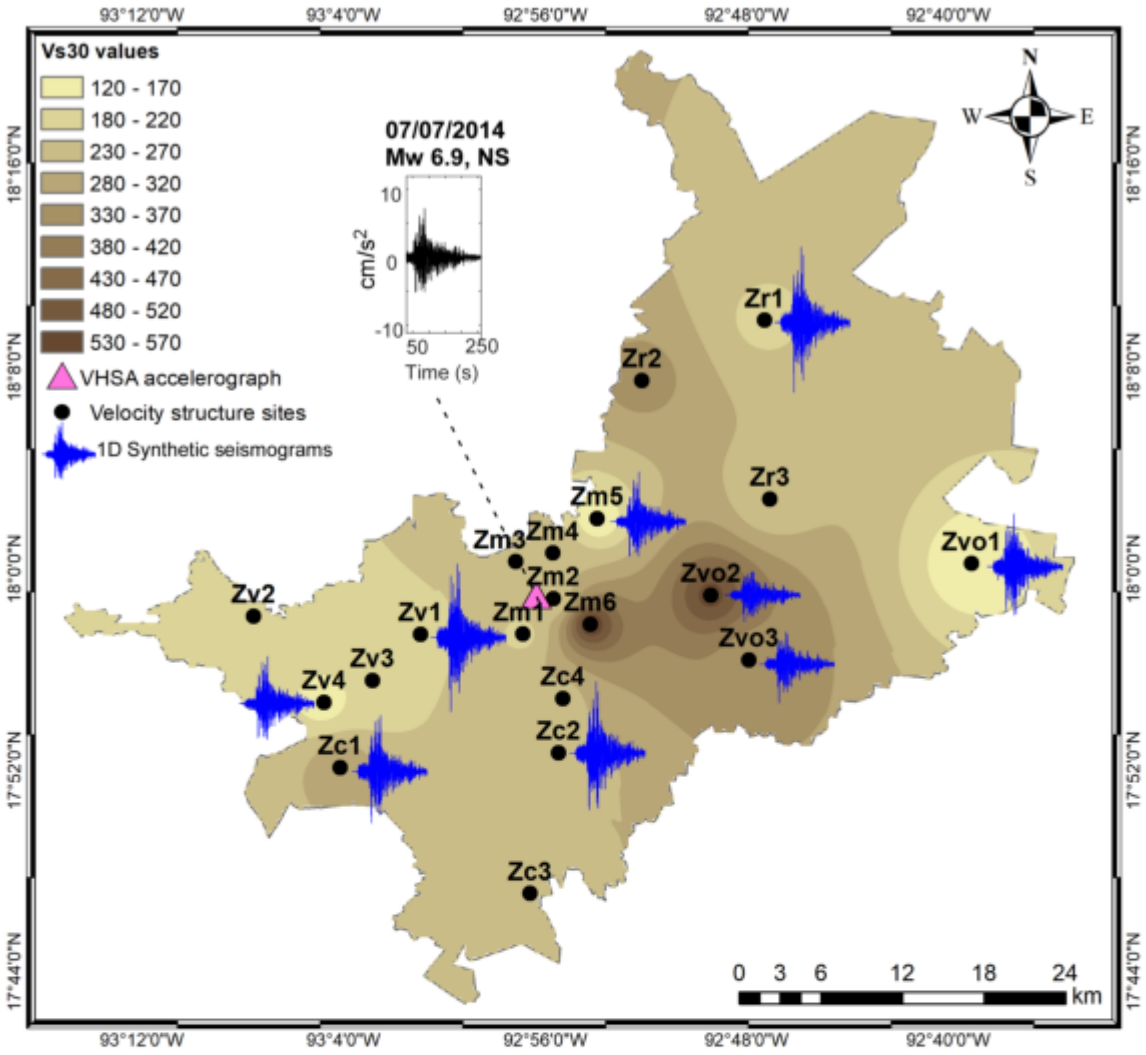

Figure 5.9. 1D synthetic seismograms for some study sites. V_{s30} values generated for Centro town, cold colors regions show the highest shear wave velocity values. Black dots represent the seismic profiles.

Next, regarding the damages caused by the Chiapas earthquake of September 8, 2017 (M_w8.2) the transfer functions with the V_{S30} distribution and some of the damages reported were correlated (Figure 5.10).

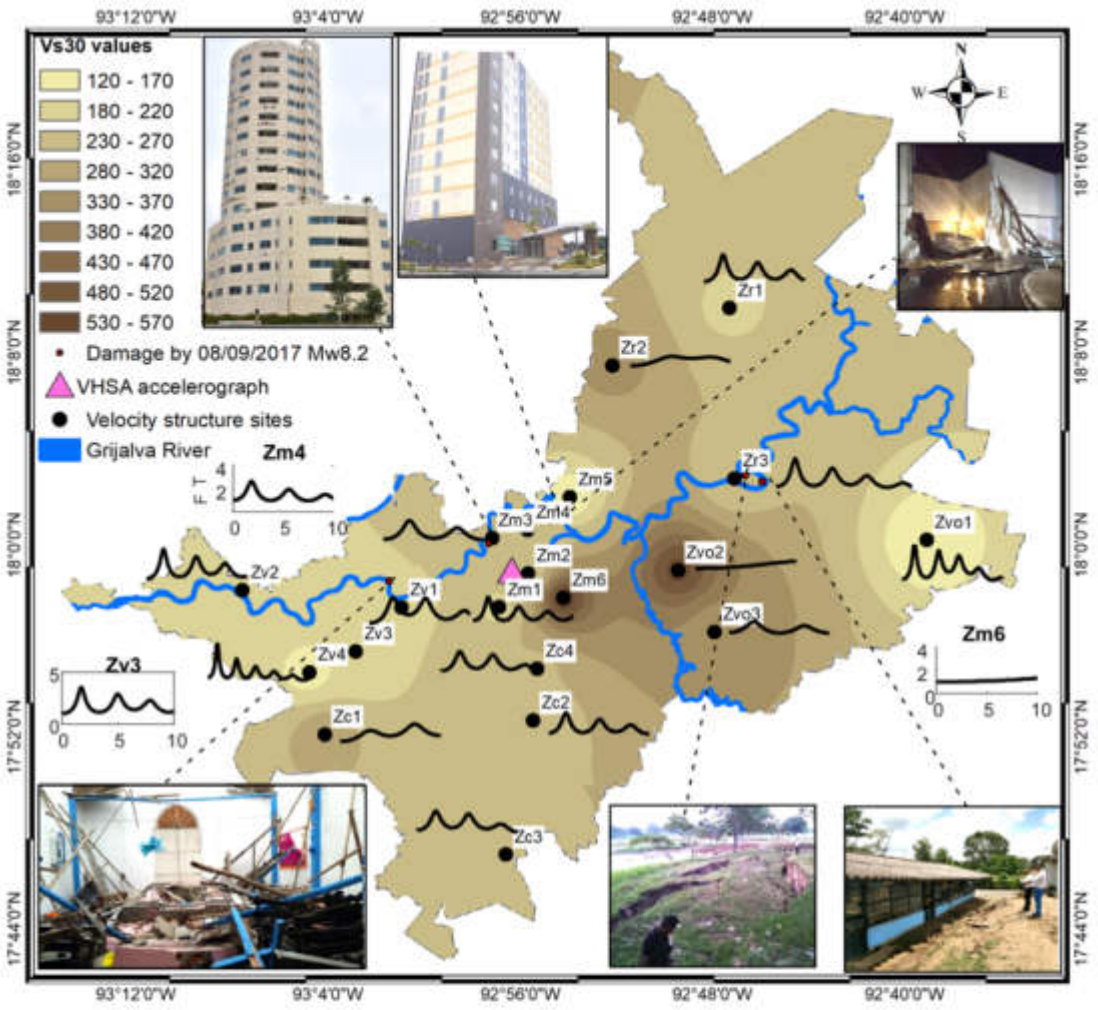

Figure 5.10. V_{S30} map with the transfer functions obtained from the velocity structures.

5.7 Fundamental frequency of Centro's buildings

Some important buildings are near some studied points. In a close distance to VHSA and Zm1 sites are located the Zafiro Tower and the Hotel Fairfield Marriot. The Zafiro Tower is a 70 meters tall building that have 16 floors and the Fairfield Marriott Hotel has 43 meters tall. To assess the correlation between the fundamental frequency of resonance of the site and the frequency of resonance of the building (f_b), the empirical relation proposed by Goel and Chopra (1997) was used in order to get the fundamental frequency of those buildings:

$$T_b = 0.052h^{0.9} \qquad (5.2)$$

where h is the height in meters, and T_b is the fundamental period. In the Table 5.2 is the comparison between f_b and f_0 of the nearest site(s) to the buildings analyzed.

Table 5.2. Parameters used in the comparison of the fundamental vibration of buildings and the site response of site more damaged.

Building	**Height (m)**	**T_b (s)**	**f_b (Hz)**	**Nearest Site 1 (f_0)**	**Nearest Site 2 (f_0)**	**Nearest Site 3 (f_0)**
Zafiro tower	70	2.38	0.42	Zm3 (2.61 Hz)	Zm4 (1.8 Hz)	VHSA (0.9 Hz)
Fairfield Marriot Hotel	43	1.54	0.65	VHSA (0.9 Hz)	Zm1 (1.52 Hz)	
Catholic Church de Nuestra Madre de Asunción de María	11	0.45	2.22	Zv1 (2.39 Hz)	-	-
Sendero mall	12	0.48	2.05	Zm4 (1.88 Hz)	Zm5 (1.55 Hz)	-

As is shown in Table 5.2 and Figure 5.10 the Zafiro tower has a f_b lower than the f_0 values of the nearest Zm3, Zm4 and VHSA sites. In the case of the Fairfield Marriott Hotel, the f_b is closest to f_0 of the VHSA site; while in the site where the Catholic Church is located both f_b and f_0 values are very similar.

In the Church site and in the Sendero mall the structure and roofing collapsed. Other damages were reported, as is the case in an elementary school, located near the Zr3 site where landslides occurred of approximately 30 cm and liquefaction processes were also present. Another municipality in Veracruz state presented liquefaction. It has the same epicentral distance from the M_w8.2 earthquake. The soils there presented $0.77 \leq f_0 \leq 1.07$ (Guzmán-Ventura *et al.,* 2020), almost identical to those obtained in this work.

5.8 Discussion

The seismic site characterization which shows the effects on the local geology, was evaluated at Centro municipality. The quaternary sedimentary material was investigated in the study area

through geophysical studies with the MASW technique. Those sediments belong to the Tertiary Basins of Southeast Mexico.

The V_{s30} parameter distribution was classified according to NEHRP as sites class C with $V_{s30} \geq 539$ m/s, class D with $181 < V_{s30} < 345$ m/s and, class E with $V_{s30} \leq 180$ m/s.

The sites classified as class C are located over silty sands of low to medium compactness, high and low compressibility silt, and low and high plasticity clays of soft to medium consistency. The competent stratum is found at varying depths of approximately 7 m, increasing towards the West-Northwest, presenting $V_{S30} \geq 400$ m/s.

The class E sites are Zm5, Zv3, Zv4, and Zvo1 points, they are on alluvial and marshy sediments of the recent Quaternary, reaching two meters. Underlying is a competent stratum with a thickness of 8 m, where silty and clayey sands of very dense compactness underlie, showing a change in the velocity values for this interface of 313 m/s, increasing to 570 m/s for the one more consolidated layer. They are characterized by V_{S30} parameters in a range of $124 \leq V_{S30} \leq 172$ m/s. In these sites, the most competent stratum is at depths greater than 25 meters like De la Fuente *et al*. (2012). These low shear-wave velocity values were located on sites with unconsolidated Quaternary deposits originating from river floodplains and lacustrine areas characteristic of the Tabasco state. In regard to, the most significant damage caused by the September 8, 2017 earthquake (M_w 8.2) was reported in the north and northeast portion of the Centro in the areas (Jesus de la Cruz *et al.*, 2017). It coincides with the lowest values of V_{s30}.

Other characteristics to consider in Tabasco are the largest number of annual rainfalls, its complex hydrological network, the low topographic relief of 20 m.s.n.m., two of the biggest rivers of Mexico passing there, and numerous streams.

All those, together with the sedimentary rocks and geological structures such as basins, help to the creation of many numbers of bodies of water of different dimensions, which means that during an earthquake, strong ground motion amplifications can be expected as well as liquefaction, failure of soils, and landslides.

The seismic site effect is confirmed by the transfer functions obtained from 1D velocity structures that had resonance frequency values varying from $0.9 \leq f_0 \leq 2.0$ Hz, it coincides with the locations

nearest to river floodplains and lacustrine areas. The TF also coincides with the spectral ratio H/V of three regional earthquakes that originated in the Mesoamerican trench recorded in the VHSA accelerograph station. With this instrument, two vibration modes in f_0 = 0.9 Hz and f_1 = 2.5 Hz (first high mode) are also identified in the TF The deconvolved acceleration record of July 7, 2014, was used as the input signal to model 1D synthetics in the study area. These synthetics records show the strong ground motion amplitudes near floodplains and lacustrine areas where damage to buildings during the September 8, 2017 earthquake (M_w8.2) was documented, as well as the liquefaction process and the failure of the ground near the Zr3 site.

As seen, Centro Tabasco presents seismic site conditions, presenting low resonance frequencies and saturation of soft soils, hence, the municipality and Villahermosa City can be considered a prone area to suffer severe damage during regionals earthquakes, as occurs in Mexico City.

Chapter VI. Uniform Hazard Spectra in some urban zones

In Southern Mexico, some economically important cities related to the oil and gas industry are located. In this work, their seismic hazard was studied in detail by one representation of the Uniform Hazard Spectra (UHS) in terms of acceleration. This chapter aims to show the seismic hazard in Tabasco state's most populated urban center because of its quick infrastructure and population rise.

The results of the UHS for Villahermosa, Tabasco; Paraíso, Tabasco; Coatzacoalcos, Veracruz; Ciudad del Carmen, Campeche; Tuxtla Gutiérrez, Chiapas; and Tapachula, Chiapas are shown in this chapter with an ascending way according to the distance to the Middle American Trench.

6.1 Tapachula, Chiapas

One of the most populated cities in Chiapas state is Tapachula, which has been widely studied by seismic hazard studies due to its closeness with the subduction zone. The spectral acceleration values obtained in previous works correspond to 1200 cm/s^2 for a return period of 500 years (Figure 6.1 down left.). Apart from its closeness to the subduction zone, in this work, this city is considered because of its importance in the fisheries industries, ports, marine transportation, tourism, etc.

In Figure 6.1, the green lines in the UHSs were obtained for rock with Vs_{30},>700 m/s. Those considering site effects for different return periods (95, 238, 475, and 950 years) are in the blue lines spectrum.

In this case, for Tapachula, Chiapas it was possible to compare the return periods of 475 and 950 years with Rodríguez-Lomelí and García-Mayordomo (2019) where two UHS are published and represented in this work with the pink line. A difference is clear in the intensity of approximately 0.35 *g* for both return periods; however, a different and wider updated catalog and different GMPS were used here.

The results in this work show higher values with respect to Prodisis; however, this software can provide a general estimation of the seismic hazard, but it is needed a more detailed study for a better definition in southern Mexico and especially in regions with low seismicity such as Tabasco's state.

In all USH the form is similar, the peak is between 0.1 and 0.4 seconds, varying each one in intensity and being smaller for Prodisis and higher for those obtained in this work with site effect.

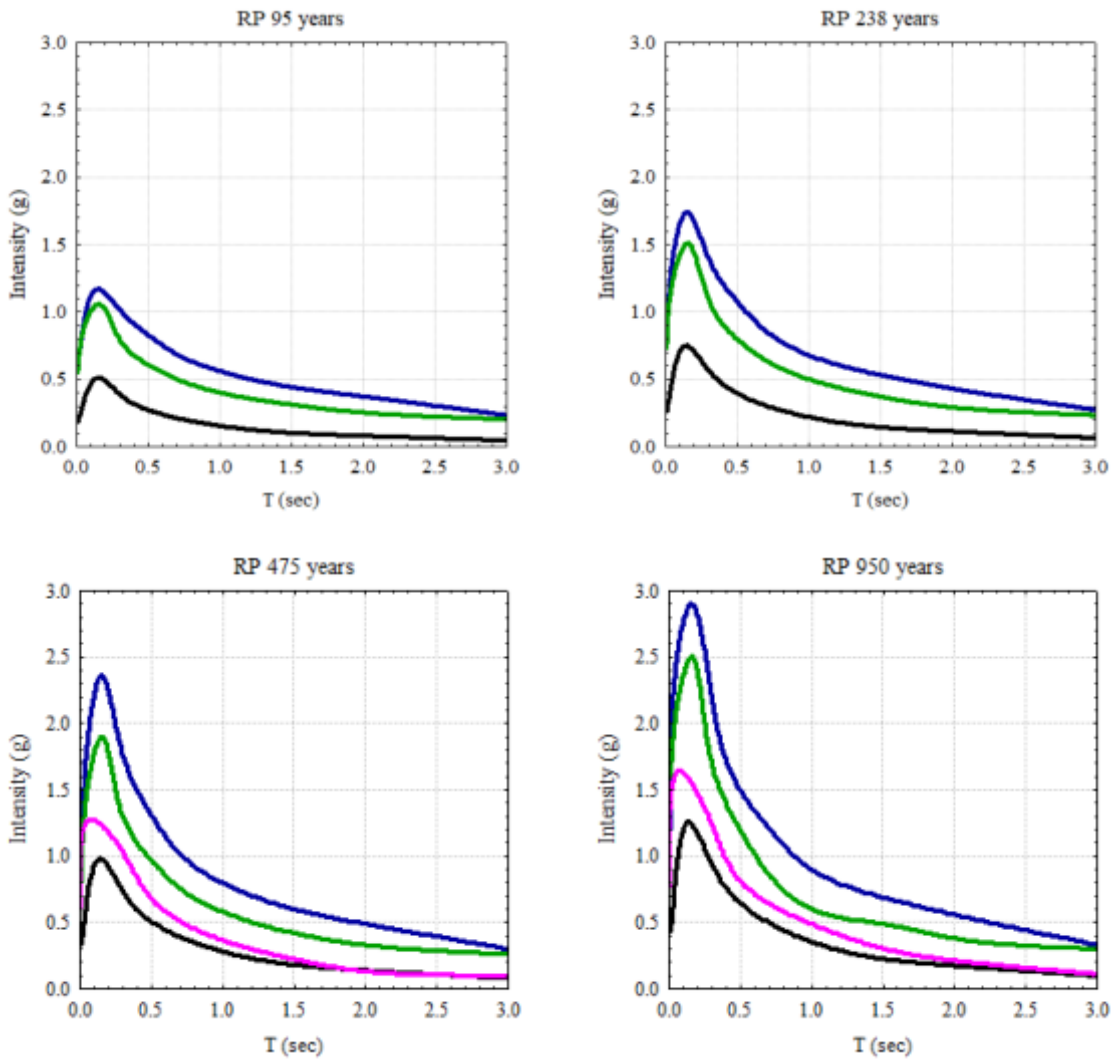

Figure 6.1 UHS in Tapachula, Chiapas for different return periods. Green line for rock, blue line considering site effect with Vs_{30} of 200 m/s, pink line are the results of Rodríguez-Lomelí and García-Mayordomo (2019), and black line data obtained from Prodisis.

6.2 Tuxtla Gutiérrez, Chiapas

The rapid growth of the urban zones in Tuxtla Gutiérrez has left to use agricultural areas for new residential ones, therefore, the city has been built in no adequate zones such as hillsides.

Seismologically, the municipality has been affected by large intraplate events such as October 21, 1995, M_w7.2 which had an A_{max} of 437 cm/s^2. Rodríguez-Lomelí and García-Mayordomo (2019) obtained the UHS for 500, 1000, and 2500 return periods. Again, the values in this work are slightly higher for 475 and 950 years of return period.

Prodisis' spectrums are smaller than in this work approximately 0.4 *g* (Figure 6.2 down). Pink lines represent the results obtained from a Chiapas seismic hazard study with 500 and 1000 years return periods, and they are smaller in this work, the differences can be attributed to the period used in the catalog and a constrained study area compared to this research.

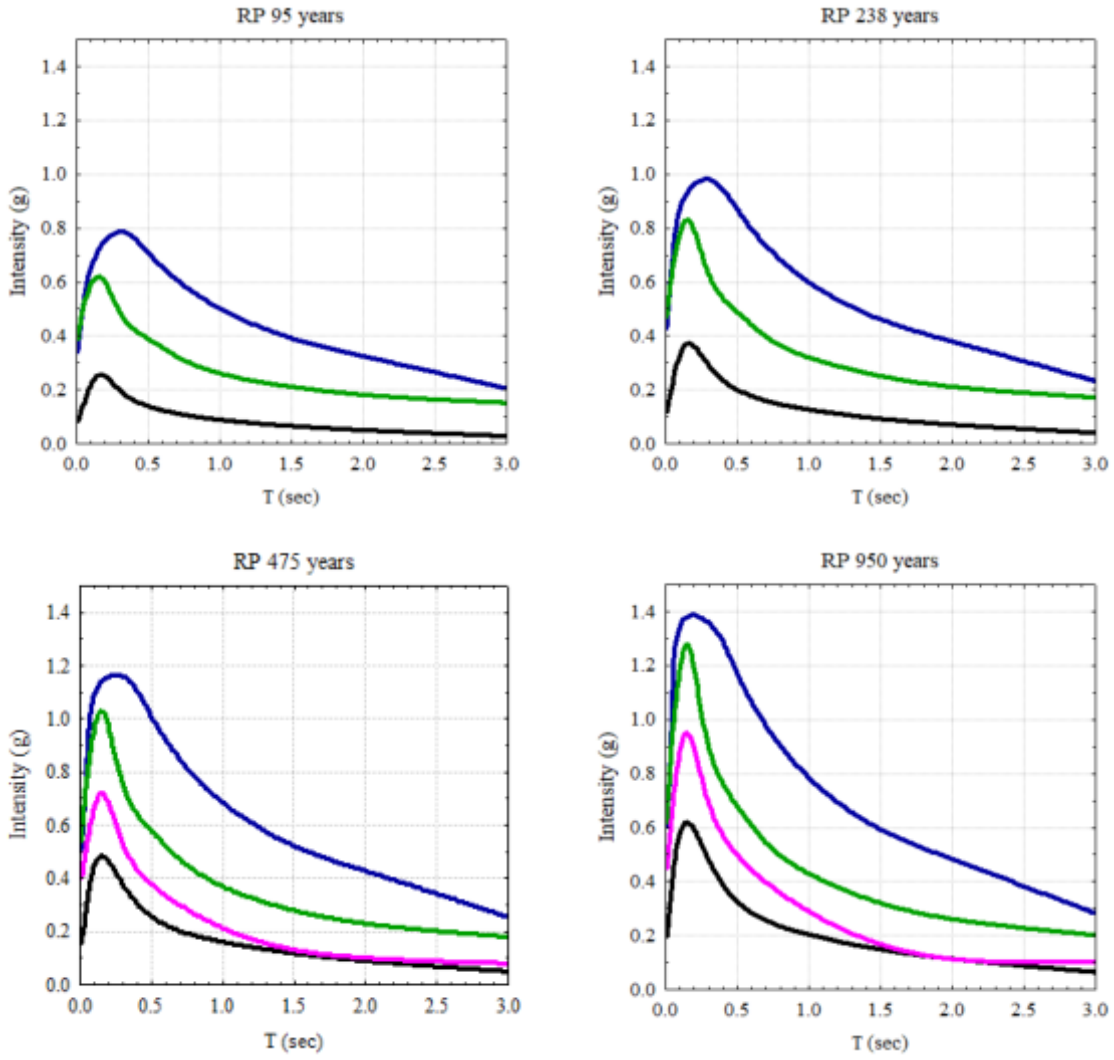

Figure 6.2. UHS in Tuxtla Gutiérrez, Chiapas for different return periods. Green line for rock, blue line considering site effect with Vs30 of 200 m/s, pink line are the results of Rodríguez-Lomelí and García-Mayordomo (2019)and black line data obtained from Prodisis.

6.3 Coatzacoalcos, Veracruz

Coatzacoalcos City is a region located on the Gulf Plain Coast of Mexico. Its economic importance lies in its commercial port, adding the oil industry which is one of its main activities. This is the place where the Jáltipan earthquake with M_w6.4 occurred and caused several damage (Singh *et al.*, 2015). Is relevant to add that the city is sited in recent quaternary sediments (Carta Geológico-Minera Coatzacoalcos E15-1-4, 2004) that amplify the subsoil movement.

With respect to studies of seismic hazard, there is no evidence in the area; however, a UHS was estimated near the city for an RP of 200 years in the southern Gulf of Mexico (Alamilla *et al.*, 2021), it is represented by the pink line in Figure 6.3 and is like Prodisis. Similarity can be attributed because an incomplete catalog was used; however, it allowed a first sight in the comprehension of the seismic hazard for the region. The values obtained in this work are higher than those presented before. We got UHS for the different return periods with 0.4 *g* greater than Prodisis.

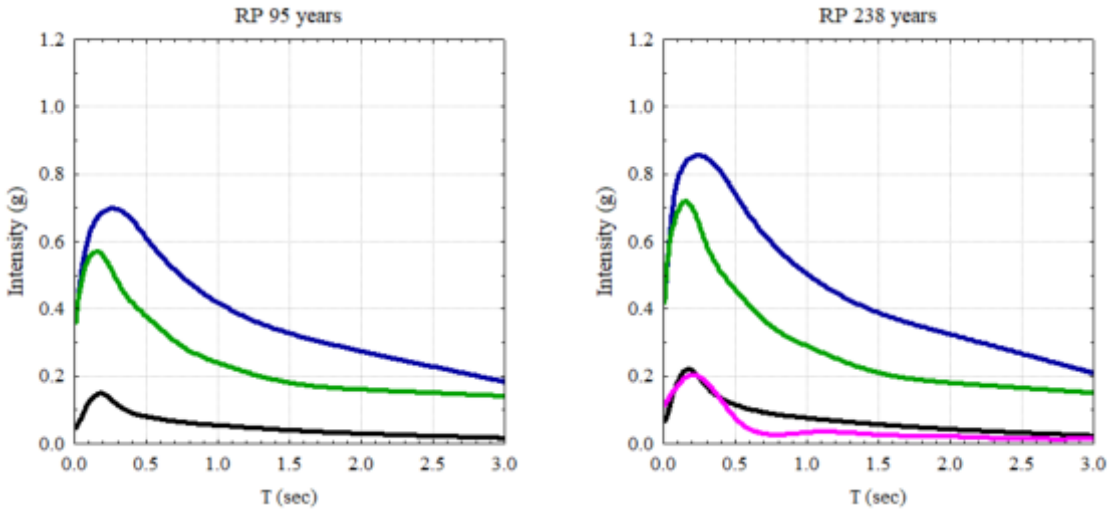

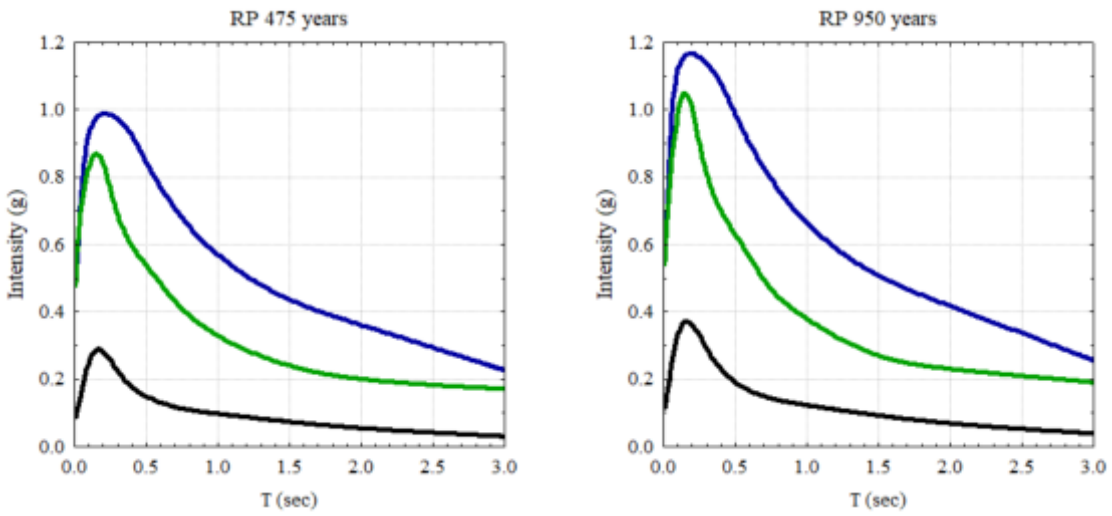

Figure 6.3. UHS in Coatzacoalcos Veracruz for different return periods. Green line for rock, blue line considering site effect with Vs_{30} of 200 m/s, pink line is the result obtained by Alamilla *et al.*, 2021 *and black line data obtained from Prodisis.*

6.4 Paraíso, Tabasco

Paraíso is a municipality located in the Gulf Coastal Plain; its growing population is related to building a new oil refinery currently under construction. The advantages of this new project are social impact, which demands construction and improvement of public convenience, and the development of urban regions. However, there are no seismic hazard studies in the region. The UHS for different return periods and considering the local site effect were estimated (Figure 6.4). The next figures show that the highest values are from the spectra computed using the local geology being 0.2 *g* greater than those on rock.

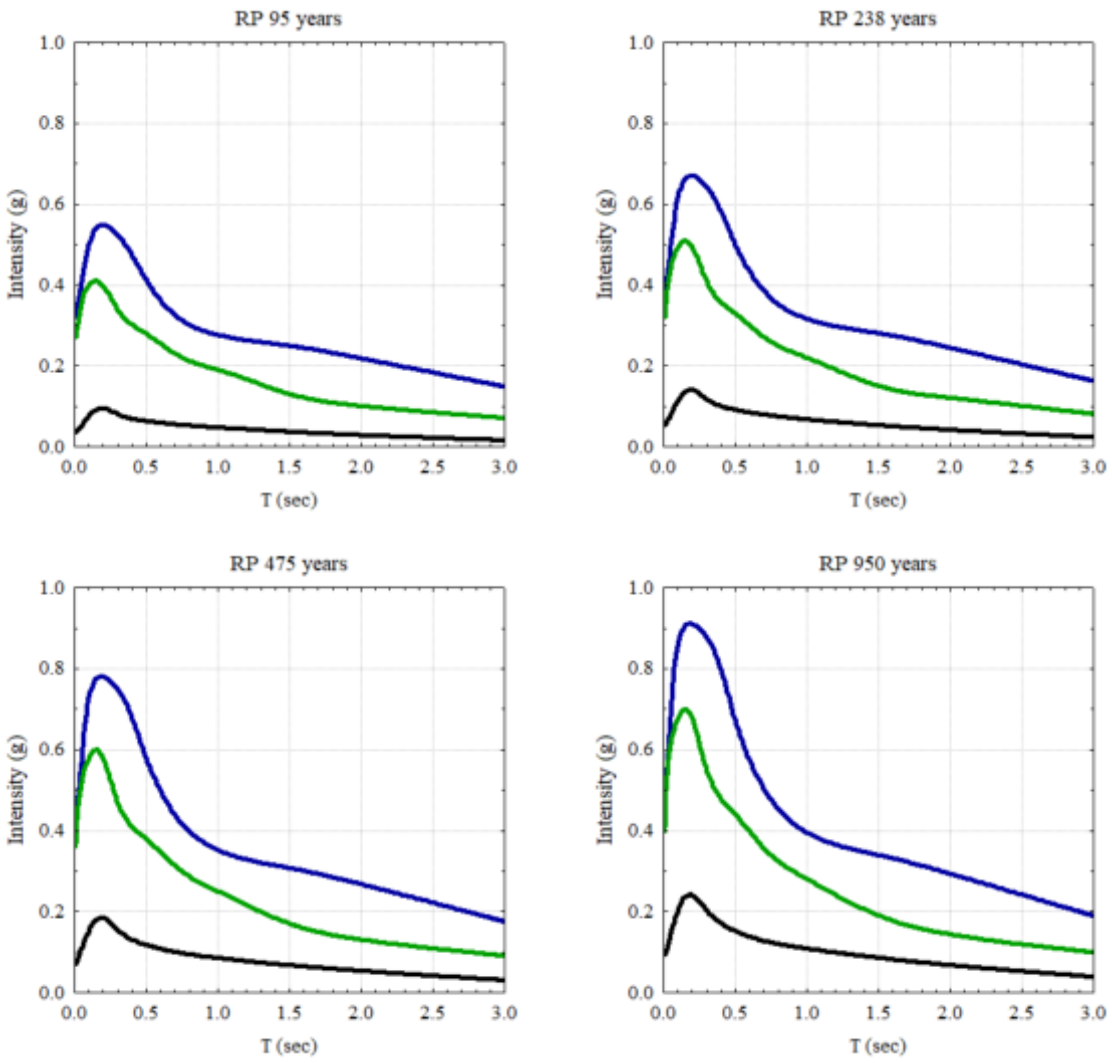

Figure 6.4 UHS for different return periods in Paraíso, Tabasco. Green line for rock, blue line considering site effect with Vs_{30} of 200 m/s, and black line data obtained from Prodisis.

6.5 Villahermosa, Tabasco

Villahermosa City is an important logistical center of Tabasco state that has been affected by seismic events and recurrent river floods (Areu-Rangel *et al.,* 2019). Currently is an important place for the oil industry in Mexico. It has 683,607 habitants (INEGI, 2023), and its population is yet under-raising because of the construction of a new oil refinery which is projected to be the larger in Mexico.

Adding that uncontrolled urbanization is located adjacent to the channels of the big rivers and the population lying in old lagoons (Figure 5.3), is needed in the assessment of the seismic hazard in the region.

The UHS for the four return periods considered were estimated (Figure 6.5). Differences between the obtained for site class C and D according to NEHRP and those obtained for rock have been observed. The spectra obtained in this work are higher than estimated by Prodisis. In the following figures, the blue lines represent the estimation made considering the local site effect. In Villahermosa, Tabasco, there are some studies of Vs_{30} parameter, which show values from 180 to 560 m/s. The UHS computed using the average shear wave velocities are approximately 0.2 *g* greater than ones computed on rock and approximately 0.4 *g* greater than Prodisis.

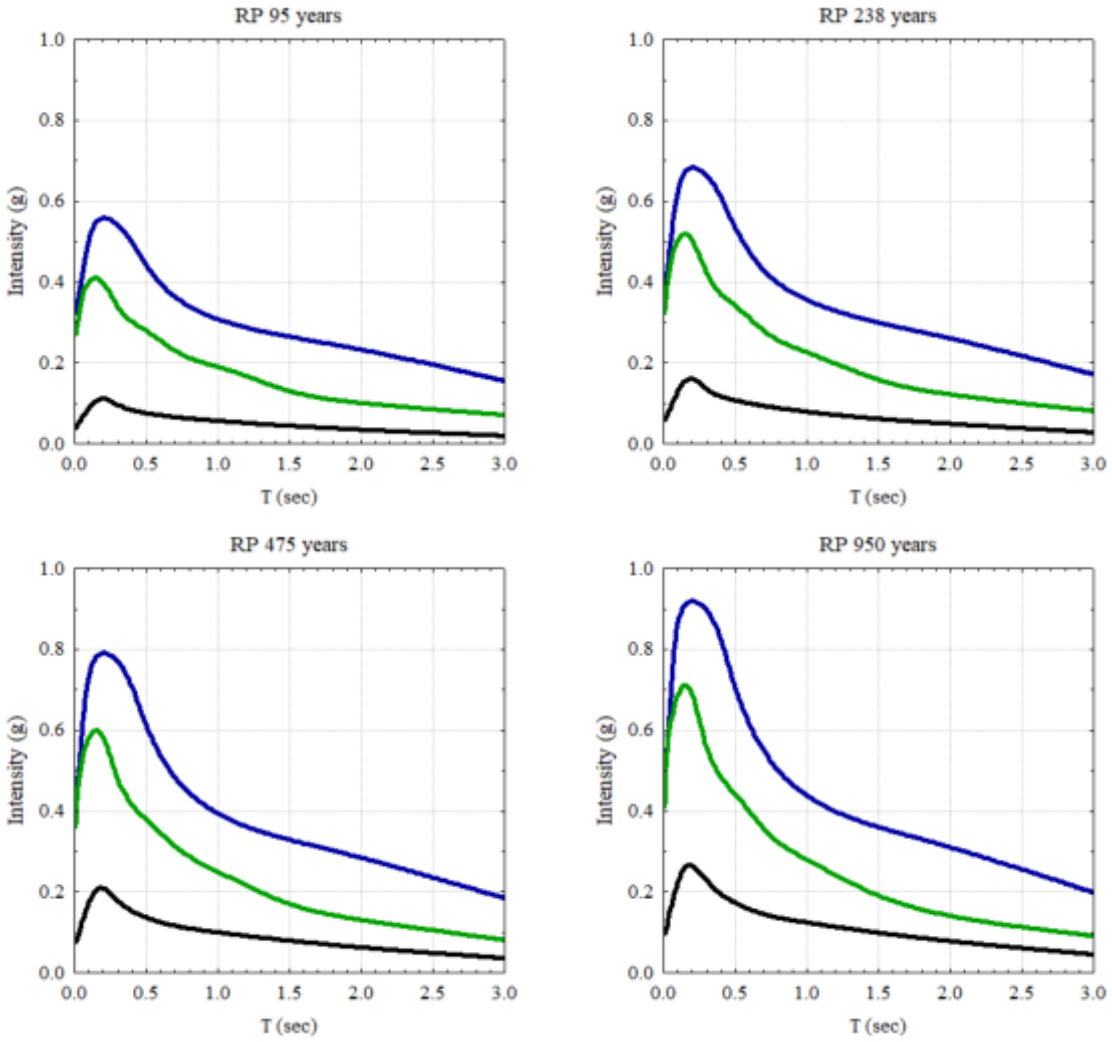

Figure 6.5 UHS for different return periods. Green line for rock, blue line considering site effect with Vs_{30} of 200 m/s, and black line data obtained from Prodisis.

6.6 Cd. del Carmen, Campeche.

Near Ciudad del Carmen Island is Cantrell, the largest oil field in Mexico, apart from this important issue, other disasters to which the city is exposed are linked to floods and meteorological phenomena.

Being a city exposed to environmental effects due to being a coastal city, the risk increases by intense storms and hurricanes affecting most of the island that is lower than 1-2 meters above sea level. All those effects, adding the seismological consequences, can be catastrophic for the 295,000 habitants (INEGI, 2023).

The seismic hazard was estimated for the city. The values were computed for rock (V_{S30}>800 m/s) and class D and E according to NEHRP. Over again, the results obtained in this work are higher than Prodisis (Figure 6.6). Even if the UHS obtained for Cd. del Carmen presents the lowest hazard of the complete study area, their knowledge is important because of the different natural phenomena together with a seismic event could have.

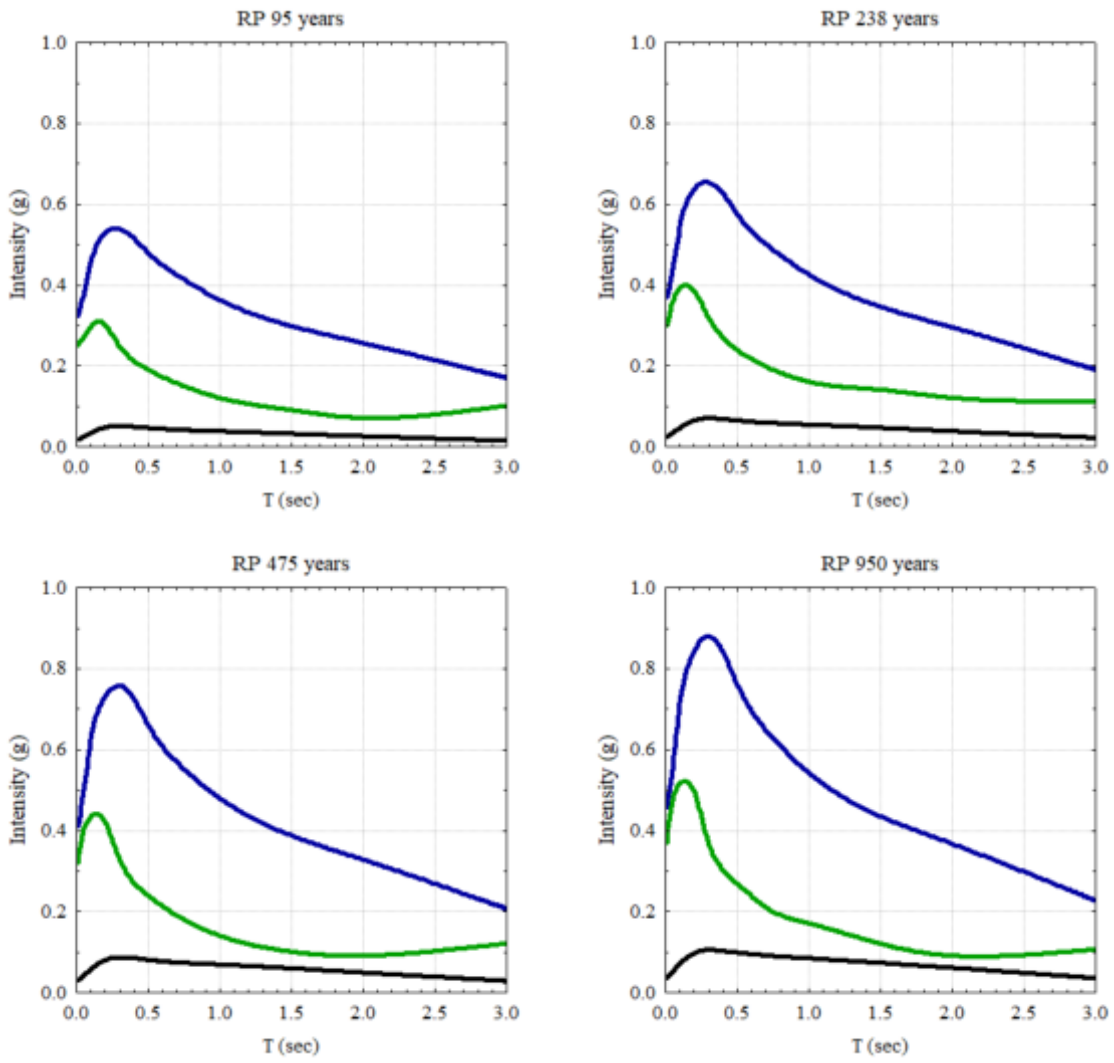

Figure 6.6 UHS in Ciudad del Carmen, Campeche for different return periods. Green line for rock, blue line considering site effect with Vs_{30} of 200 m/s, and black line data obtained from Prodisis.

6.7 Discussion

In Chapter IV, the contour maps have the higher hazard level near the Middle American Trench which is an active tectonic zone, while in Chapter V we demonstrated the relationship between damage to the tallest buildings and regional events. Now we show the seismic hazard for some economically important and most populated cities in southern Mexico.

The state's capital of Tabasco has tall constructions higher than 80 meters; however, the predominant ones are those with one to three stages. It shows the importance of studying the seismic hazard in specific places.

Under this scope, the UHS for the most socioeconomic important cities was evaluated. It is remarkable that chosen cities that are close to the Gulf of Mexico Coastal Plain have the lowest values of the study area, while the hazardous zones are those nearest and parallel to the subduction zone of Mexico and Guatemala.

The results of PGA in this work compared with Prodisis (*Comisión Federal de Electricidad, CFE*), are dissimilar since they provide the UHS computed on rock, related to a certain return period. Villahermosa's hazard level is 0.3 *g* less than this work estimated on rock for Prodisis.

In Paraíso, the difference is 0.3 g for 95 and 238 years of return period, while 0.4 g for 475 and 950 years. In Coatzacoalcos Veracruz, are 0.3, 0.4, 0.5, and 0.6 *g* for 95, 238, 475 and 950 years return period respectively.

There are some UHS published for the study area, examples are in Figure 6.1, 6.2, and 6.3 represented by pink lines that are the UHS for a return period of 200, 500, and 1000 years estimated for the southern Gulf of Mexico (Figure 6.3) and cities close to the subduction zone (Figure 6.1 and 6.2).

The UHS estimated to the southern Gulf of Mexico for 200 years return period (Figure 6.3) is similar to Prodisis; however, the information of Alamilla *et al.,* 2021 from which it was obtained was estimated with an incomplete catalog for the complete Gulf of Mexico.

The UHSs for Tuxtla Gutiérrez and Tapachula in Chiapas state are lower in previous studies in comparison with this work. It is important to mention elements such as an updated seismic catalog, a wider zone, and different and recent GMPE's among other input parameters were used in this work and are different in previous works. Even updated geological and tectonics information was used to estimate the seismic hazard.

Another important issue is that considering that the Prodisis program estimates the UHS with a regional seismic source zonation, a regional catalog, and again probably different GMPE's, the differences could result in an underestimation of computed spectra.

The UHS of published authors and spectrums obtained in this work have a similar form, where the peak is over 0.2 to 0.5 seconds, but in dissimilar scales. Bearing in mind that Villahermosa

municipality has tall buildings, and there is evidence of their damage by regional events, the results of the T_b (fundamental period of the buildings) and F_0 (resonance frequency) are consistent with the findings in this work (Chapter V).

After all, is important to consider that buildings settled in cities belonging to the Gulf of Mexico Coastal Palin have evidence of damage by earthquakes the Middle American Trench occurred at a distance of 350 km. Adding that, the local geological structures, thickness, and seismic velocity of the sedimentary deposits in Tabasco state, not only condition the amplification of ground motion but the frequency range at which the movement is major, such as the well-known case of Mexico City. With all this is shown the necessity of a better understanding or more detailed seismic studies, such as UHS for specific periods according to the frequency that is related to distant events.

Chapter VII. Conclusions

Based on the setting tectonic and geological analysis, pre-instrumental and instrumental seismicity, examination of attenuation relationships, and site effects, the conclusions of the seismic hazard assessment and study cases in urban zones of Tabasco's state are presented as follows:

- To better understand the seismic hazard in SEM, an earthquake catalog was prepared for a period of 1533 to 2020 with a magnitude range $3.3 \leq M_w \leq 8.6$ containing 62965 events. It was decluttered and homogenized using an empirical magnitude conversion for Mexican earthquakes.

- A cluster on the catalog of events that occurred in the Gulf of Mexico for the period studied was analyzed through CLVD, missing out on the relationship with the oil and gas industrial activity.

- Seismic hazard assessment in SEM was carried out considering crustal events on North American plate, interface events of the subduction zone between Cocos and North American, and shallow and deep in-slab events of Cocos plate.

- Considering the local and regional geology, the tectonic setting, a gravimetric anomaly map, and a focal mechanism catalog; the study area was subdivided into 21 seismic source zones. Between them are crustal, interface, shallow in-slab, and deep in-slab zones.

- In crustal areas, the scarcity of studies of active faults such as paleoseismological, seismic reflection, refraction, GPS, and so on prevented the model of geological structures individually, and because of this were treated as seismic sources.

- The GMPEs used in this work were Chiou and Young (2014), Abrahamson *et al.* (2014), and Parker *et al.* (2020). Because all equations must be adequate to use in a seismic hazard study, some characteristics such as magnitude range, distance definition, consideration of site effect, units (cm/s^2, m/s^2, and g), fault mechanism, etc. were checked in the beginning for all studied equations.

- Seismic hazard maps for 95, 238, 475, and 950 years of return period were performed covering southern Mexico but focusing on Tabasco state. The contour lines obtained in the seismic hazard maps on rock are very similar to the direction of the isodepth of Cocos plate, subducting under the North American plate.
- Two sets of seismic hazard maps were developed, the first group was for rock sites with shear wave velocities >800 m/s, and the second maps group considered site effect.
    - The second group considers the soil class definition of the NEHRP classification based on the Vs_{30} values obtained by the MASW technique. These results of surface waves ranged between 120 to 570 m/s in some localities of Tabasco state which correspond to C, D, and E classes.
    - The Vs_{30} parameter distribution for Centro, Tabasco was classified according to NEHRP as sites class C (dense soil) with $Vs_{30} \geq 539$ m/s, class D (stiff soil), with $181 < Vs_{30} < 345$ m/s and, class E (soft soil) with $Vs_{30} \leq 180$ m/s.
    - The velocity structure of the subsoil in one municipality of Tabasco state was derived by the MASW technique. The values obtained of Vs_{30} obtained from 20 profiles agree with some published studies of SPT. The basement depth was encountered from 25 up to 40 meters, showing the deepest values in the Northeastern and the southwestern of the municipality.
    - The resonance frequency values varying from $0.9 \leq f_0 \leq 2.0$ Hz, coincide with low surficial wave velocities and more damaged areas during the M_w8.2 earthquake. After that, Centro municipality can be considered a prone area to suffer severe damage during regional earthquakes originating in the MAT.
    - Transfer functions obtained by velocity structures varying from $0.9 \leq f_0 \leq 2.0$ Hz coinciding with soft soil areas and with the spectral ratio H/V of regional earthquakes.
    - For the M_w8.2 that occurred in the September 08, 2017 earthquake, the most damage was in buildings of 1 story, corresponding to T_b=0.45 seconds and T_b=2.38 seconds for 16 stories. It reveals the damage that regional earthquakes can cause to Tabasco

state. The strong evidence is on building cracks in Villahermosa city. Additionally, it means that low-frequency events have caused damage in the study area.

  - The analysis performed of the geology and tectonic of the SEM, shows Tabasco is located on sedimentary basins, which are formed by alluvial deposits and younger sedimentary rocks. Their thickness can reach thickness up to ten kilometers. This type of material shows low seismic wave velocities; a consequence is that in the cities underlying this type of material, the waves become trapped in the basins and can be potentially damaged, as was the case of M_w8.2 Chiapas earthquake.

- The local geological conditions in Tabasco highlight the influence of the quaternary sediments on which the state is positioned, with an increment in the seismic hazard.

- The probabilistic seismic hazard map was prepared, using an updated and homogenized earthquake catalog to create a seismic zonation model. The seismicity parameters were estimated for each region being from b=0.56 to 1.96 varying from shallow to deep zones. The results of the seismic hazard maps for rock and taking into consideration site effect, show that the more hazardous zones are in the coastal regions.

- The PGA values obtained on rock for the regional maps were 0.15 - 0.7 *g* for 95 years of return period, 0.15 – 1 *g* for 238 years of return period, 0.2 – 1.15 for 475 years of return period, and 0.2 – 1.15 *g* for 950 years of return period. While for site effect the PGA values were 0.2 to 0.7 *g* for 95 years of return period.0.2 to 1 *g* for 238 years of return period, 0.3 to 1.2 *g* for 475 years of return period, and 0.3 to 1.6 years of return period.

  - In Tabasco state, the PGA values on rock varied from 0.15 to 0.35 *g* for 95 years, 0.15 to 0.4 g for 238 years of the return period, 0.2 to 0.5 *g* for 475 years of return period, and 0.25 to 0.55 *g* for 950 years of return period.

  - While for the seismic hazard's maps considering local geology effect the PGA values are 0.25 to 0.35 *g* for 95 years of return period, 0.3 to 0.43 *g* for 238 years of return period, 0.3 to 0.45 *g* for 475 years of return period, and 0.3 to 0.56 *g* for 950 years of return period.

- This study's outcomes indicate higher values compared to those provided by Prodisis (CFE). This disparity is attributed to incorporating an updated seismic catalog, attenuation relationships, and a meticulous consideration of site conditions, and their association with the soil amplification in this work. However, it is noteworthy that the UHS shapes between 0.1 to 0.5 seconds are consistent with those observed in analogous areas.

- Under the scope, of the seismic hazard at which Tabasco state is placed, some urban areas have been studied in detail. The population, socioeconomic importance, and urban development were three factors considered in selecting them. The first one was Villahermosa City, the most populated city in Tabasco state, and its importance as a key meeting point for oil issues. The second one was the Petroleum Refinery because it is probably the largest oil refinery in Mexico and is under construction. The next ones were Coatzacoalcos Veracruz and Ciudad del Carmen, Campeche, due its closeness to Tabasco state and its similarity with Tabasco in geological and epicentral distances from the Middle American Trench.

    - The results of seismic hazard represented by UHS, showed differences between the spectrum estimated for site class C and D, corresponding to Vs_{30} of 200 m/s, and those estimated for rock. In all cases, the UHS observed in rock and soils are larger than Prodisis and even spectrum published.

- The need to prepare a more detailed study based on ground motion values has been observed considering different spectral acceleration that support the current seismic design criteria.

- A wider comprehension of the seismic hazard in terms of maps and UHS is needed, especially in areas with high seismic hazards and new oil and gas investment construction.

- Another important issue to bear in mind, is that natural phenomena such as floods together with the occurrence of a seismic event in Tabasco, and the local site effect in the study area have affected Tabasco and at the same time, becoming it more vulnerable. It was evidenced by subsidence in some localities in Centro municipality during the M_w8.2 earthquake, defined as a distant event.

References

Abe, K. and Noguchi, S. I. (1983). Revision of magnitudes of large shallow earthquakes, 1897–1912. Physics of the Earth and Planetary Interiors, 33(1), 1-11.

Abrahamson, N. A. and Silva, W. J. (1997). Empirical response spectral attenuation relations for shallow crustal earthquakes. Seismological research letters, 68(1), 94-127.

Abrahamson, N. A., Silva, W. J. and Kamai, R. (2014). Summary of the ASK14 ground motion relation for active crustal regions. Earthquake Spectra, 30(3), 1025-1055.

Aki, K., & Richards, P. G. (2002). Quantitative seismology

Alamilla, J. L., Vai, R. and Esteva, L. (2021). Probabilistic seismic hazard analysis under incomplete data and imperfect source characterization: the Gulf of Mexico case study. Journal of Seismology, 25, 487-498.

Alejandro Almeida, E., (2020), Clasificación local de sitio utilizando métodos de ondas superficiales activos y pasivos en Teapa, Tabasco, México. Tesis de licenciatura. Universidad Juárez Autónoma de Tabasco.

Algermissen S.T., D.M.Perkins, W.Isherwood, D.Gordon, G.Reagor, C.Howard, 1976. Seismic risk evaluation of the Balkan region. UNESCO SSBR, U.S. Geological Survey, Denver, Colorado 80225, 43+20 p.

Alvarado, G. E., Benito, B., Staller, A., Climent, Á., Camacho, E., Rojas, W., & Lindholm, C. (2017). The new Central American seismic hazard zonation: Mutual consensus based on up to day seismotectonic framework. Tectonophysics, 721, 462-476.

Ambraseys, N. Y. and Adams, R. D. (1996). Large-magnitude Central American earthquakes, 1898–1994. Geophysical journal international, 127(3), 665-692.

Andreani, L. and Gloaguen, R. (2015). Geomorphic analysis of transient landscapes from the Sierra Madre de Chiapas and Maya Mountains (northern Central America): implications for the North American-Caribbean-Cocos plate boundary. Earth Surface Dynamics, 3(3).

Andreani, L., Le Pichon, X., Rangin, C., and Martínez-Reyes, J. (2008a). The southern Mexico block: main boundaries and new estimation for its quaternary motion, B. Soc. Geol. Fr., 179, 209– 223, 944, 946, 950, 973, 974, 990

Andreani, L., Rangin, C., Martínez-Reyes, J., Le Roy, C., Aranda-García, M., Le Pichon, X., and Peterson-Rodriguez, R. (2008b). The Neogene Veracruz fault: evidences for left-lateral slip along the southern Mexico block, B. Soc. Geol. Fr., 179, 195–208, 949

Areu-Rangel, O. S., Cea, L., Bonasia, R., & Espinosa-Echavarria, V. J. (2019). Impact of urban growth and changes in land use on river flood hazard in Villahermosa, Tabasco (Mexico). Water, 11(2), 304.

Arroyo, D., García, D., Ordaz, M., Mora, M. A., & Singh, S. K. (2010). Strong ground-motion relations for Mexican interplate earthquakes. Journal of Seismology, 14, 769-785.

Authemayou, C., Brocard, G., Teyssier, C., Simon-Labric, T., Guttiérrez, A., Chiquín, E. N. and Morán, S. (2011). The Caribbean–North America–Cocos Triple Junction and the dynamics of the Polochic–Motagua fault systems: Pull-up and zipper models. Tectonics, 30(3).

Baker, J. W. (2008). An introduction to probabilistic seismic hazard analysis (PSHA). White paper, version, 1, 72.

Beauval, C., Yepes, H., Palacios, P., Segovia, M., Alvarado, A., Font, Y. and Vaca, S. (2013). An earthquake catalog for seismic hazard assessment in Ecuador. Bulletin of the Seismological Society of America, 103(2A), 773-786.

Bender, B; Perkins, D (1982). SEISRISK II. A Computer Program for Seismic Hazard Estimation. USGS Open file report, pp 82-293.

Bender, B; Perkins, D (1987). SEISRISK III. A Computer Program for Seismic Hazard Estimation. USGS Bulletin 1772.

Benito, M. B., Lindholm, C., Camacho, E., Climent, A., Marroquín, G., Molina, E. and Torres, Y. (2012). A new evaluation of seismic hazard for the Central America region. Bulletin of the Seismological Society of America, 102(2), 504-523.

Borcherdt, R. D. (1994). Estimates of site-dependent response spectra for design (methodology and justification). Earthquake Spectra, 10(4), 617-653.

Böse E (1903) Informe sobre los temblores de Zanatepec a fines de Septiembre de 1902 y sobre el estado actual del volcán de Tacana. Parergones del Instituto geológico de Mexico 1(1): 20

Bravo, H., Rebollar, C. J., Uribe, A., & Jimenez, O. (2004). Geometry and state of stress of the Wadati-Benioff zone in the Gulf of Tehuantepec, Mexico. Journal of Geophysical Research: Solid Earth, 109(B4).

Building Seismic Safety Council, 2003. NEHRP Recommended Provisions for Seismic Regulations for New Buildings and Other Structures (FEMA 450). Part 1 338.

Cabañas, L., Benito, B., Cabañas, C., López, M., Gómez, P., Jiménez, M. E. and Alvarez, S. (1999). Caracterización del movimiento del suelo en ingeniería sísmica. Fisica de la Tierra, 11.

Calò, M. (2021). Tears, windows, and signature of transform margins on slabs. Images of the Cocos plate fragmentation beneath the Tehuantepec isthmus (Mexico) using Enhanced Seismic Models. Earth and Planetary Science Letters, 560, 116788.

Campbell, K. W., & Bozorgnia, Y. (2008). NGA ground motion model for the geometric mean horizontal component of PGA, PGV, PGD and 5% damped linear elastic response spectra for periods ranging from 0.01 to 10 s. Earthquake spectra, 24(1), 139-171.

CENAPRED (2020), Centro Nacional de Prevención de Desastres. Impacto socioeconómico de los principales desastres ocurridos en México. Resumen ejecutivo.

CENAPRED (2021), Centro Nacional de Prevención de Desastres. Impacto socioeconómico de los principales desastres ocurridos en México. Resumen ejecutivo.

Chiou, B. S. J., and Youngs, R. R. (2014). Update of the Chiou and Youngs NGA model for the average horizontal component of peak ground motion and response spectra. Earthquake Spectra, 30(3), 1117-1153.

Cid Villegasa, G., Mendozab, C., & Ferrarib, L.(2017) Mexico Quaternary Fault Database Base de datos de fallas cuaternarias de México.

Cornell, C. A. (1968). Engineering seismic risk analysis. Bulletin of the seismological society of America, 58(5), 1583-1606.

Cornu, F. N., & Ponce, L. (1989). Zonas sísmicas de Oaxaca, México: sismos máximos y tiempos de recurrencia para el periodo 1542-1988. Geofísica Internacional, 28(4), 587-641.

Cotton, F., Scherbaum, F., Bommer, J. J. and Bungum, H. (2006). Criteria for selecting and adjusting ground-motion models for specific target regions: Application to central Europe and rock sites. Journal of Seismology, 10, 137-156.

CRED (2016), Centre for Research on the Epidemiology of Disasters. Annual Disaster Statistical Review 2016. The number and trends.

Crone, A. J. and Wheeler, R. L. (2000). Data for Quaternary faults, liquefaction features, and possible tectonic features in the central and eastern United States, east of the Rocky Mountain Front (p. 342). US Department of the Interior, US Geological Survey.

Das, R., Wason, H. R. and Sharma, M. L. (2011). Global regression relations for conversion of surface wave and body wave magnitudes to moment magnitude. Natural hazards, 59, 801-810.

De la Cruz-Reyna, D., & Martin Del Pozzo, A. L. (2009). The 1982 eruption of El Chichón volcano, Mexico: eyewitness of the disaster. Geofísica internacional, 48(1), 21-31.

De la Fuente HA, Sánchez MA, Tenorio AE, Lavariega DO, Rodriguez JF, Zúñiga AR (2012) Zonificación geotécnica del municipio de Centro, Tabasco. Sociedad Mexicana de Ingeniería Geotécnica

DeMets, C., Gordon, R. G., Argus, D. F. and Stein, S. (1994). Effect of recent revisions to the geomagnetic reversal time scale on estimates of current plate motions. Geophysical research letters, 21(20), 2191-2194.

Di Giacomo, D., Bondár, I., Storchak, D. A., Engdahl, E. R., Bormann, P. and Harris, J. (2015). ISC-GEM: Global Instrumental Earthquake Catalogue (1900–2009), III. Re-computed MS and mb, proxy MW, final magnitude composition and completeness assessment. Physics of the Earth and Planetary Interiors, 239, 33-47.

Dobry, R., Borcherdt, R. D., Crouse, C. B., Idriss, I. M., Joyner, W. B., Martin, G. R., & Seed, R. B. (2000). New site coefficients and site classification system used in recent building seismic code provisions. Earthquake spectra, 16(1), 41-67.

Douglas, J. (2003). Earthquake ground motion estimation using strong-motion records: a review of equations for the estimation of peak ground acceleration and response spectral ordinates. Earth-Science Reviews, 61(1-2), 43-104.

Douglas, J. (2021). Ground motion prediction equations 1964–2021. Department of Civil and Environmental Engineering University of Strathclyde, Glasgow, United Kingdom.

Ekström, G., Nettles, M., Dziewon ski, A.M. (2012). The global CMT project 2004-2010: centroid-moment tensors for 13,017 earthquakes. Phys. Earth Planet. Inter. 200–201, 1–9. https://doi.org/10.1016/j.pepi.2012.04.002.

Esteva L. (1967) Criterios para la construcción de espectros para diseño sismico Proceedings of XII Jornadas Sudamericanas de Ingeniería Estructural y III simposio panamericano de Estructuras, Caracas. Published later in Boletin del Instituto de Materiales y Modelos estructurales, Universidad Central de Venezuela, No. 19, 1967.

Esteva L. (1970), Regionalizacion sismica de Mexico para fines de ingenieria. Report 246, Universidad Nacional Autonoma de Mexico

Esteva L.(1963), Regionalizacion sismica de la Republica Mexicana. Revista Sociedad Mexicana de Ingenieria Sismica, 1(1):31–35.

Figueroa, J. (1963). Isosistas de macrosismos mexicanos, Ingenieffa (Mexico) 33 (1), 45-67.

Franco, A., Lasserre, C., Lyon-Caen, H., Kostoglodov, V., Molina, E., Guzman-Speziale, M. and Manea, V. C. (2012). Fault kinematics in northern Central America and coupling along the subduction interface of the Cocos Plate, from GPS data in Chiapas (Mexico), Guatemala and El Salvador. Geophysical Journal International, 189(3), 1223-1236.

Franco, S. I., Canet, C., Iglesias, A. and Valdés-González, C. (2013). Seismic activity in the Gulf of Mexico. A preliminary analysis. Boletín de la Sociedad Geologíca Mexicana, 65(3), 447-455.

Franco, S. I., Iglesias, A. and Fukuyama, E. (2020). Moment tensor catalog for Mexican earthquakes: almost two decades of seismicity. Geofísica internacional, 59(2), 54-80.

Galvis, F., Miranda, E., Heresi, P., Dávalos, H., & Silos, J. R. (2017). Preliminary statistics of collapsed buildings in Mexico City in the September 19, 2017 Puebla-Morelos Earthquake. John A. Blume Earthquake Engineering Center and Department of Civil and Environmental Engineering Stanford University, http://learningfromearthquakes. org.

García Acosta, V. G. and Suárez Reynoso, G. (1996). Los sismos en la historia de México: el análisis social. CIESAS (2).

Garcia Peláez, J., Gee, R., Styron, R, and Poggi, V. (2023), GEM Global Mosaic of Hazard Models, Caribbean and Central America, https://hazard.openquake.org/gem/models/CCA/ , last viewed June 15th, 2023.

García, D., Singh, S. K., Herráiz, M., Ordaz, M. and Pacheco, J. F. (2005). Inslab earthquakes of central Mexico: peak ground-motion parameters and response spectra. Bulletin of the Seismological Society of America, 95(6), 2272-2282.

Gardner, J. K. and Knopoff, L. (1974). Is the sequence of earthquakes in Southern California, with aftershocks removed, Poissonian?. Bulletin of the seismological society of America, 64(5), 1363-1367.

Gasperini, P., Lolli, B. and Vannucci, G. (2013). Body-Wave Magnitude mb Is a Good Proxy of Moment Magnitude M w for Small Earthquakes (m b< 4.5–5.0). Seismological Research Letters, 84(6), 932-937.

Gazel, E., Flores, K. E. and Carr, M. J. (2021). Architectural and tectonic control on the segmentation of the Central American volcanic arc. Annual Review of Earth and Planetary Sciences, 49, 495-521.

Godínez, E., Tena, A., Archundia, H., Gómez, A., Ruíz, R. and Escamilla, J. (2019). Structural damage in housing and apartment buildings located in the Southeast of Mexico due to the September 7th, 2017 Tehuantepec earthquake, Mw= 8.2. Revista Internacional de Ingeniería de Estructuras, 24, 2.

Goel RK, Chopra AK (1997) Period formulas for moment-resisting frame buildings. J Struct Eng 123: 1454

Graham, R., Pindell, J., Villagómez, D., Molina-Garza, R., Granath, J. and Sierra-Rojas, M. (2021). Integrated Cretaceous–Cenozoic plate tectonics and structural geology in Southern Mexico. Geological Society, London, Special Publications, 504(1), 285-314.

Gutenberg B, Richter CF (1954) Seismicity of the earth. Princeton University Press, Princeton

Guzmán Ventura JA, Williams Linera F, Riquer Trujillo G, Vargas Colorado A, Leyva Soberanis R (2020) Fallas de licuación de suelos inducidas por el sismo de Tehuantepec del 7 de septiembre de 2017 (M_w 8.2) en la Ciudad de Coatzacoalcos, Veracruz, México. Ingeniería Sísmica 102:82-106

Guzmán-Speziale, M. (2001). Active seismic deformation in the grabens of northern Central America and its relationship to the relative motion of the North America–Caribbean plate boundary. Tectonophysics, 337(1-2), 39-51.

Guzmán-Speziale, M. (2010). Beyond the Motagua and Polochic faults: Active strike-slip faulting along the western North America–Caribbean plate boundary zone. Tectonophysics, 496(1-4), 17-27.

Guzmán-Speziale, M., & Meneses-Rocha, J. J. (2000). The North America–Caribbean plate boundary west of the Motagua–Polochic fault system: a fault jog in Southeastern Mexico. Journal of South American Earth Sciences, 13(4-5), 459-468.

Guzman-Speziale, M., & Molina, E. (2022). Seismicity and seismically active faulting of Guatemala: A review. Journal of South American Earth Sciences, 115, 103740.

Guzmán-Speziale, M., Pennington, W. D., & Matumoto, T. (1989). The triple junction of the North America, Cocos, and Caribbean plates: Seismicity and tectonics. Tectonics, 8(5), 981-997.

Hanks, T. C., & Kanamori, H. (1979). A moment magnitude scale. Journal of Geophysical Research: Solid Earth, 84(B5), 2348-2350.

Hayes, G.P., Moore, G.L., Portner, D.E., Hearne, M., Flamme, H., Furtney, M., Smoczyk, G.M. (2018). Slab2, a comprehensive subduction zone geometry model. Science (80-.). 362, 58–61. https://doi.org/10.1126/science.aat4723.

Heath, D. C., Wald, D. J., Worden, C. B., Thompson, E. M., & Smoczyk, G. M. (2020). A global hybrid VS 30 map with a topographic slope–based default and regional map insets. Earthquake Spectra, 36(3), 1570-1584.

Hussaini, T. M., Chowdhury, I. N., al Faysal, H., Chakraborty, S., Vaccari, F., Romanelli, F., & Magrin, A. (2022). Neo-deterministic seismic hazard assessment studies for Bangladesh. In Earthquakes and Sustainable Infrastructure (pp. 559-581). Elsevier.

INEGI (2023) Estadísticas sobre las afectaciones de los sismos de septiembre de 2017 en las actividades económicas. INEGI, Ciudad de México.

IPCET (2020). Instituto de Protección Civil del Estado de Tabasco. https://tabasco.gob.mx/ipcet
Işık, E., & Harirchian, E. (2022). A comparative probabilistic seismic hazard analysis for Eastern Turkey (Bitlis) based on updated hazard map and its effect on regular RC structures. Buildings, 12(10), 1573.
Jesús de la Cruz H, Jiménez-Peralta E, Jiménez-López J, García-Pérez AA, Jiménez-Cabrera JD (2017) Caso de estudio: municipio de centro tabasco sismo pijijiapan, chiapas del 07 de septiembre de 2017: report.

Jiménez, C. (2018). Seismic source characteristics of the intraslab 2017 Chiapas-Mexico earthquake (Mw8. 2). Physics of the Earth and Planetary Interiors, 280, 69-75.

Johnston, A. C., Coppersmith, K. J., Kanter, L.R. & Cornell, C.A., (1994). The earthquakes of stable continental regions: assessment of large earthquake potential, TR-102261, Vol. 1–5, ed. Schneider, J.F., Electric Power Research Institute (EPRI), Palo Alto, CA.
Kanamori, H. and Stewart, G. S. (1978). Seismological aspects of the Guatemala earthquake of February 4, 1976. Journal of Geophysical Research: Solid Earth, 83(B7), 3427-3434.

Kelleher, J., Sykes, L., & Oliver, J. (1973). Possible criteria for predicting earthquake locations and their application to major plate boundaries of the Pacific and the Caribbean. Journal of Geophysical Research, 78(14), 2547-2585.

Kijko, A. (2004). Estimation of the maximum earthquake magnitude, Pure Appl. Geophys. 161, 1–27.
Larios-Romero, J., & Hernández, J. (1992). Fisiografía, ambientes y uso agrícola de la tierra en Tabasco. Unidad de Centros Regionales, Universidad Autónoma Chapingo. Chapingo, México.

León, J. A., Ordaz, M., Haddad, E. and Araújo, I. F. (2022). Risk caused by the propagation of earthquake losses through the economy. Nature communications, 13(1), 2908.

Lyon-Caen, H., Barrier, E., Lasserre, C., Franco, A., Arzu, I., Chiquin, L. and Wolf, R. (2006). Kinematics of the North American–Caribbean-Cocos plates in Central America from new GPS measurements across the Polochic-Motagua fault system. Geophysical Research Letters, 33(19).

Manea, M., Manea, V. C., Ferrari, L., & Orozco-Esquivel, T. (2019). Delamination of sub-crustal lithosphere beneath the Isthmus of Tehuantepec, Mexico: Insights from numeric modelling. Journal of Geodynamics, 129, 262-274.

Manea, V. C., Manea, M. and Ferrari, L. (2013). A geodynamical perspective on the subduction of Cocos and Rivera plates beneath Mexico and Central America. Tectonophysics, 609, 56-81.

Marmureanu, G., Cioflan, C. O., Marmureanu, A., Ionescu, C., & Manea, E. F. (1993). Bridging the Gap Between Nonlinear Seismology as Reality and Earthquake Engineering. Perspectives on European Earthquake Engineering and Seismology, 218, 409.

Marzocchi, W., Taroni, M., & Selva, J. (2015). Accounting for epistemic uncertainty in PSHA: Logic tree and ensemble modeling. Bulletin of the Seismological Society of America, 105(4), 2151-2159.

McGuire, R. K. (2008). Probabilistic seismic hazard analysis: Early history. Earthquake Engineering & Structural Dynamics, 37(3), 329-338.

McGuire, R.K. (1976) FORTRAN Computer Program for Seismic Risk Analysis. United States Geological Survey Open-File Report No. 76-67, U.S. Geological Survey, Washington DC. https://doi.org/10.3133/ofr7667

MDOC-DV (1993) Manual de Diseño de Obras Civiles–Diseño por Sismo. Comisión Federal de Electricidad (in Spanish)

MDOC-DV (2015) Manual de Diseño de Obras Civiles–Diseño por Sismo. Comisión Federal de Electricidad (in Spanish)

MDOC-DV (2018) Manual de Diseño de Obras Civiles–Diseño por Sismo. Comisión Federal de Electricidad (in Spanish)

Meletti, C., Galadini, F., Valensise, G., Stucchi, M., Basili, R., Barba, S. and Boschi, E. (2008). A seismic source zone model for the seismic hazard assessment of the Italian territory. Tectonophysics, 450(1-4), 85-108.

Melgar, D., Ruiz-Angulo, A., Garcia, E. S., Manea, M., Manea, V. C., Xu, X. and Ramirez-Guzmán, L. (2018). Deep embrittlement and complete rupture of the lithosphere during the M w 8.2 Tehuantepec earthquake. Nature Geoscience, 11(12), 955-960.

Meneses-Rocha, J. J., Bartolini, C., Buffler, R. T. and Cantú-Chapa, A. (2001). Tectonic evolution of the Ixtapa Graben, an example of a strike-slip basin of southeastern Mexico: Implications for regional petroleum systems. MEMOIRS-AMERICAN ASSOCIATION OF PETROLEUM GEOLOGISTS, 183-218.

Montero, W., Peraldo, G. and Rojas, W. (1997). Proyecto de amenaza sísmica de América Central. Informe final del proyecto del Instituto Panamericano de Geografía e Historia (IPGH).

Nishenko, S. P. and Singh, S. K. (1987). Relocation of the great Mexican earthquake of 14 January 1903. Bulletin of the Seismological Society of America, 77(1), 256-259.

Ordaz M, Cardona O, Salgado-Gálvez MA, Bernal G, Singh K, Zuloaga D (2014) Probabilistic seismic hazard assessment at global level. Int J Disaster Risk Reduct 10:419–427

Ordaz, M. (1991). CRISIS. Brief description of program CRISIS, Internal report, Institute of Solid Earth Physics, University of Bergen, Norway, 16 pp.

Ordaz, M., Faccioli, E., Martinelli, F., Aguilar, A., Arboleda, J., Meletti, C., D'Amico, V., (2021). R-CRISIS Ver 20.3.0. Program for Computing Seismic Hazard, Institute of Engineering. UNAM, Mexico.

Ortiz, D., Reinoso, E., & Villalobos, J. A. (2021). Assessment of business interruption time due to direct and indirect effects of the Chiapas earthquake on September 7th 2017. Natural Hazards, 108(3), 2813-2833.
Pacheco, J. F. and Sykes, L. R. (1992). Seismic moment catalog of large shallow earthquakes, 1900 to 1989. Bulletin of the Seismological Society of America, 82(3), 1306-1349.

Padilla y Sánchez, R. J. (2007). Evolución geológica del sureste mexicano desde el Mesozoico al presente en el contexto regional del Golfo de México. Boletín de la Sociedad Geológica Mexicana, 59(1), 19-42.

Palma-López, D.J., Zavala-Cruz, J., Bautista-Zúñiga, F., Morales-Garduza, M.A., López-Castañeda, A., Shirma-Torres, E.D., Sánchez-Hernández, R., Peña-Peña, A.J. & Tinal-Ortiz, S. (2017). Clasificación y cartografía de suelos del estado de Campeche, México. AgroProductividad 10(12): 71-78.

Papazachos, B. C., Scordilis, E. M., Panagiotopoulos, D. G., Papazachos, C. B., & Karakaisis, G. F. (2004). Global relations between seismic fault parameters and moment magnitude of earthquakes. Bulletin of the Geological Society of Greece, 36(3), 1482-1489.

Park, C. B., Miller, R. D., & Xia, J. (1999). Multichannel analysis of surface waves. Geophysics, 64(3), 800-808.

Park, C. B., Miller, R. D., Xia, J., & Ivanov, J. (2007). Multichannel analysis of surface waves (MASW)—active and passive methods. The Leading Edge, 26(1), 60–64.doi:10.1190/1.2431832

Parker, G. A., Stewart, J. P., Boore, D. M., Atkinson, G. M. and Hassani, B. (2022). NGA-subduction global ground motion models with regional adjustment factors. Earthquake Spectra, 38(1), 456-493.

Pelc, S. and Koderman, M. (2018). Nature, Tourism and Ethnicity as Drivers of (De) Marginalization. Nature, 3.

Peraldo, G. and Montero, W. (1999). Sismología histórica de América Central. Inst. Panamericano de Geogra. Historia, México, 347.

Perevochtchikova, M. and de la Torre, J. L. L. (2010). Causas de un desastre: Inundaciones del 2007 en Tabasco, México. Journal of Latin American Geography, 73-98.

Pindell, J. and Miranda, E. (2011). Linked kinematic histories of the Macuspana, Akal-Reforma, Comalcalco, and deepwater Campeche Basin tectonic elements, southern Gulf of Mexico.

Plafker, G. (1976). Tectonic aspects of the Guatemala earthquake of 4 February 1976. Science, 193(4259), 1201-1208.

Porfido, S., Esposito, E., Spiga, E., Sacchi, M., Molisso, F. and Mazzola, S. (2014). Re-evaluation of the 1976 Guatemala earthquake taking into account the environmental effects. In EGU General Assembly Conference Abstracts (6525).

Ramírez-Herrera, M. T., Corona, N., Ruiz-Angulo, A., Melgar, D. and Zavala-Hidalgo, J. (2018). The 8 September 2017 tsunami triggered by the M w 8.2 intraplate earthquake, Chiapas, Mexico. Pure and Applied Geophysics, 175, 25-34.

Reasenberg, P. (1985). Second-order moment of central California seismicity, 1969–1982. Journal of Geophysical Research: Solid Earth, 90(B7), 5479-5495.

Rebollar, C. J., Espíndola, V. H., Uribe, A., Mendoza, A. and Vertti, A. P. (1999). Distributions of stresses and geometry of the Wadati-Benioff zone under Chiapas, Mexico. Geofísica Internacional, 38(2), 95-106.

Reiter, L. 1990. Earthquake Hazard Analysis – Issues and Insights. Columbia University Press, New York.

Research Group for Active Fault of Japan (1991) Active Faults in Japan: Sheet Maps and Inventories. University of Tokyo Press, Tokyo, 437.

Rodríguez Vazquez, A. (2018), Caracterización geofísica de sitio para la obtención del parámetros Vs30 mediante la técnica MASW en Villahermosa, Tabasco. Tesis de licenciatura. Universidad Juárez Autónoma de Tabasco.

Rodríguez-Lomelí, A. G. and García-Mayordomo, J. (2019). Seismic hazard at a triple plate junction: the state of Chiapas (México). Natural Hazards, 97, 1297-1325.

Rodríguez-Pérez, Q., & Zuñiga, F. R. (2018). Imaging b-value depth variations within the Cocos and Rivera plates at the Mexican subduction zone. Tectonophysics, 734, 33-43.

Rodríguez-Pérez, Q. (2014). Ground-Motion Prediction Equations for Near-Trench Interplate and Normal-Faulting Inslab Subduction Zone Earthquakes in Mexico. Bulletin of the Seismological Society of America, 104(1), 427-438.

Román-Ramos, Juan R., Cruz-Mercado, M.A., Salofscmón-Mora, L.E., Rosas-Lara, C., Sánchez-Ferrer, F., Biegert, E., Bartsch, E., (2009). Continental-Oceanic Boundary Deep Structure in a Shear Margin: Western Main Transform, Offshore Veracruz, Southern Gulf of Mexico, in: Bartolini, C., Román-Ramos, J. R. (Eds.), Petroleum Systems in the Southern Gulf of Mexico. American Association of Petroleum Geologists, Tulsa, Oklahoma, U.S.A., pp. 409–420. https://doi.org/10.1306/13191094M903416

Salgado, A., Escamirosa, F., & Calvo, A. (2004). Zonificación sísmica de tres centros históricos del sureste mexicano. Sociedad Mexicana de Ingeniería Estructural, 11-15.

Sarlis, N. V., Skordas, E. S., Varotsos, P. A., Ramírez-Rojas, A., & Flores-Márquez, E. L. (2019). Investigation of the temporal correlations between earthquake magnitudes before the Mexico M8. 2 earthquake on 7 September 2017. Physica A: Statistical Mechanics and its Applications, 517, 475-483.

Sawires, R., Peláez, J. A. and Santoyo, M. A. (2023). Probabilistic seismic hazard assessment for Western Mexico. Engineering Geology, 313, 106959.

Sawires, R., Santoyo, M. A., Peláez, J. A. and Corona Fernández, R. D. (2019). An updated and unified earthquake catalog from 1787 to 2018 for seismic hazard assessment studies in Mexico. Scientific data, 6(1), 241.

Sawires, R., Santoyo, M. A., Peláez, J. A. and Henares, J. (2021). Western Mexico seismic source model for the seismic hazard assessment of the Jalisco-Colima-Michoacán region. Natural Hazards, 105(3), 2819-2867.

Schulte, S. M., & Mooney, W. D. (2005). An updated global earthquake catalogue for stable continental regions: reassessing the correlation with ancient rifts. Geophysical Journal International, 161(3), 707-721.

Scordilis, E. M. (2006). Empirical global relations converting MS and mb to moment magnitude. Journal of seismology, 10, 225-236.

Scott, C., Adam, R., Arrowsmith, R., Madugo, C., Powell, J., Ford, J., ... & Ingersoll, S. (2023). Evaluating how well active fault mapping predicts earthquake surface-rupture locations. Geosphere, 19(4), 1128-1156.
Silva, V., Amo-Oduro, D., Calderon, A., Costa, C., Dabbeek, J., Despotaki, V. and Pittore, M. (2020). Development of a global seismic risk model. Earthquake Spectra, 36(1_suppl), 372-394.

Singh, S. K., Corona-Fernandez, R. D., Santoyo, M. Á., & Iglesias, A. (2023) Repeating Large Earthquakes along the Mexican Subduction Zone. Seismological Research Letters. https://doi.org/10.1785/0220230243

Singh, S. K., Pacheco, J. F., Pérez-Campos, X., Ordaz, M. and Reinoso, E. (2015). The 6 September 1997 (Mw 4.5) Coatzacoalcos-Minatitlan, Veracruz, Mexico earthquake: implications for tectonics and seismic hazard of the region. Geofísica internacional, 54(2), 191-199.

Singh, S. K., Reinoso, E., Arroyo, D., Ordaz, M., Cruz-Atienza, V., Pérez-Campos, X. and Hjörleifsdóttir, V. (2018). Deadly intraslab Mexico earthquake of 19 September 2017 (M w 7.1): Ground motion and damage pattern in Mexico City. Seismological Research Letters, 89(6), 2193-2203.

Solano-Hernández, E. A., Caamal, L. V. and Melgar, D. (2022). Tsunami modeling and inundation maps of the~ M8. 6, 1787 earthquake along the Oaxacan coast.Journal of South American Earth Sciences, 119, 103982

SSN (2023). Universidad Nacional Autónoma de México, Instituto de Geofísica, Servicio Sismológico Nacional, México. Dirección electrónica: http://www.ssn.unam.mx

Suárez, G. (2000). Reverse faulting in the Isthmus of Tehuantepec: Backarc deformation induced by the subduction of the Tehuantepec ridge. Special Papers-Geological Society of America, 263-268.

Suárez, G. (2021). Large earthquakes in the Tehuantepec subduction zone: evidence of a locked plate interface and large-scale deformation of the slab. Journal of Seismology, 25(2), 449-460.

Suárez, G. and Albini, P. (2009). Evidence for great tsunamigenic earthquakes (M 8.6) along the Mexican subduction zone. Bulletin of the Seismological Society of America, 99(2A), 892-896.

Suárez, G., & López, A. (2015). Seismicity in the southwestern Gulf of Mexico: evidence of active back arc deformation. Revista mexicana de ciencias geológicas, 32(1), 77-83.

Suárez, G., Santoyo, M. A., Hjorleifsdottir, V., Iglesias, A., Villafuerte, C. and Cruz-Atienza, V. M. (2019). Large scale lithospheric detachment of the downgoing Cocos plate: The 8 September 2017 earthquake (Mw 8.2). Earth and Planetary Science Letters, 509, 9-14.

Trugman, D. T., Borsa, A. A., & Sandwell, D. T. (2014). Did stresses from the Cerro Prieto geothermal field influence the El Mayor-Cucapah rupture sequence?. Geophysical Research Letters, 41(24), 8767-8774.

Van Stiphout T, Zhuang J, Marsan D (2012) Seismicity declustering, Community online resource for statistical seismicity analysis. https://doi.org/10.5078/corssa-52382934. Available at http:// www.corssa.org

Vanneste, K., Vleminckx, B., Stein, S., & Camelbeeck, T. (2016). Could M max be the same for all stable continental regions?. Seismological Research Letters, 87(5), 1214-1223.

Velázquez-Bucio, M. M., Ferrario, M. F., Muccignato, E., Porfido, S., Sridharan, A., Chunga, K. and Michetti, A. M. (2023). Environmental effects caused by the Mw 8.2, September 8, 2017, and Mw 7.4, June 23, 2020, Chiapas-Oaxaca (Mexico) subduction events: comparison of large intraslab and interface earthquakes. Quaternary International, 651, 62-76.

Villagran, M., Lindholm, C., Dahle, A., Cowan, H., & Bungum, H. (1996). Seismic hazard assessment for Guatemala City. Natural hazards, 14, 189-205.

Ward, P. J., Blauhut, V., Bloemendaal, N., Daniell, J. E., de Ruiter, M. C., Duncan, M. J., Emberson, R., Jenkins, S. F., Kirschbaum, D., Kunz, M., Mohr, S., Muis, S., A. Riddell, G., Schäfer, A., Stanley, T., Veldkamp, T. I. E., and Winsemius, H. C. (2020). Natural hazard risk assessments at the global scale. Natural Hazards and Earth System Sciences, 20(4), 1069-1096.

Wells, D. L. and Coppersmith, K. J. (1994). New empirical relationships among magnitude, rupture length, rupture width, rupture area, and surface displacement. Bulletin of the seismological Society of America, 84(4), 974-1002.

White, R. A. (1984). Catalog of historic seismicity in the vicinity of the Chixoy-Polochic and Motagua faults, Guatemala. US Geological Survey.
White, R. A. (1985). The Guatemala earthquake of 1816 on the Chixoy-Polochic fault. Bulletin of the Seismological Society of America, 75(2), 455-473.

White, R. A. and Harlow, D. H. (1993). Destructive upper-crustal earthquakes of Central America since 1900. Bulletin of the Seismological Society of America, 83(4), 1115-1142.

White, R. A., Ligorría, J. P., & Cifuentes, I. L. (2004). Seismic history of the Middle America subduction zone along El Salvador, Guatemala, and Chiapas, Mexico: 1526–2000.

Wiemer, S. (2001). A software package to analyze seismicity: ZMAP. Seismological Research Letters, 72(3), 373-382.

Witt, C., Brichau, S. and Carter, A. (2012). New constraints on the origin of the Sierra Madre de Chiapas (south Mexico) from sediment provenance and apatite thermochronometry. Tectonics, 31(6).

Xiang, Y., Yue, J., Cai, D., & Wang, H. (2019). Rapid determination of source parameters for the 2017 Mw 8.2 Mexico earthquake based on high-rate GPS data. Advances in Space Research, 64(5), 1148-1159.

Youngs, R. R., Chiou, S. J., Silva, W. J. and Humphrey, J. R. (1997). Strong ground motion attenuation relationships for subduction zone earthquakes. Seismological research letters, 68(1), 58-73.

Zhao, J.X., Zhang, J., Asano, A., Ohno, Y., Oouchi, T., Takahashi, T., Ogawa, H., Irikura, K., Thio, H.K., Somerville, P.G., Fukushima, Yasuhiro, Fukushima, Yoshimitsu, (2006). Attenuation relations of strong ground motion in Japan using site classification based on predominant period. Bull. Seismol. Soc. Am. 96, 898–913. https://doi.org/10.1785/0120050122.

Zúñiga FR, Suárez O, Ordaz M, García-Acosta V (1997) México, Proyecto: Peligro sísmico en Latinoamérica y el Caribe. Instituto Panamericano de Geografía e Historia and Centro Internacional de Investigaciones para el desarrollo Ottawa, Canadá Proyecto 89-0190, vol 2, p 82

Zúñiga, F. R., Suárez, G., Figueroa-Soto, Á., & Mendoza, A. (2017). A first-order seismotectonic regionalization of Mexico for seismic hazard and risk estimation. Journal of Seismology, 21, 1295-1322.